MONITORING OF THE DYNAMIC GAS-OIL CONTACT DISPLACEMENT FOR WELLS IN NATURALLY FRACTURED RESERVOIRS BY ANALYZING PRODUCTION TUBING DATA

A Thesis

by

PEDRO RUBEN SANCHEZ LOERA

Submitted to the Office of Graduate and Professional Studies of
Texas A&M University
in partial fulfillment of the requirements for the degree of

MASTER OF SCIENCE

Chair of Committee,	David S. Schechter
Committee Members,	Ding Zhu
	Debjyoti Banerjee
Head of Department,	A. Daniel Hill

August 2016

Major Subject: Petroleum Engineering

ABSTRACT

Reservoir monitoring allows petroleum engineers to acquire a better understanding of the phenomenon happening inside a hydrocarbon reservoir under development; multiple methods exist currently to monitor a reservoir, depending on the data required and the studies the data is needed for. In naturally fractured reservoirs with a gas cap present, where the fracture network dominates the fluid flow from the reservoir to the production wells, it is of vital importance to be able to have a continuous surveillance of the behavior of the fluid contacts, in order to successfully plan and optimize the development of the reservoir. A well-documented monitoring methodology consists on installing permanent sensors at open-hole well completions, metering the pressure and temperature outside a production tubing designed to be in contact with all the fluids in the well. With the data gathered through these sensors, and basic knowledge of the reservoir fluid properties, the fluid contacts in the fracture network can be estimated at any time whenever data is available.

An alternate methodology is presented in this document, for those well cases in which the placement of permanent sensors at the well completion is not viable and therefore pressure data outside of the production tubing for the aforementioned well is not available. This thesis proposes two methodologies to calculate the fluid contact by performing a small-aperture orifice to the well completion design at the gas cap level, this modification allows to collect gas inflow pressure and rates data by introducing to the well surface-run tools;

A derived mathematical expression is fed with the obtained data to estimate the conditions outside the production tubing at the gas cap level, such correlation is also presented as a series of dimensionless type curves; finally, with the estimated pressure conditions and the corresponding fluid properties, the position of the gas-oil contact is calculated. The methodologies presented can be adapted to different forms of fluid flow through orifices equations in case the reader prefers to use a different one to those selected here; the methodology has to be calibrated before being implemented in the field in order to reduce uncertainty.

DEDICATION

To you who have walked beside me during this adventure.

To you who took interest in reading beyond the abstract and conclusions.

ACKNOWLEDGMENTS

I would like to express my deepest gratitude to my advisor, Dr. David S. Schechter, for his guidance, time and support during my pursuit of the M.S. Degree. His support has positively influenced my professional growth. I would also like to extend my sincere appreciation to Dr. Ding Zhu and Dr. Debjyoti Banerjee, my committee members, for their continuous advice and support throughout my research. I want to thank the professors and department staff for being so much more than the person in front of a class or behind a desk, your genuine interest in helping people achieve their goals is admirable. To Petroleos Mexicanos, CONACYT and Dr. Nemesio Miguel Hernandez, I would also like to extend my gratitude, for allowing me to take the opportunity to achieve this professional goal, they have fully supported me through all the process.

Thanks to all my graduate friends, “Wets”, “Chatas” and aggies for making my time at Texas A&M University an incredible experience, one I will surely never forget. Thanks to my family, my friends and co-workers back in Mexico for keeping the friendship alive not mattering the distance. Finally, thanks to my mother and my father, you have never stopped encouraging me to pursue new goals, I am truly grateful for that and for still having you with me, you have always believed in me and I can only hope to someday become the person you see when you see me.

NOMENCLATURE

A	Area
C_D	Orifice flow discharge coefficient, dimensionless
C_C	Coefficient of contraction
C_p	Specific heat of the gas at constant pressure
C_v	Specific heat of the gas at constant volume
C_V	Actual flow velocity vs ideal flow velocity ratio
CT	Coiled Tubing
d_{ch}	Diameter of the orifice or channel, inches or 64ths of an inch
D	Diameter of the tubing, inches
DGOC	Dynamic Gas-Oil Contact
DTTC	Deep Tubing Tail Completion
DTS	Distributed Temperature Sensing
DWOC	Dynamic Water-Oil Contact
Δz	Vertical depth differential, ft
γ_g	Gravity of the gas (relative to air), dimensionless
GLR	Gas-Liquid Ratio, volume unit of gas / volume unit of liquid
GOC	Gas-Oil Contact
Grad	Fluid gradient, psi/ft
IDTTC	Instrumented Deep Tubing Tail Completion
k	Heat capacity ratio (HCR), dimensionless
K	Kelvin, temperature unit

l	Orifice length (thickness of the tubing hosting the orifice), inches
M	Molecular weight, lbm / lbmol
$\dot{m}$	Mass flow rate, mass unit / time unit
NFR	Naturally Fractured Reservoir
P	Pressure, psi
P_{crit}	Critical pressure, psi
P_{dwn}	Pressure downstream of an orifice or restriction, psi
$(P_{dwn}/P_{ups})_c$	Critical pressure ratio, dimensionless
PNLT	Pulsed Neutron Logging Tools
PTT	Pressure Transient Testing
P_{ups}	Pressure upstream of an orifice or restriction, psi
P_{ws}	Static pressure, psi
Q_g	Gas volumetric flow rate, volume unit / time unit
Q_{gD}	Dimensionless gas flow rate, dimensionless
R	Universal Gas Constant, J / Kg mol K
ρ_g	Density of the gas, lbm / ft^3
sc	Standard Conditions
T	Temperature, ^oR
t	Time
TVD	True Vertical Depth, ft
$\vec{V}$	Flow velocity
WOC	Water-Oil Contact

TABLE OF CONTENTS

Page

Page

LIST OF FIGURES

Page

Page

Page

Page

LIST OF TABLES

Page

1. INTRODUCTION

1.1 Motivation

This thesis work originates from the need in the petroleum industry to achieve a better understanding of the reservoir conditions, in order to do so, multiple reservoir parameters such as pressure, temperature, rock saturation and fluid conditions like their position inside the reservoir, among others have to be continuously monitored; Performing the previous parameters monitoring is not easy, because the complexity and conditions of the reservoir systems and the wells drilled to produce the fluids contained in them are not always in line with the range of applicability of current wellbore data metering tools, providing an area for technologies and methodologies to be developed or improved.

1.2 Concepts and Definitions

In order to be able to put the reader in context of the terms that will be used in this thesis, the following definitions are provided.

Fluids contact. - interface between 2 different fluids contained in a reservoir porous media, usually being the fluids in contact gas and oil, gas and water, or oil and water.

Naturally fractured reservoir. - petroleum system reservoirs characterized by a matrix porous media and a fracture porous media surrounding the matrix blocks, this type of reservoir is also known as double porosity reservoirs.

Orifice geometry. - is the shape given to an orifice or restriction in order to restrict the flow from upstream conditions to downstream conditions depending on parameters like specific flow shape or pressure drop required, different shapes will result in different pressure drops and flow behavior.

Pressure gauge. - device capable of metering pressure changes in the media surrounding the device.

Sonic flow. - is the condition for fluids exhibiting a velocity greater than the sonic velocity; at conditions of sonic flow, perturbations downstream cannot propagate upstream since they cannot travel faster than sonic velocity.

Well completion. - section or interval of a wellbore in charge of connecting the target reservoir system pay zone to the well production system. A well can have more than one completion.

2. LITERATURE REVIEW

2.1 Importance of Fluid Position Monitoring Inside Wells Producing in NFR

Naturally Fractured Reservoirs (NFR) have a very characteristic property, they possess 2 fluid systems when 2 or more different fluids are present, as (Edwards et al. 2011) explains, more often than not, in mature fields, or fields in which the bubble point has been reached, the reservoir rock matrix develops one gas-oil-water contact while the fracture system develops a different gas-oil-water contact; in these cases a gradients difference provokes oil from the rock matrix system surrounded by the gas cap to leave the rock and migrate by gravity segregation through the fracture network to the oil rim formed in the fracture system; wells drilled in these reservoirs produce the oil by intersecting the fractures containing the oil rim, since the fracture system allows the fluids in the reservoir to move fairly easily when compared to the rock matrix system, the oil rim under exploitation exhibits a very dynamic behavior; Because of the previous statement, It is a top priority to be able to know and track the changes in the oil rim position and thickness, and avoid conditions where the wells get disconnected from it.

NFR are also good candidates for a Gas flooding process or a Double Displacement Process, which basically consist in making the most of the gravity drainage effect by producing water from the bottom of the reservoir, while injecting gas on the top, in order to lower the position of the oil rim and expose to the gas cap the most possible volume of

reservoir rock matrix, increasing the volume of oil able to migrate down to the oil rim, and maximizing the recovery factor; This procedure makes very relevant the need to monitor the progress of the oil rim movement, in order to know the velocity at which this is moving down the reservoir, track the thickening or thinning of the oil rim as more reservoir rock matrix is exposed to the gas cap, increasing the gravity drainage effect, and plan accordingly to these changes in order to adapt the wells to be able to follow the moving oil rim. Very similar to the Double Displacement Process, exists a Temperature Assisted Gas-Oil Gravity Drainage process, in which gas is injected into the reservoir to increase the temperature, reduce the oil viscosity, and increase its mobility, facilitating the migration to the oil rim; the previous process also requires a continuous monitoring of the fluid contacts inside the reservoir, for very similar reasons to those of the double displacement process.

An additional point worth mentioning regarding the importance of a fluid contact monitoring philosophy is presented by (Ladron De Guevara et al. 2012), putting emphasis in how wells in NFR initially completed with an open-hole way below the gas-oil contact (GOC) gas out when the GOC moves down the reservoir and generates conditions around the well completion where the mobility of the gas prevents for any liquid in the well to be extracted; Ladron De Guevara et al. modified the well completion, installing a hanging tubing with a packer at the liner, the hanging tubing is designed with production slots at the lower end, or the bottom end open and is long enough that it penetrates the oil rim deep enough for oil production to be resumed with a great reduction in the gas-liquid ratio,

in some cases completely eliminating gas production; such design is known as a Deep Tubing Tail Completion, and when paired with tools to monitor reservoir parameters like pressure gauges, it is known as an Instrumented Deep Tubing Tail Completion (Ladron De Guevara et al. 2012); The main benefits of having a way to acquire data from the well-reservoir conditions in these type of well completions, according to Ladron de Guevara et al. are:

- Continuous tracking of the Dynamic and Static conditions of the near well reservoir region.
- Tracking of the changes in the oil rim thickness and position.
- Changes in the monitored fluid gradients.
- Real time reservoir pressure and/or temperature monitoring.
- Estimation of reservoir and well parameters by means of transient pressure test analysis availability.
- Tuning and optimization of the artificial lift system in cases where this exists.

2.2 Types of Gas-Oil Contacts in NFR

As described in the previous chapter, a NFR under exploitation possess 2 main GOC, one in the reservoir rock matrix system, and a second one in the fracture network (Edwards et al. 2011), this happens because of the limited mobility fluids have inside the rock matrix relative to the mobility through the fracture network, delaying the change in position of

the GOC in the first system. The previous GOC are usually referred to areas of the reservoir where a condition of semi-balance is present, conditions also known as “static conditions”, this means that, the effects of a producing well are not directly altering the condition of the reservoir area under study.

Reservoir areas subject to producing wells usually are influenced by the pressure drawdown generated to transport the hydrocarbons to the surface, the new conditions generated by this perturbation in the reservoir are known as “dynamic conditions”, and they directly affect the fluids in the reservoir near the well; the dynamic condition experienced while producing a well force the GOC in the very near region to change its depth until such perturbance is stopped, depending on the magnitude of the pressure drawdown, the characteristics of the well completion, the reservoir rock properties and fracture network properties, the change in the GOC depth can go from a few to several feet; the position of the GOC while under dynamic conditions is known as the Dynamic Gas-Oil Contact (DGOC), an example of the GOC and DGOC is displayed on fig. 2.1; more information on how the DGOC monitoring benefits engineers to achieve better reservoir exploitation practices is presented by (Ladron De Guevara et al. 2012).

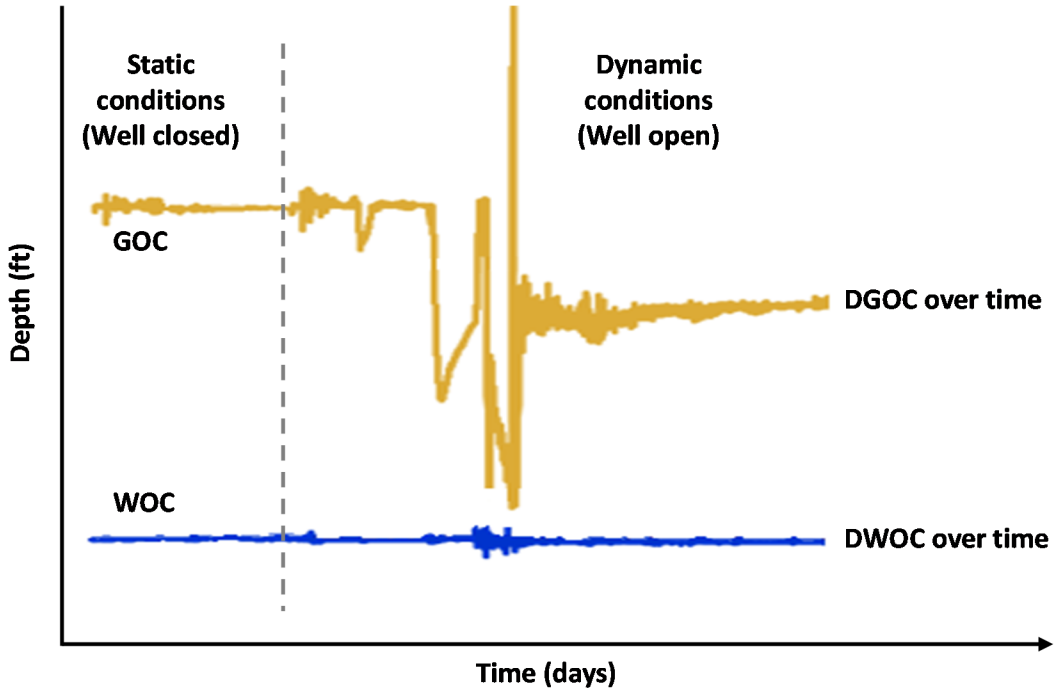

Fig. 2.1– DGOC and DWOC position monitoring over time using pressure gauges data.

2.3 Well Completion Types Suited for GOC and DGOC Monitoring in NFR

Depending on many factors, including the purpose of a well, the geology and shape of the reservoir, budget, etc., a well completion can be very different from another in the same reservoir. In the Petroleum Production Systems book by (Economides et al. 2012) four main completion designs are described, open-hole completion, gravel pack completion, cemented, cased and perforated completion, and the slotted liner horizontal well completion; each of those completions has its own specific characteristics, advantages, limitations and ideal conditions for implementation; other completion designs exist, but they are basically iterations or more complex designs of the four mentioned previously.

The completion designs better suited to allow an efficient DGOC monitoring are the open-hole completion, and the cemented, cased and perforated completion, diagrams of these two completions appear in Fig. 2.2; the open-hole completion in Fig. 2.2(A) consists in perforating the producing section of the well and leaving the hole directly in contact with the reservoir rock. Fig. 2.2(B) shows a cemented, cased and perforated completion, this type of completion consist in installing a tubing casing at the bottom of the well and cement it to the reservoir, in order to support the casing, it also prevents the well walls from collapsing, in reservoirs where wall conformity is an issue, after cementation the casing is perforated in a way that vertical direct communication exists between the well completion and the reservoir area surrounding the well.

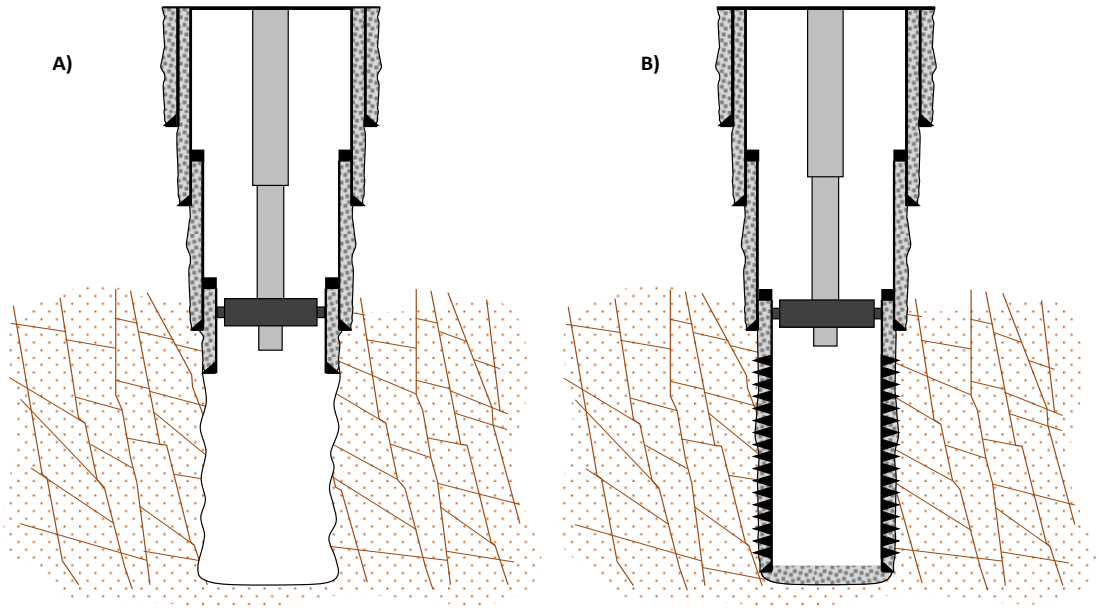

Fig. 2.2– A) Open-hole well completion B) Cemented, cased and perforated completion.

The open-hole completion and the cemented, cased and perforated completion are great for fluid contacts monitoring since their characteristics minimize reservoir isolation, which allows the conditions inside the well completion to be almost the same as the reservoir conditions surrounding the well, this of course includes, the DGOC position; if the well completion was cased and cemented, the fluid levels inside the completion would not be representative of those at the reservoir (Fig. 2.3).

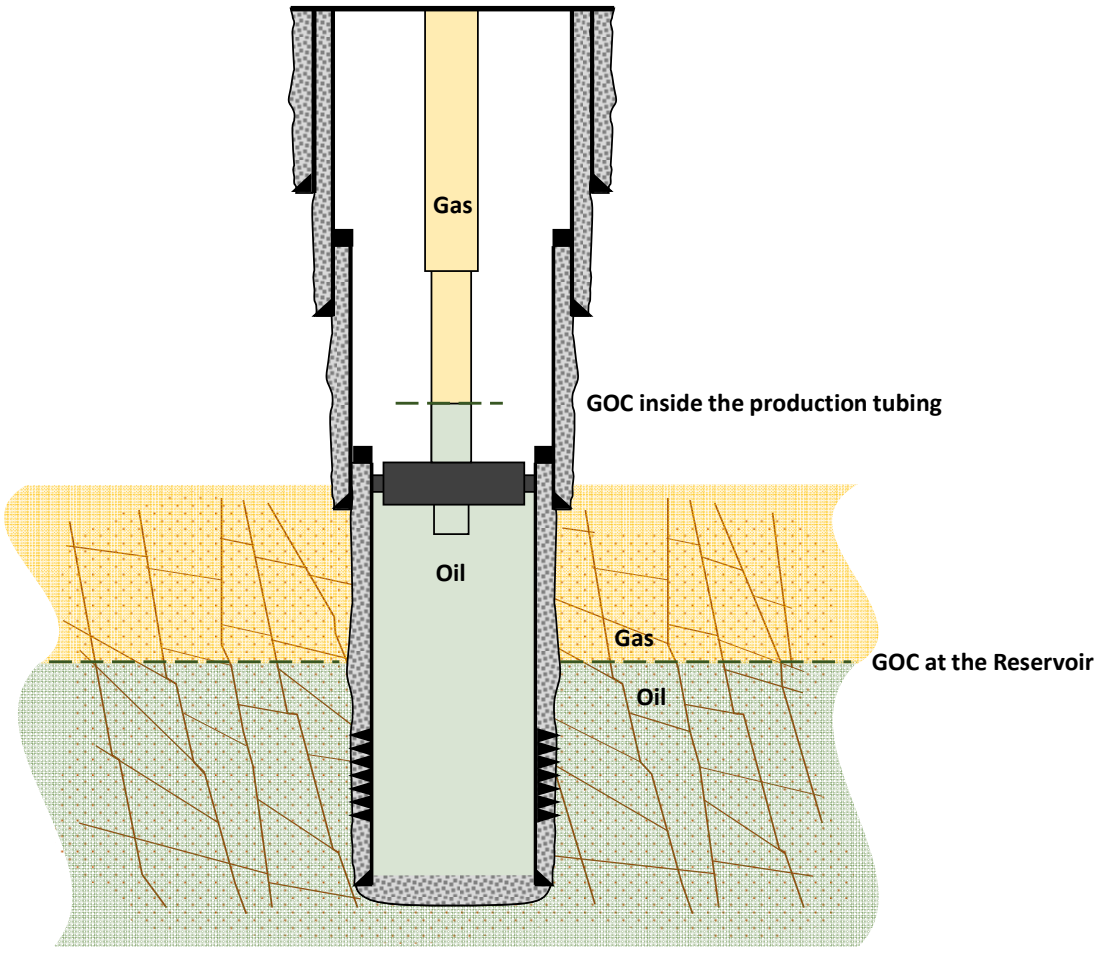

Fig. 2.3– Schematics of a closed well displaying the difference between fluid column inside a well and the GOC position at the reservoir.

2.4 Current Technologies and Methodologies to Monitor the GOC and DGOC

Multiple technologies currently exist focused on monitoring different reservoir parameters at the well completion, the technology to implement is selected depending on the characteristics of the completion, budget and data required. Brief descriptions are provided here of the most widely applied in the industry in order to give the reader a sense of the application range and restrictions that current GOC monitoring technologies possess.

2.4.1 Wireline Intervention Tools

The use of wireline intervention tools usually provide means to acquire data inside the production tubing or even at the bottom of the well completion if the production tubing is not closed at the bottom end; the basic configuration of this tool consist of a coiled wireline that is used to introduce different tools into a wellbore or a tubing; because of the nature of the wireline, its use is limited to vertical wells or wells with limited deviation since the introduction of the tool all the way to the bottom of the borehole or the tubing will depend on the weight of the tools being introduced and the resistance the walls of the wellbore or the tubing oppose, if the well is highly deviated, the metering tools will rest in the wall of the wellbore or tubing and won't be able to travel to the required depth.

The tools introduced in wells for data gathering usually include (but are not limited to), pressure sensors, flow spinners, gradiomanometers, electric probes, calipers, etc. The

usual wireline procedure consist on making an initial calibration run to the bottom of the wellbore or tubing, or the deepest location possible without restrictions or risks of getting the tool stuck, once the calibration run has been performed, multiple runs up and down the hole are performed along stops at different depths, and at flowing or closed well conditions depending on the data required to be gathered inside the well configuration(Edwards et al. 2011).

If the production tubing bottom side is located below the reservoir GOC in an open-hole well completion, making use of the pressure data taken at multiple stops when the well is closed will allow us to detect the liquid level inside the tubing, this data is important when gas lift design and optimization is being performed but will not allow us to estimate the GOC position at the well; if the production tubing bottom side is located above the reservoir GOC in an open-hole well completion, in other words in direct contact with the gas cap (Fig. 2.4), making use of the pressure data taken at multiple depth stops when the well is closed will allow us to detect the position of the GOC inside the well (Onyekonwu. 1997).

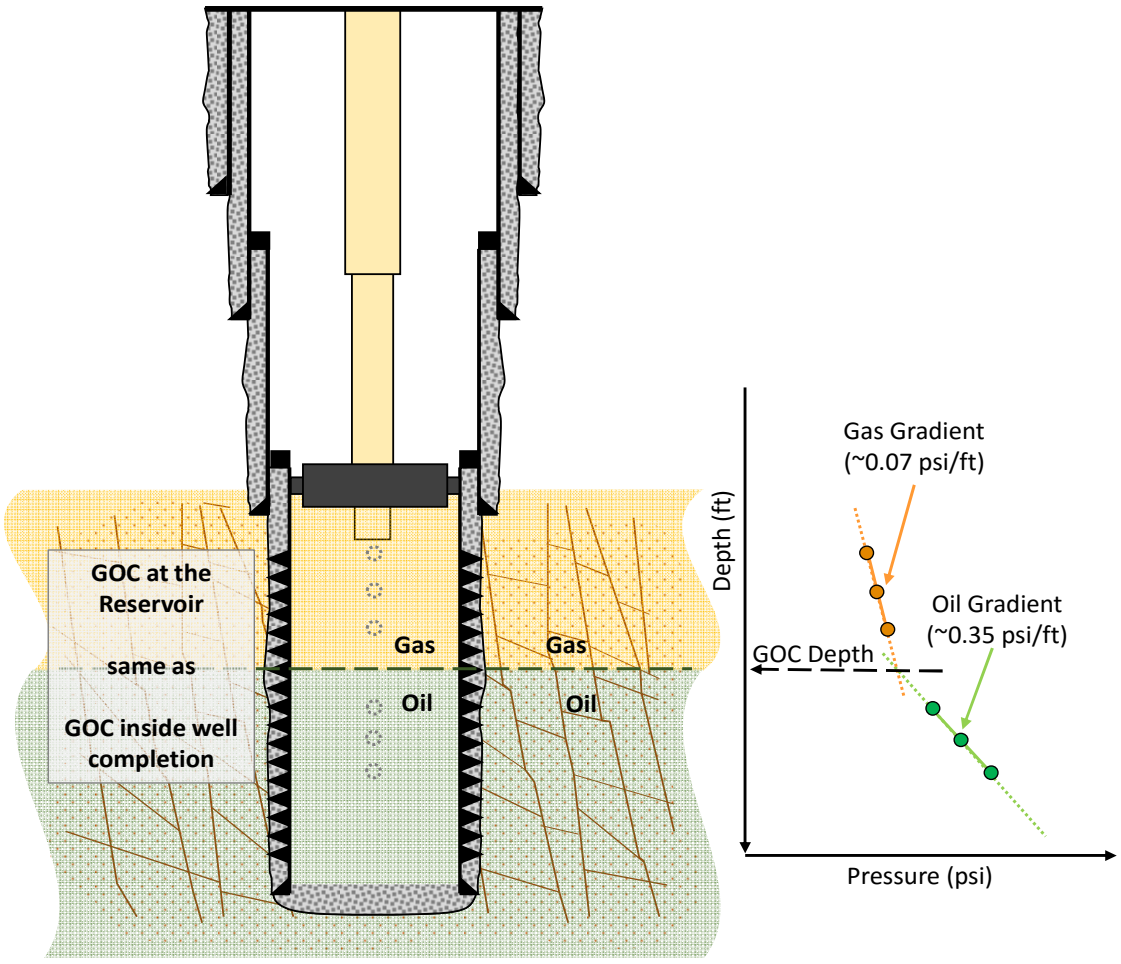

Fig. 2.4 – Closed well with direct communication to the gas cap, displaying same GOC inside and outside the well completion, obtained with pressure data acquired at different depth stops.

2.4.2 Pulsed Neutron Logging Tools

Pulsed neutron logging tools (PNLT) can be run in open or cased wellbores, surrounded by liquid or air, they are used primarily to perform formation evaluation, they provide measurements of "sigma" (the cross section formation capture), ratio of near to far detectors, porosity, carbon and oxygen (C/O), gamma ray spectra of inelastic neutron

scattering and thermal neutron capture in one logging trip in the wellbore (Schneider et al. 1996; AlSharif et al. 2013). This type of tools can help detect fluid contacts, an example is given in the work performed by (Schneider et al. 1996) where he explains how he used a combination of data analysis from the PNLT and existing open hole log data to evaluate and find the fluid contacts in a CO_2 flooding project in a mature reservoir.

2.4.3 Distributed Temperature Sensing

Distributed Temperature Sensing (DTS) technologies can be implemented in a well using optic fiber, this fiber is designed to resist high temperatures and many corrosive components regularly found in wells; the resolution of the fiber optic temperature readings is really good, capable of detecting changes every few feet, or even less; in order to use the DTS to detect fluid contacts inside a well, a perturbation must be introduces that does not change the position of the fluid contacts but reveals their depth, when a well is under production the produced fluids will surround the optic fiber, making difficult to detect a fluids level, for this reason the DTS measurements and respective perturbations must be performed in a closed well in equilibrium (Edwards et al. 2011). In their work, (Edwards et al. 2011) explain how using a U tube inside a closed well crossing the fluid contacts allows them to pump a cool fluid inside the sealed loop and measure the thermal perturbation with an optic fiber installed inside the same U tube(Fig. 2.5); the DTS fiber measures the cooling process and the subsequent stabilization of the temperature as the reservoir heats the pumped fluid, the temperature recovery, called thermal relaxation, will

be different for each section of the DTS fiber depending on the fluid surrounding it (Edwards et al. 2011). For the reasons mentioned previously, this tool proves an excellent method for GOC monitoring, but its limited when trying to measure the DGOC because of the thermal equilibrium and the constant fluid flow surrounding the DTS fiber.

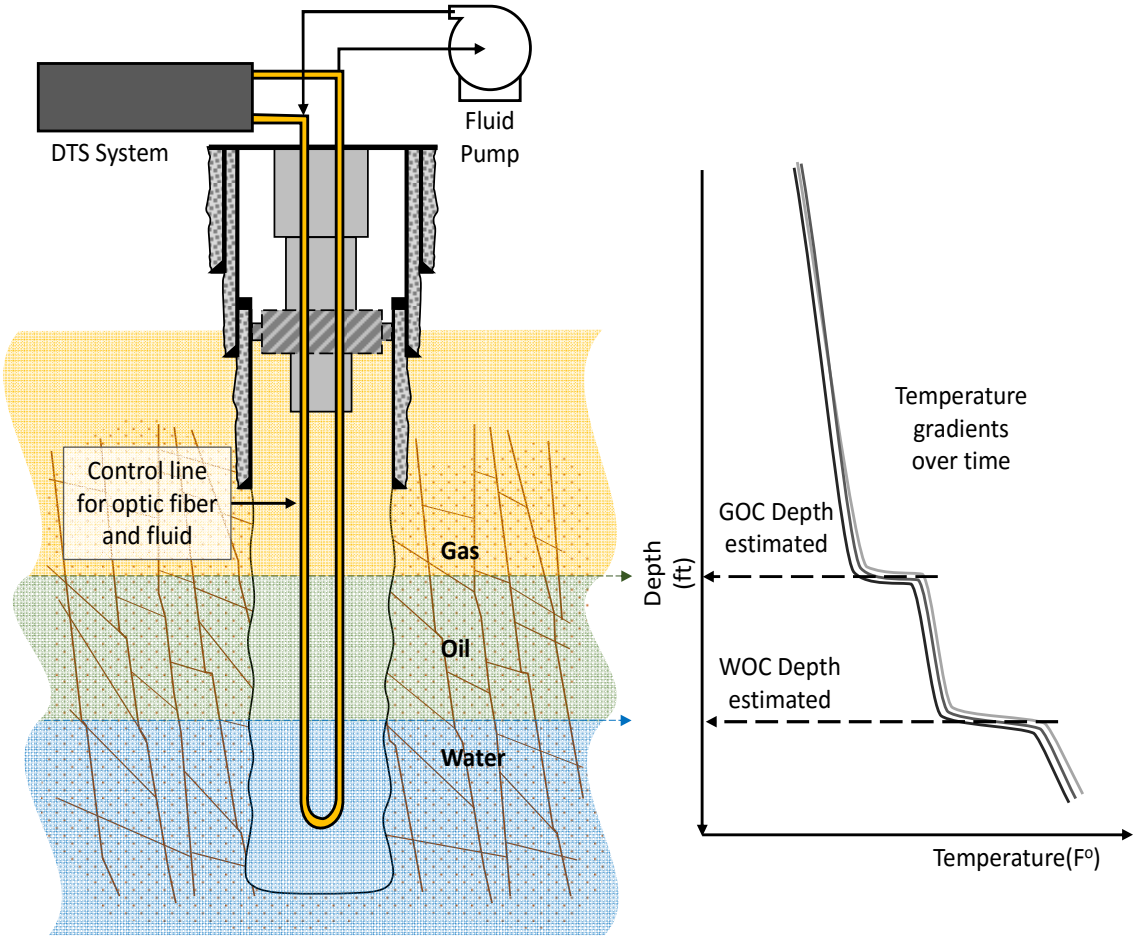

Fig. 2.5 – Schematics for a DTS configuration and data interpretation. Reprinted with permission from Edwards et al. 2011.

2.4.4 Pressure Transient Testing

Pressure transient test are widely used in the hydrocarbon industry as a mean to acquire reservoir and well data such as skin or permeability; with the introduction of pressure derivative log-log plots multiple well reservoir and boundary signature responses have been characterized and can now be identified, diagnosed and their model parameters can now be calculated (Nnadi et al. 2015). According to Nnadi et al. the implementation of bottom hole pressure tests and permanent pressure gauges has allowed fluids contact movement can be detected from late time pressure derivative responses, and when the historic responses of pressure transient tests taken in the same well at different times are superimposed on the same pressure derivative log-log plot the detection of the advancing fluid contacts becomes possible. (Nnadi et al. 2015) have tested their methodology primarily in gas reservoirs with presence of a water front with great success, while their methodology allows for a static fluids contact to be estimated, they require direct communication to the gas in order to perform such estimations and detect the gas-water contact as a boundary response.

2.4.5 Instrumented Deep Tubing Tail Completion

The deep tubing tail completion (DTTC) has been widely implemented in NFR with consistent success, either being instrumented or not, one of its main benefits is to reduce the pressure drawdown required to bring the oil to the surface (Posadas-Mondragon.

2006), while also reducing the gas produced by means of placing the producing section of the tubing tail below enough of the GOC; (Tovar Rodriguez et al. 2011), (Ladron De Guevara et al. 2012; Tovar Rodriguez et al. 2011) and (Ramondenc et al. 2016) have all presented successful production cases for instrumented and non-instrumented iterations of the DTTC, The difference between an Instrumented completion and a non-instrumented basically resides in the presence or absence of permanent sensor gauges at the completion.

As shown in Fig. 2.6, an instrumented tubing tail completion (IDTTC) consists of an open hole or cemented, cased and perforated completion, where a packer/hanger is anchored at the last cemented casing string, the packer/hanger holds a tubing extension known as the tail, which depending on the design can end up between 5 to 15 feet from the bottom of the borehole, the tail will be either an open ended production tubing or a slotted liner, always below enough the GOC, only allowing production to flow from the bottom of the completion if the water-oil contact is known to be far enough, or positioned at the middle of the oil rim promoting oil production over undesired fluids when water is present; the tubing tail will also host a series of pressure and temperature sensors connected to the surface though a cable, these sensors are distributed along the tubing tail in a way that allows for data to be taken from al the fluids or sections of interest inside the well (Ladron De Guevara et al. 2012).

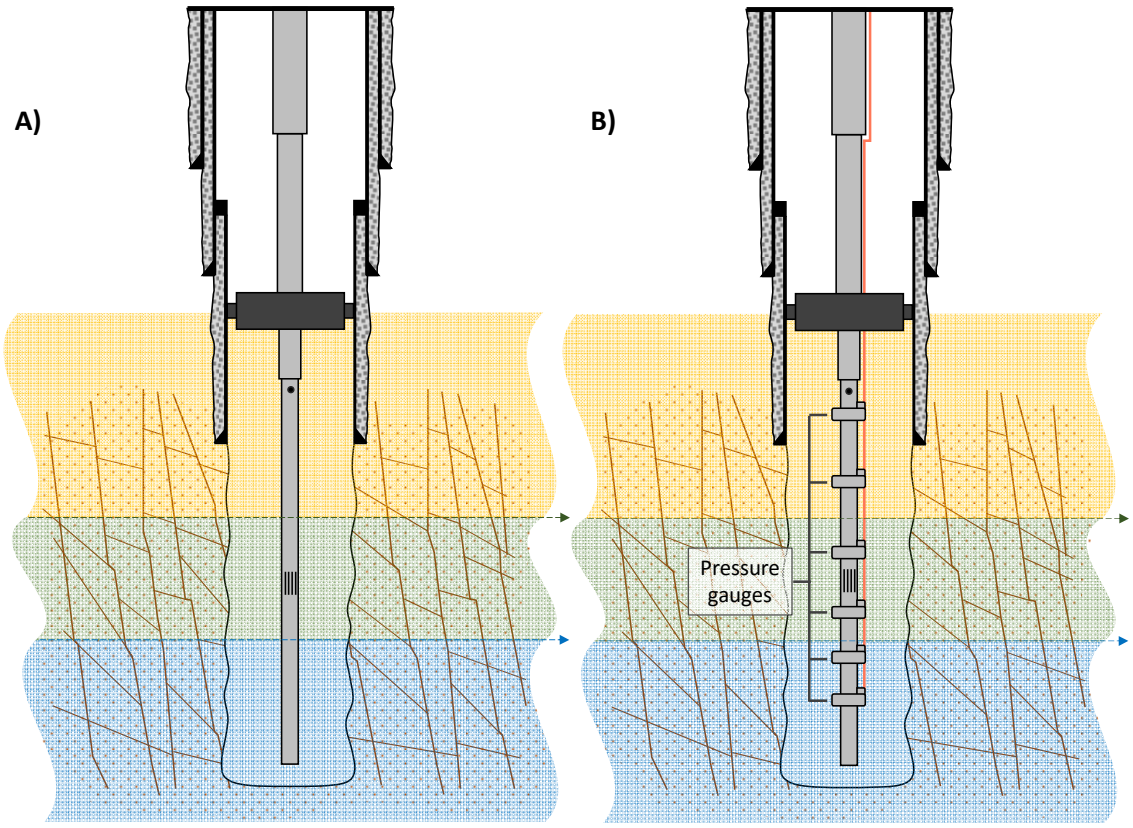

Fig. 2.6 – A) non-instrumented deep tubing tail completion B) Instrumented deep tubing tail completion.

The main benefit obtained from installing pressure and temperature sensors in a DTTC is the continuous monitoring of fluid gradients and dynamic or static conditions when the well is producing or shut down respectively, the monitoring of these parameters also means that a continuous surveillance of the GOC and DGOC can be achieved (Fig. 2.1). fig. 2.7 shows an example of an Instrumented DTTC configuration in a NFR well that experiences both production and shut down periods and how does the fluid gradients and contacts behave over time, the slots in the completion diagram are sliding sleeves where the upper one is open and the lower one in closed, such reservoir is under a gas flooding

process, this means that the oil rim is expected to be displaced down the reservoir, when this happens, the upper sliding sleeve will be closed and the lower one will be opened to continue production at the new position of the oil rim.

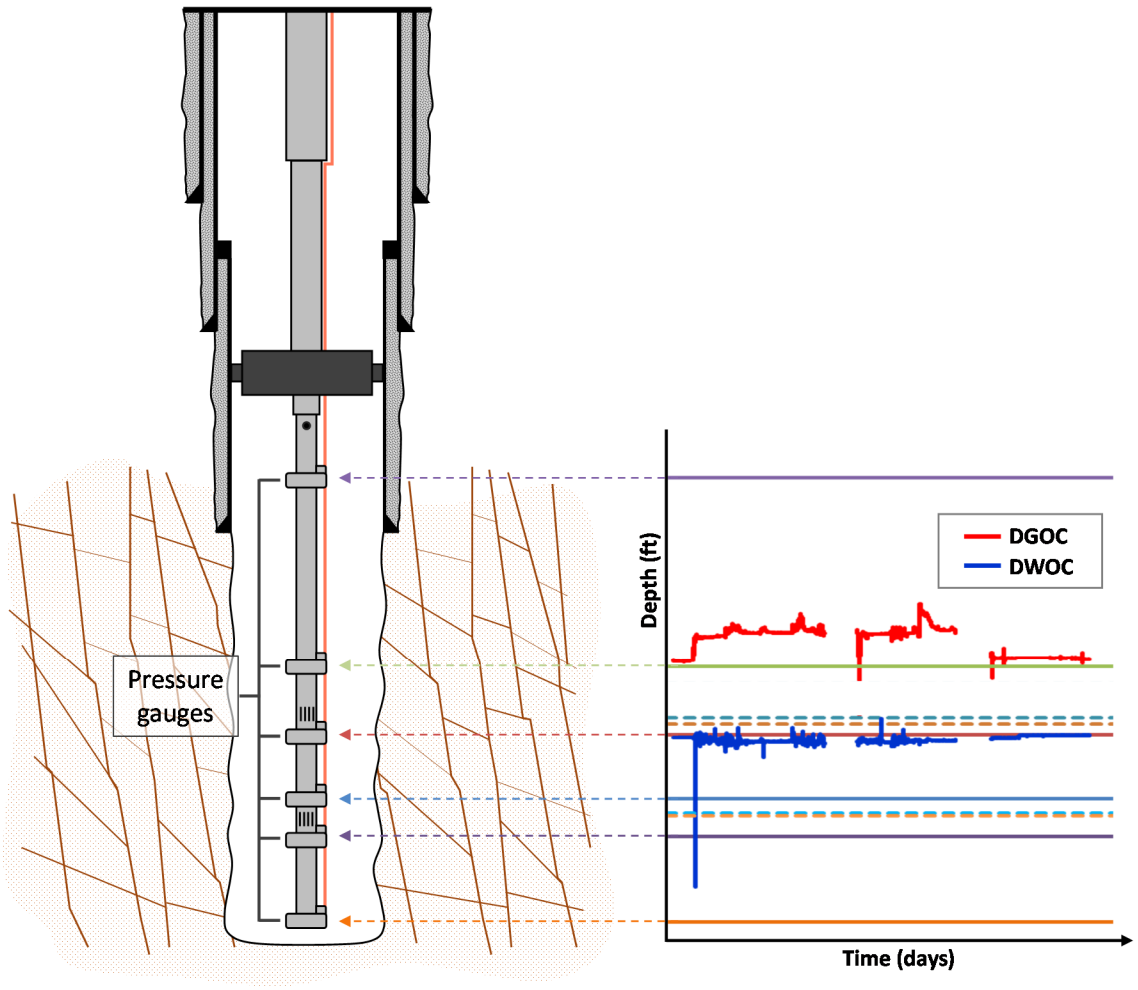

Fig. 2.7 – IDTTC monitoring both the DGOC and the DWOC using gradients from the pressure gauges.

Having such a continuous monitoring capability provides means to optimize the production in a well, it can diminish bottom-hole condition uncertainties, extend the productive life and increase the success of the completion regarding final oil recovery. A key factor for this kind of monitoring to be successful is to have a 100% certainty of the vertical position of the sensors, since their position plays a key part of the fluids contacts position calculation, any divergence with their true vertical depth will make the gradient calculations not be representative of the fluids present inside the well, thus producing calculation errors (Onyekonwu. 1997; Ladron De Guevara et al. 2012).

2.4.6 DGOC Position Monitoring Through Physical Evidence

An iteration of the deep tubing tail completion is presented by (Lagunas Tapia et al. 2015) where monitoring of the dynamic gas-oil contact can be achieved to a certain extension, in wells drilled in NFR where pressure data outside of the production tubing for the aforementioned well is not available because the placement of permanent sensors at the well completion is not viable (the reason either being technical, mechanical, personnel safety or project budget related), their proposed solution relies on making small alterations to the tubing tail, alterations that won't increase the diameter of the tubing, and will allow to estimate a depth interval where the DGOC is placed at the moment when data metering tool are run inside the tubing to detect physical evidence of the DGOC position (controlled inlet gas flow to the production tubing).

Installation of an instrumented deep tubing tail completion requires an economic investment to modify the well completion to be able to allocate the pressure-temperature sensors, and such investment is not always possible because of budget limitations; or the need for the physical characteristics of the wellbore (mainly the diameter and severity of the well trajectory) to allow for the additional equipment to be installed without risk of the completion tubing getting stuck during the installation since the jackets that hold the sensors tend to increase the outside diameter of the completion (Fig. 2.8).

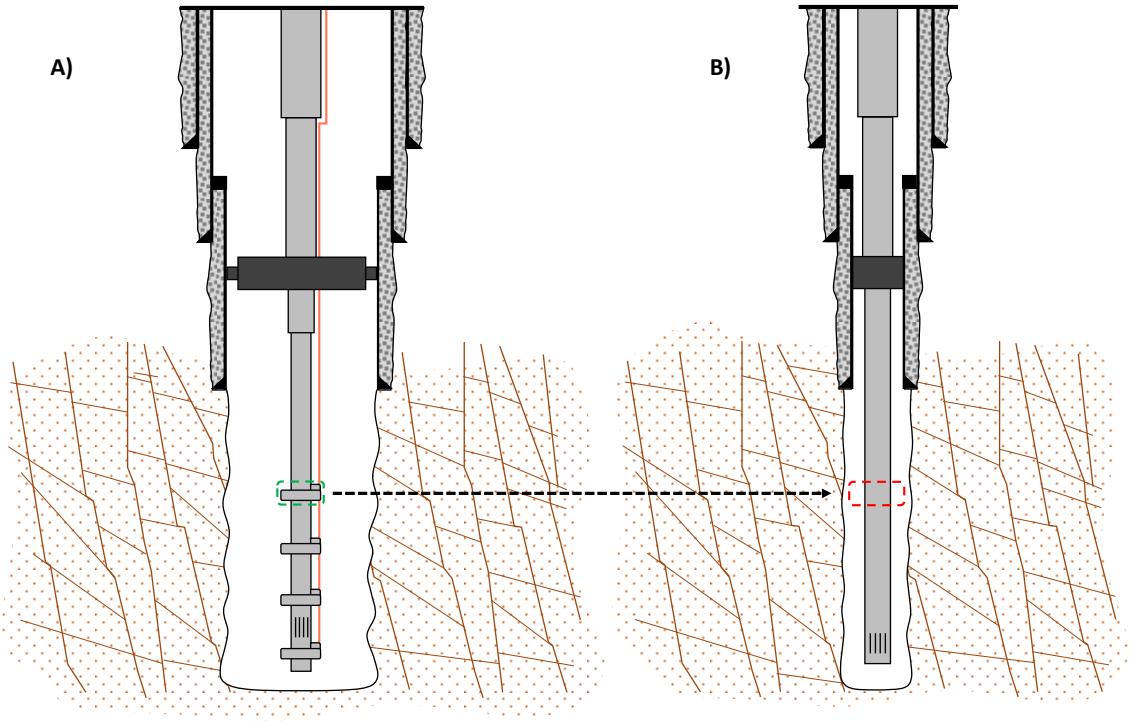

Fig. 2.8 – A) Well completion with sufficient space to safely allocate instrumented tubing tail B) Well completion without sufficient space to safely allocate instrumented tubing tail.

Due to the circumstances stated in the previous paragraph, wells with small hole diameter are not candidates for monitoring technologies relying on annular space pressure data gathered with external sensors; The approach to solve this problem presented by Lagunas Tapia et al. (2015) consists in making alterations to the tubing tail, small diameter orifices (usually around 8/64" – 16/64") denominated as "witnesses" are designed and perforated above the production slots at specific intervals, depending on the characteristics of the completion, the vertical length available between the production slots and the packer/hanger, and the resolution required for the contact estimate.

The main objective of Lagunas Tapia et al. (2015) methodology is to allow a small amount of gas to enter the non-instrumented tubing tail through each orifice as they become exposed to the gas cap by means of the displacement of the gas-oil contact. In this way it can be concluded that the gas-oil contact position must be somewhere in the interval between the deepest orifice where exists evidence of gas inlet and the next orifice bellow it, giving a better idea of the movement of the contact in time; when the next orifice admits gas, it is assumed that the gas-oil contact has displaced somewhere between the new orifice admitting gas and the next one down along the tubing tail, a diagram displaying this completion design and methodology is shown in fig. 2.9 and fig. 2.10, where the same flowing well is analyzed at two different times, being the principal change between t_1 and t_2 the displacement of the DGOC down the reservoir, further exposing to gas cap gas additional witness orifices to those already exposed at t_1, and the physical response this displacement provokes inside the modified tubing tail installed in the well.

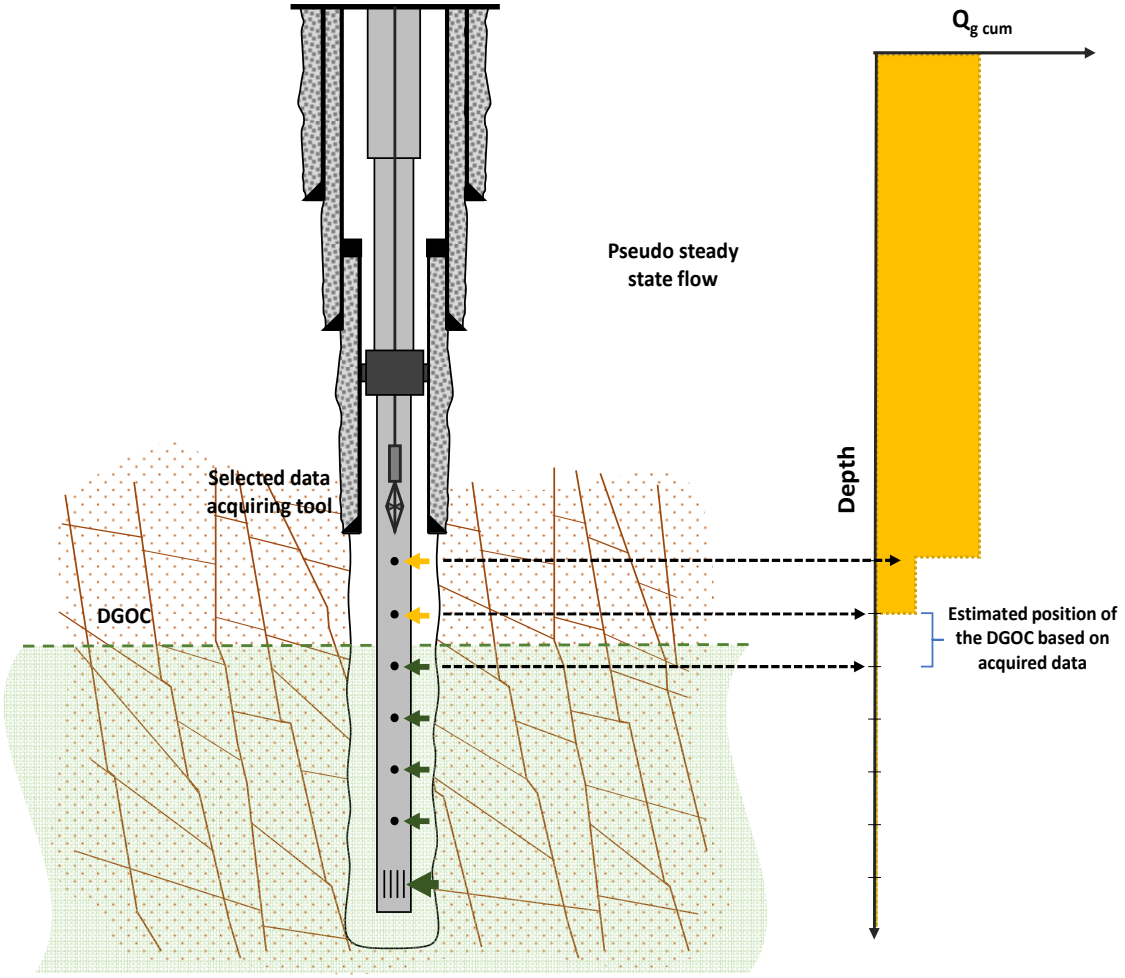

Fig. 2.9 – Completion design based on the GOC monitoring methodology by Lagunas Tapia et al. (2015) at t_1.

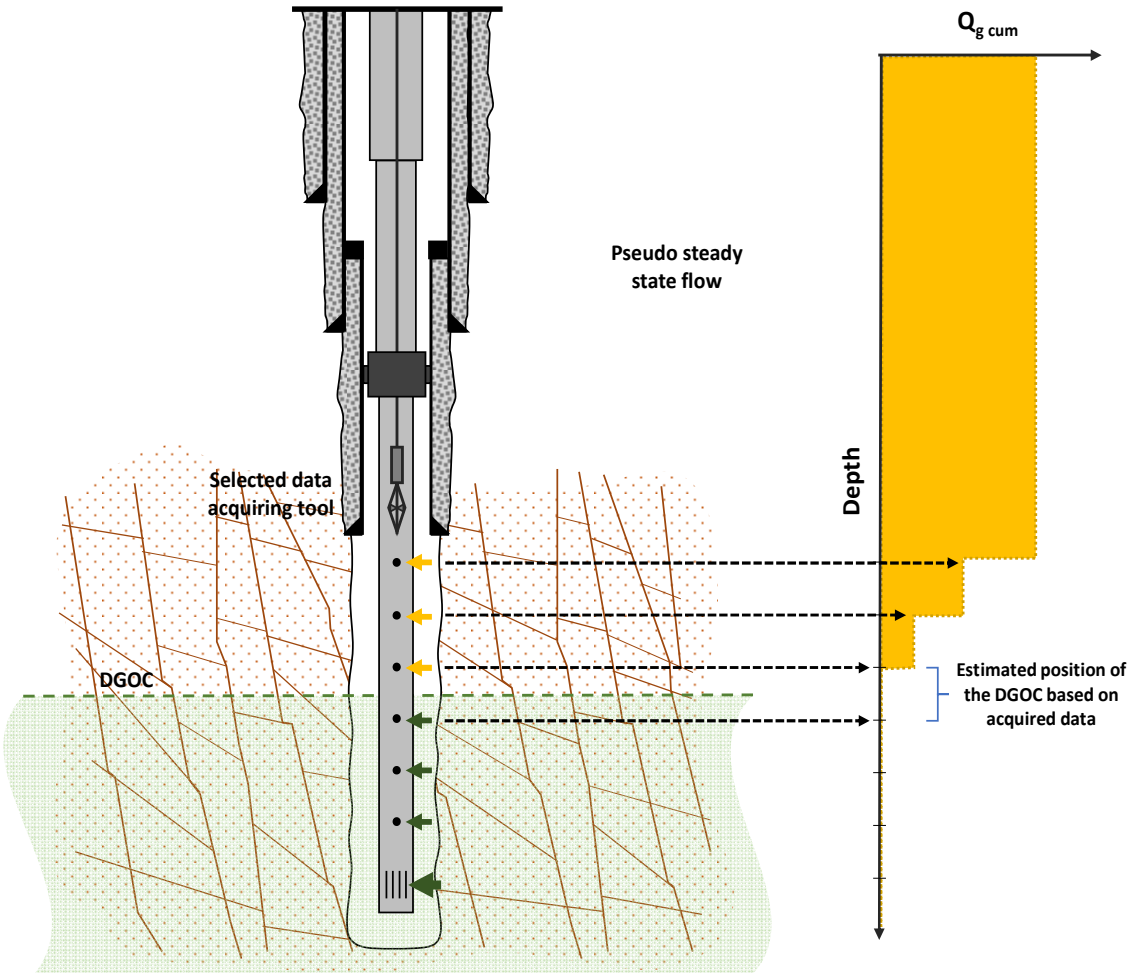

Fig. 2.10 – Completion design based on the GOC monitoring methodology by Lagunas Tapia et al. (2015) at t_2.

The easiest way to obtain the gas inlet evidence is to run wireline intervention tools like spinners, gradiomanometers and electric probes inside the tubing tail like those mentioned previously in this section, positioning them in front of every witness orifice in order to collect fluid rates and pressure data.

The additional gas production coming from the witness orifices in contact with the gas cap should not reduce the total liquid production since a design analysis is done beforehand, applying gas lift performance curves theory (Economides et al. 2012) fig. 2.11; The maximum gas-liquid ratio is calculated for the well conditions and then this value is used as the limit for the amount of total gas that cumulatively all the witness orifices should allow to enter the production tubing to achieve such maximum gas-liquid ratio and the corresponding production rate, in a scenario where every hole was exposed to the gas cap.

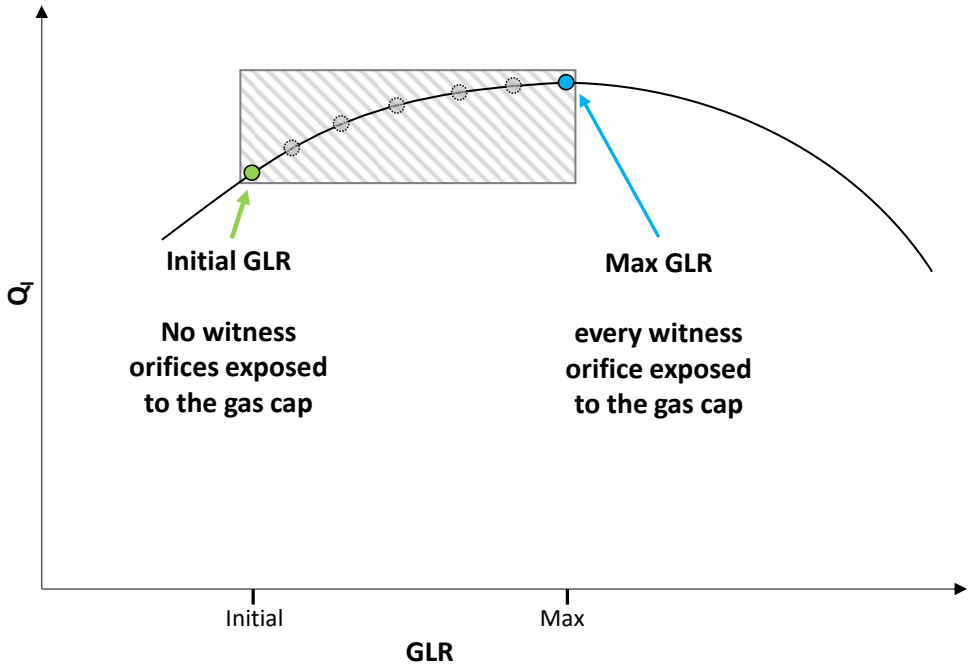

Fig. 2.11 – GLR vs liquid production rate example curve.

The main limitation regarding the use of this type of completion to monitor the DGOC is the reduced resolution that can be achieved without allowing too much gas into the well; this means that too many orifices will increase the resolution of the estimated interval, but will also increase the amount of gas entering the completion, while not enough orifices will result in an estimated interval allocating the DGOC so big that it basically invalidates the benefit of having the orifices perforated in the tubing tail.

2.5 Heat Capacity Ratio for Gases

The heat capacity ratio for gases (k) also known as specific heat ratio (Bahadori. 2012b), or adiabatic gas exponent (Szilas. 1985a), is an expression for the relation between two specific heat values of a gas under two different conditions, it is expressed as (Szilas. 1985b):

$$k = \frac{C_p}{C_v} \quad \text{---------- 2.1}$$

Where C_p is the specific heat of the gas at constant pressure and C_v is the specific heat of the gas at constant volume. The heat capacity ratio is relatively insensitive to changes in molecular weight or temperature within the family of gaseous hydrocarbons, for this reason is safe to make calculations assigning it a constant value (Szilas. 1985a).

For air usually the heat capacity ratio has a value of 1.4, while the heat capacity ratio for natural gas is around 1.28; if we calculate the critical pressure ratio for air and natural gas using the previously mentioned values, air critical pressure ratio has a value of 0.528 and natural gas critical pressure ratio has a value of 0.549 (Gould. 1974).

2.6 Compressible Flow Through Restrictions and Chokes

According to Majid et al. (2014-2015) the amount of fluid that can pass through an orifice in a pipe depend on the pressure differential existing across the orifice and the discharge coefficient for such hole, under pseudo-steady state flow, where such conditions remain fairly constant, the amount of fluid passing through the orifice should also remain constant.

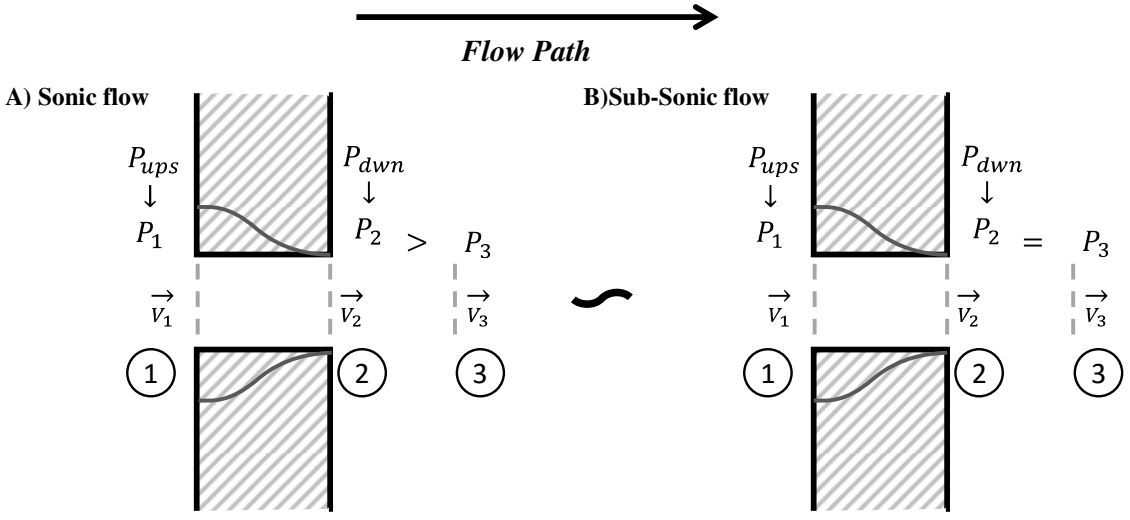

Fig. 2.12 – Nozzle/Choke schematic reference points for A) sonic flow B) Sub-sonic flow.

If the pressure differential is big enough when a gas flows through a choke, the fluid may be accelerated sufficiently to reach sonic velocity at position 2 of fig. 2.12 (Economides et al. 2012). Fluids exhibiting a velocity greater than the sonic velocity are considered under sonic flow behavior, where any downstream perturbation in unable to propagate upstream because the maximum velocity pressure perturbation can achieve is sonic velocity (Economides et al. 2012; Bahadori. 2012a), meaning that the mass flow rate will reach a maximum value dependent only of upstream parameters, independent of any change in pressure differentials (Bahadori. 2012a; Morris. 1996; Grace and Frawley. 2011), so any perturbation occurring downstream of the orifice will not affect upstream conditions (Nøkleberg and Søntvedt. 1998), this also means that pressure at location 2 in fig. 2.12 under sonic flow conditions will be greater than pressure at location 3 of that same figure (Kayser and Shambaugh. 1991). If the system is under sub-sonic flow and pressure P_1 upstream is increased parting from pressure P_2 downstream, the lowest pressure P_1 value at which sonic flow begins is known as the critical pressure P_{crit}, the differential between the P_{crit} upstream and the pressure P_2 downstream is known as the critical pressure differential "$P_{crit} - P_2$". The pressure relation at which gas flow achieves sonic flow is known as the critical pressure ratio "$(P_2/P_1)_c$" (where $(P_2/P_1)_c=(P_{dwn}/P_{ups})_c =(P_{dwn}/P_{crit})$), it is expressed as a function of the heat capacity ratio for gases (Szilas. 1985a):

$$\left(\frac{P_2}{P_1}\right)_c = \left(\frac{P_{dwn}}{P_{ups}}\right)_c = \left(\frac{2}{k+1}\right)^{\frac{k}{k-1}} \quad \text{---------- 2.2}$$

Based on the previous equation, table 2.1 shows the corresponding $(P_{dwn}/P_{ups})_c$ for a given set of the most common heat capacity ratio values:

k	$(P_{dwn}/P_{ups})_c$	k	$(P_{dwn}/P_{ups})_c$
1.49	0.514	1.29	0.548
1.48	0.515	1.28	0.549
1.47	0.517	1.27	0.551
1.46	0.518	1.26	0.553
1.45	0.520	1.25	0.555
1.44	0.522	1.24	0.557
1.43	0.523	1.23	0.559
1.42	0.525	1.22	0.561
1.41	0.527	1.21	0.563
1.40	0.528	1.20	0.564
1.39	0.530	1.19	0.566
1.38	0.532	1.18	0.568
1.37	0.533	1.17	0.570
1.36	0.535	1.16	0.572
1.35	0.537	1.15	0.574
1.34	0.539	1.14	0.576
1.33	0.540	1.13	0.578
1.32	0.542	1.12	0.581
1.31	0.544	1.11	0.583
1.30	0.546	1.10	0.585

Table 2.1 – Heat capacity ratio vs critical pressure ratio

For Sub-sonic flow behavior, the gas flow speed is less than the speed of sound, so pressure at location 2 in figure 2.12 under sub-sonic flow conditions will be equal to the pressure at location 3 of that same figure (Kayser and Shambaugh. 1991), it is concluded that gas flow rate for such conditions depends on the pressure differential across the choke, additionally any perturbation occurring downstream will have an impact on the upstream

pressure, becoming the pressure differential across the choke a parameter of mayor influence for the flow rate (Schuller et al. 2006). Fig. 2.13 shows the gas flow rate model at pressure differential ratios spanning sub-sonic and sonic flow regions, exposing the behavior it attains, dependent of the pressure ratio when flow is sub-sonic, and independent of pressure ratio when flow achieves a sonic velocity (Economides et al. 2012).

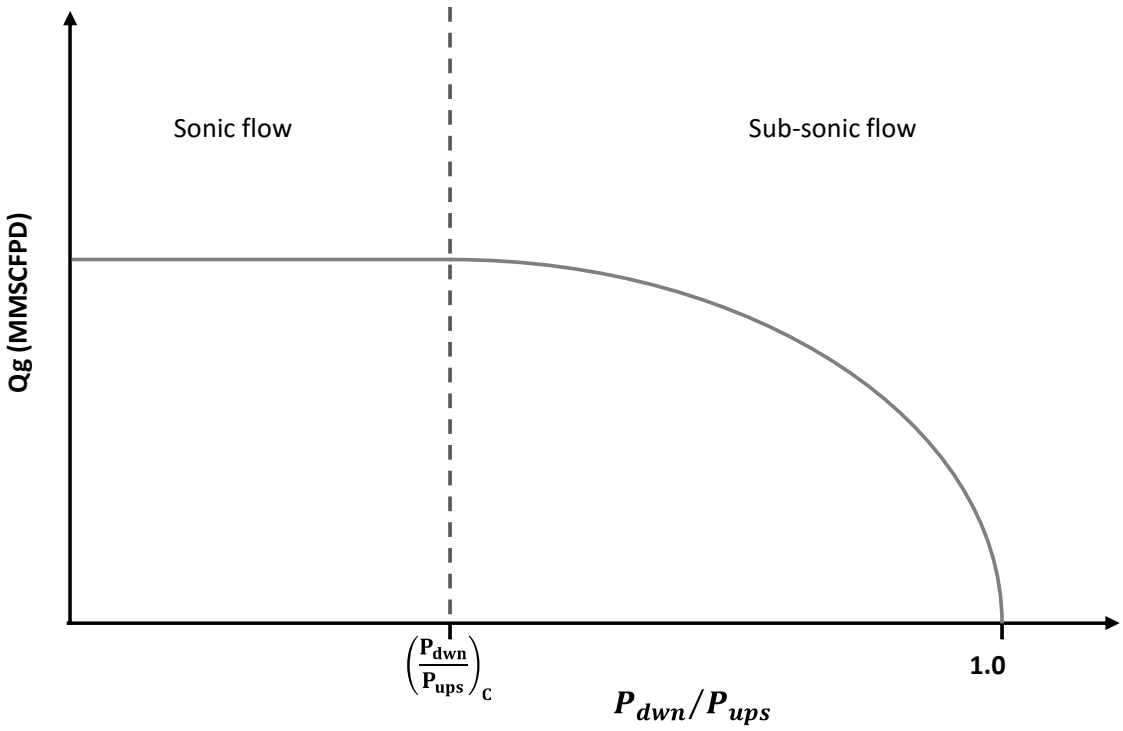

Fig. 2.13 – Pressure differential ratio vs gas rate curve behavior for sonic and sub-sonic flows

Bear in mind that even when the sonic gas flow rate velocity has become choked, we can still increase the mass flow rate by means of either decreasing the upstream temperature, or increasing the upstream pressure (Bahadori. 2012a; Bahadori. 2012b; Ashford and Pierce. 1975; Liu et al. 2007).

It is easily concluded from available literature that a universal equation does not exist for flow rates estimation across chokes that fits accurately all types of chokes and fluids passing through them (Bahadori. 2012a; Nøkleberg and Søntvedt. 1995), there exist many models to estimate choke flow behavior, depending on the fluid properties, sonic or subsonic flow and choke configuration, one model or another will be better suited to our specific scenario, and new studies are performed every day with the objective to improve current correlations.

The general form of many compressible gas flow equation models found in literature for flow through small round orifices have the following structure (Szilas. 1985a; Economides et al. 2012):

$$Q_g = \sqrt{2R}\frac{\pi}{4}d_{ch}^2 P_{ups}\frac{T_{sc}}{P_{sc}}C_D\sqrt{\frac{1}{MT_1}\frac{k}{k-1}\left[\left(\frac{P_{dwn}}{P_{ups}}\right)^{\frac{2}{k}}-\left(\frac{P_{dwn}}{P_{ups}}\right)^{\frac{k+1}{k}}\right]} \quad \text{---------- 2.3}$$

The general assumptions involving the derivation of the previous equation are mentioned here (Binder. 1958; Emanuel. 1986; Kayser and Shambaugh. 1991; Szilas. 1985a):

- Flow of an ideal gas.
- The gas has constant heat capacity.
- Isentropic, frictionless and adiabatic flow.
- The flow does not produce chemical reactions.
- There exists pseudo steady-state flow.

In this thesis we will make use of the form of the equation for compressible gas flow through small round orifices using field units:

$$Q_g = (3.505) C_D d_{64}^2 \frac{P_{ups}}{P_{sc}} \sqrt{\frac{1}{\gamma_g T}} \sqrt{\frac{k}{k-1}\left[\left(\frac{P_{dwn}}{P_{ups}}\right)^{\frac{2}{k}} - \left(\frac{P_{dwn}}{P_{ups}}\right)^{\frac{k+1}{k}}\right]} \quad \text{---------- 2.4}$$

Equation 2.4 is governed by the critical pressure ratio (equation 2.2), the usual methodology to calculate the gas flow rate using these equations requires for the critical pressure ratio to be calculated first using equation 2.2, if P_{ups} and P_{dwn} are known we check if the pressure ratio P_{dwn}/P_{ups} is bigger or smaller than the critical pressure ratio, when pressure ratio P_{dwn}/P_{ups} is bigger than the critical pressure ratio then equation 2.4 can be used as it is written, but if pressure ratio P_{dwn}/P_{ups} is equal or smaller than the critical pressure ratio, then the pressure ratio P_{dwn}/P_{ups} must be replaced in every term of equation 2.4 for the critical pressure ratio $(P_{dwn}/P_{ups})_c$, due to the fact that under sonic flow conditions the flow rate will be insensitive to any perturbation or change in the pressure downstream; such

setting for sonic flow conditions results in the following equation (Szilas. 1985a; Economides et al. 2012):

$$Q_g = (3.505)C_D d_{64}^2 \frac{P_{ups}}{P_{sc}} \sqrt{\frac{1}{\gamma_g T}} \sqrt{\frac{k}{k-1}\left[\left(\frac{P_{dwn}}{P_{ups}}\right)_c^{\frac{2}{k}} - \left(\frac{P_{dwn}}{P_{ups}}\right)_c^{\frac{k+1}{k}}\right]} \text{ ---------- } 2.5$$

Fig. 2.14 has been created using the previous methodology, for different choke diameters, displaying the sonic and sub-sonic flows; it is clear from fig. 2.14 that when pressure ratios are smaller than the critical pressure ratio for the same flow conditions, the gas flow rate depends only on the choke diameter and the pressure upstream of the choke (Szilas. 1985a).

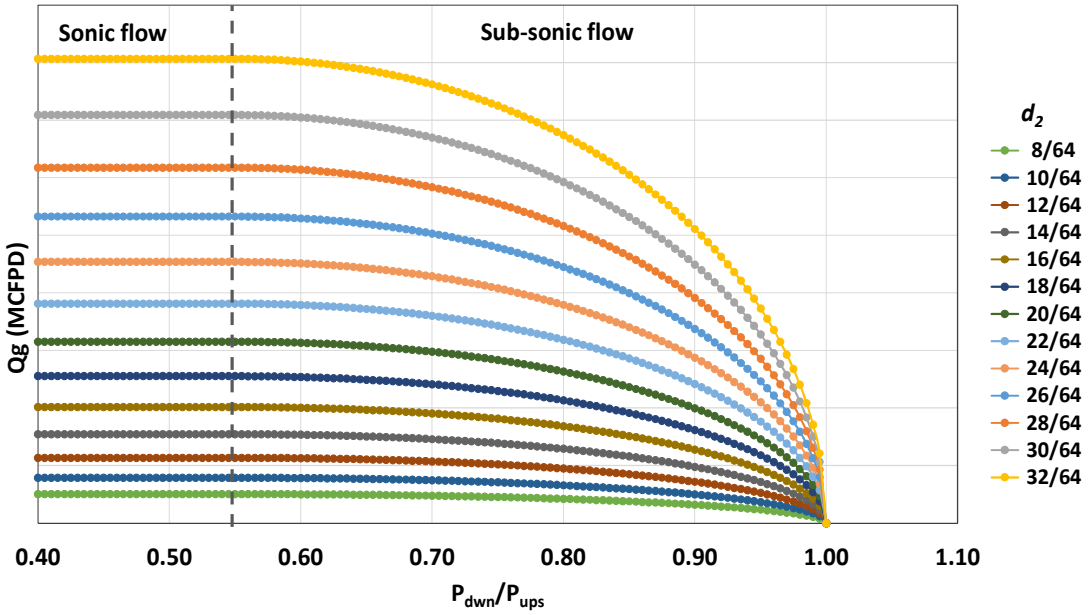

Fig. 2.14 – Pressure differential ratio vs gas rate.

One last comment worth mentioning regarding compressible flow through small orifices is that according to (Fortunati. 1972; Nejatian et al. 2014), pressure and temperature conditions for fields currently under exploitation are most likely to result in wells operating at sub-sonic flows.

2.7 Orifice Geometries

Different orifice and nozzle geometries have been developed in the literature, depending on the requirements some are better that others, usually the designs aim to achieve sonic stabilized flow with the minimum pressure differential across the orifice or nozzle.

The shape and geometry of an orifice greatly affects the behavior and conditions of the compressible flow across it. Taking for example small diameter orifices, the length to diameter ratio, also known as the plate thickness to diameter ration, affects the compressible flow through a small straight bore orifice since the vena contracta may develop within the length of the orifice, changing the actual flow behavior compared to larger diameter orifices at similar conditions (Kayser and Shambaugh. 1991).

Two types of geometries are presented in this work, their selection was based on their simplicity, characteristics, known influence and behavior over compressible flow conditions and easiness of implementation; the first type is the straight-bore orifice, the second type is the sharp or knife-edge orifice, such geometries are presented in Fig. 2.15:

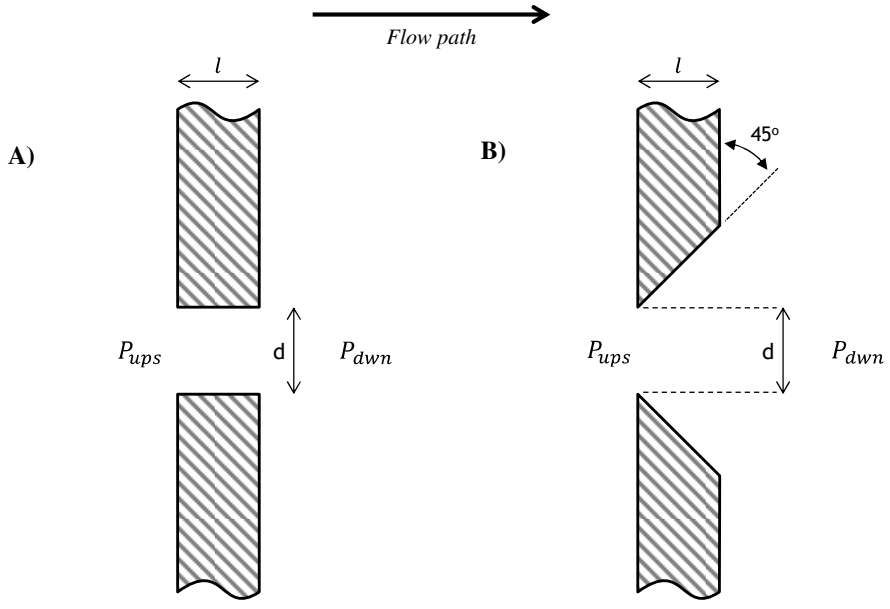

Fig. 2.15 – Cross-section of orifice geometries A) straight-bore orifice B) sharp-edge orifice.

It is worth mentioning that for the knife-edge orifices, incredibly sharp edges are not optimal because they tend to deteriorate easily; based on (Kayser and Shambaugh. 1991) flow experiment for this type of orifices have used edges of 25 μm flat surfaces parallel to the flow without signs of deterioration.

When the orifices are designed at a non-flat surface, like the side-wall of a pipe, the ratio between the orifice diameter "d" and the pipe diameter "D" will greatly affect the shape of the vena contracta, with larger d/D ratios the shape of the vena contracta will deform increasing the error of flow rate predictions, while having small d/D ratios will give the vena contracta a shape that approaches to that of a circle, increasing the accuracy of the flow rate estimations (McLemore et al. 2013).

2.8 Discharge Coefficients for Orifices and Nozzles

The discharge coefficient C_D can be defined as the representation of the relationship between the measured or actual mass flow rate through an orifice and the calculated isentropic, adiabatic mass flow rate through the orifice under identical upstream temperature, upstream pressure, and pressure drop across the orifice (Guo et al. 2011; Kayser and Shambaugh. 1991), another excellent description defines the discharge coefficient as the ratio of the mass flow rate at the orifice area and the mass flow at the vena contracta area, accounting for the difference in geometrical flow area to effective flow area (Grace and Frawley. 2011). It usually is expressed as:

$$C_D = \frac{\dot{m}_{actual}}{\dot{m}_{isen,adiab}} \quad \text{---------- 2.6}$$

Given the following expressions for the mass flow rate and the volumetric flow rate:

$$\dot{m}_{isen,adiab} = q_g * \rho_g \quad \text{---------- 2.7}$$

$$Q_g = \sqrt{2R} A_2 P_{ups} \frac{T_{sc}}{P_{sc}} \sqrt{\frac{1}{MT_1} \frac{k}{k-1} \left[\left(\frac{P_{dwn}}{P_{ups}} \right)^{\frac{2}{k}} - \left(\frac{P_{dwn}}{P_{ups}} \right)^{\frac{k+1}{k}} \right]} \quad \text{---------- 2.8}$$

Where for round shaped orifices:

$$A_2 = \frac{\pi}{4} d_{ch}^2 \quad \text{---------- 2.9}$$

Resulting in:

$$\dot{m}_{isen,adiab} = \sqrt{2R} \frac{\pi}{4} d_{ch}^2 P_{ups} \frac{T_{sc}}{P_{sc}} \rho_g \sqrt{\frac{1}{MT_1} \frac{k}{k-1} \left[\left(\frac{P_{dwn}}{P_{ups}} \right)^{\frac{2}{k}} - \left(\frac{P_{dwn}}{P_{ups}} \right)^{\frac{k+1}{k}} \right]} \quad \text{----------2.10}$$

The final form of the expression to calculate the discharge coefficient for round shaped orifices takes the following form:

$$C_D = \frac{\dot{m}_{actual}}{\sqrt{2R}\frac{\pi}{4}d_{ch}^2 P_{ups}\frac{T_{sc}}{P_{sc}}\rho_g \sqrt{\frac{1}{MT_1}\frac{k}{k-1}\left[\left(\frac{P_{dwn}}{P_{ups}}\right)^{\frac{2}{k}} - \left(\frac{dwn}{P_{ups}}\right)^{\frac{k+1}{k}}\right]}} \quad \text{----------2.11}$$

A variation of an excellent procedure given by (Kayser and Shambaugh. 1991) to apply the aforementioned equation, where is assumed that the pressure, temperature and actual mass flow rate are measured parameters, is detailed as follows:

- If the heat capacity ratio k is not going to be assumed as constant, it has to be calculated at the upstream temperature T_1.
- Calculate the critical pressure ratio $(P_{dwn}/P_{ups})_c$ using the heat capacity ratio from the previous step.
- We check if the pressure ratio P_{dwn}/P_{ups} is bigger or smaller than $(P_{dwn}/P_{ups})_c$, if pressure ratio P_{dwn}/P_{ups} is equal or smaller than the critical pressure ratio, then the pressure ratio P_{dwn}/P_{ups} must be replaced in every term of equation 2.11 for the critical pressure ratio $(P_{dwn}/P_{ups})_c$.
- If possible accurate measurements of either the area or the diameter of the orifice have to be conducted at a reference temperature and adjusted by the thermal expansion at conditions of T_1.
- With all the elements required, fill the equation and calculate the value of the discharge coefficient for the given flow conditions.

As an alternate method, the discharge coefficient can also be described by the following equation (McLemore et al. 2013):

$$C_D = C_C * C_V \quad \text{----------2.12}$$

Where the reduction of flow jet area at the vena contracta is accounted for the coefficient of contraction C_C, and the coefficient of velocity C_V accounts for the ratio between the actual flow velocity and the ideal flow velocity, this way of calculating the discharge coefficient won't be required during the development of the present thesis and is just presented as an alternative for future works.

Flow orifices are widely used in the industry, depending on the allocation of the orifice either being across a pipe, in a plate, at the lateral wall of a pipe, or otherwise; they are generally influenced by different aspects (Hüning. 2010):

- Radius or chamfer at the inlet and outlet.
- Friction, specifically the Reynolds number.
- Angle of the orifice with respect to the inlet and outlet surface.
- Geometry of the cross-section of the orifice.
- The D/d or d/D ratios when applicable (usually for cross-pipe orifices).
- The l/d ratio when applicable (usually for lateral pipe-wall or plate orifices where D/d is not available).

- Pressure differential across the orifice.
- Inlet and outlet flow obstructions or direction changes.
- Cross-flow at inlet and outlet.

The correct characterization of an orifice behavior is of great importance if accurate measurements and monitoring are to be conducted; Manufacturers used to conduct flow experiments and develop orifice discharge coefficients or empirical relationships that were generally proprietary and not always distributed, this has caused in the past a great deal of uncertainty between buyers and sellers when different manufacturers meters were used, deriving in the establishment of the Gas Measurement Committee, which has done extensive orifice research (Fling. 1988); in addition to the Gas Measurement Committee, many have been the research groups, Universities and individuals involved in the research and development of studies focused on the characterization of the orifice discharge coefficient. Nowadays leading manufacturers provide technical information, test data, sizing catalogs, calculator programs, etc. that result in better estimations (Emerson Process Management Technologies. 2015).

According to (Hüning. 2010) there are 2 methods to characterize the orifice discharge coefficient in order for us to be able to replicate its behavior and take advantage of that replicating it for computer applications, the first method to characterize C_D is to plot measured experimental data and proceed to do a curve fitting to such data, by finding fitting mathematical expressions, which are most suitable for scaling factors in between

the minimum and maximum experimental data points; the second one consist in developing an actual physical model conception of all the parameters and flow physics and adjusting it by means of matching factors to experimental data.

The available literature reviewed displays both methodologies, for the purpose of this research we will be making use of correlations for C_D based on the first methodology (Kayser and Shambaugh. 1991).

Many studies have been done regarding the analysis of the discharge coefficient, (Kayser and Shambaugh. 1991) studied the specific case of the discharge coefficient behavior for compressible flow through small-diameter orifices and convergent nozzles, four different geometries where tested, in this work we will focus on the premises of their studies and the results and conclusions achieved for two of those geometries, the straight-bore orifices, and the sharp-edge orifices.

The main objectives of (Kayser and Shambaugh. 1991) were to obtain and present experimental data of the compressible flow through small-diameter orifices and convergent nozzles and plot the flow data against multiple dimensionless parameters so important data behaviors could be isolated, studied, and if possible modeled. Their experiments span a range of 4 different geometries, elliptical entry nozzles, rounded entry nozzles, straight-bore orifices, and sharp-edge orifices, each one tested using 4 different orifice diameters, for a total of 16 different elements; the experiments were performed at

different temperatures ranging from 295 to 700 K; The flow across the orifices and nozzles was conducted using Mono-, di- and triatomic gases whose molecular weights ranged from 4 to 44, characterized by heat capacity ratios going from 1.28 to 1.67. The characteristics of the gas used in the experiments performed by (Kayser and Shambaugh. 1991) are relevant to us since natural gas properties fall right into the spectrum of the tested gases; natural gas, depending on the reservoir usually has a molecular weight close to 19, (Economides et al. 2012) propose a molecular weight for natural gas of 18.92 and a gas gravity(to air) of 0.65 when there is a lacking data regarding detailed composition of a natural gas, additionally to this data (Bahadori. 2012b; Gould. 1974) specify a heat capacity ratio around 1.28 for natural gas.

The resulting data of (Kayser and Shambaugh. 1991) for the experiments on straight-bore orifices and sharp-edge orifices has been extracted from their graphs as accurately as possible, in order to generate the graphs presented here; (Kayser and Shambaugh. 1991) implement in their results the "dimensionless pressure drop" term in order to better isolate flow behaviors, and it is defined as the ratio between the current pressure differential $\left(P_{ups} - P_{dwn}\right)$ and the critical pressure differential $(P_{crit} - P_{down})$:

$$Dim.Press.Drop = \frac{(P_{ups} - P_{dwn})}{(P_{crit} - P_{dwn})} \quad \text{----------2.13}$$

It is clear then, that when the dimensionless pressure drop is greater than 1.0 the pressure differential across the orifice is greater than the critical pressure differential and the fluid

going across the orifice will achieve sonic flow, if the dimensionless pressure drop is lower than 1.0 then the fluid going across the orifice will do so at sub-sonic flow.

The experiments done by (Kayser and Shambaugh. 1991) on sharp-edge orifices gave the following results:

- Fig. 2.16 shows how the discharge coefficient is virtually independent from temperature or orifice diameter when plotted against the dimensionless pressure drop.

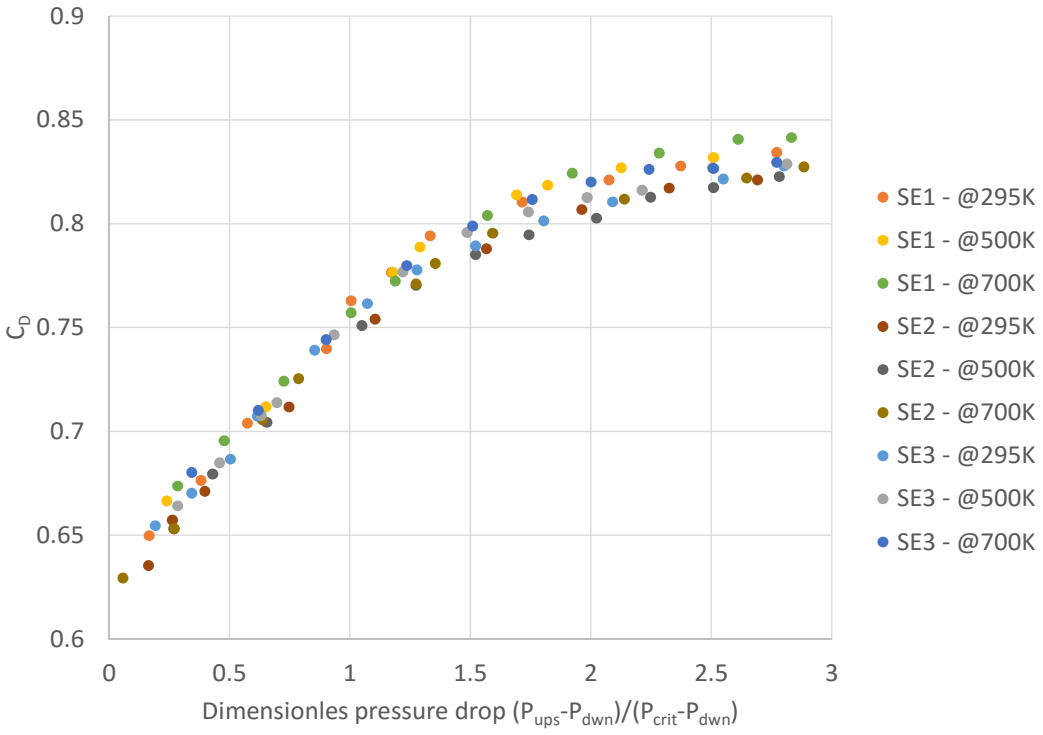

Fig. 2.16 – C_D for sharp-edge orifices at different upstream temperatures and diameters flowing the same gas. Reprinted with permission from Kayser and Shambaugh, 1991.

- Fig. 2.17 shows how the discharge coefficient is virtually independent from the gas composition when plotted against the dimensionless pressure drop, at least for the range of gases used in their experiments:

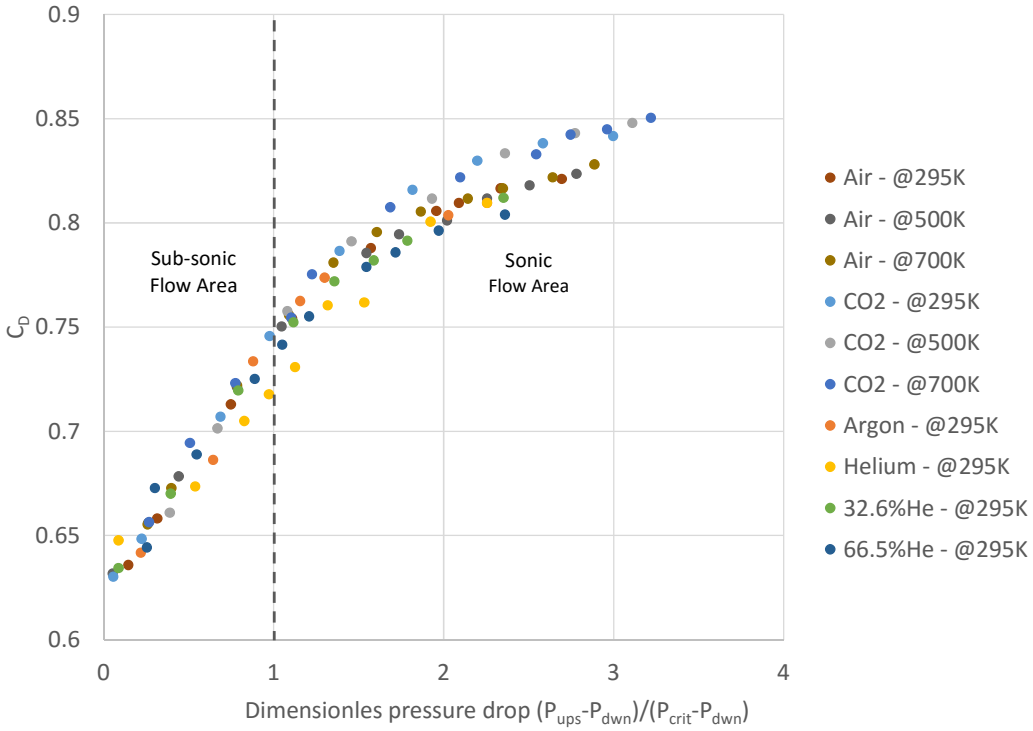

Fig. 2.17 – C_D for a sharp-edge orifice with different upstream temperatures and gas compositions. Reprinted with permission from Kayser and Shambaugh, 1991.

- From fig. 2.17 it becomes evident that the subsonic area data from the tests is well correlated to the dimensionless pressure drop, fig. 2.18 shows in detail data in the subsonic area for three sharp-edge orifices with different diameters, tested at different

temperatures using different gas compositions, the data is complemented with a best-fit line correlation that can be used confidently to calculate the discharge coefficient, based on the pressure differential, independently of the gas composition, the temperature, or the orifice diameter, as long as the calculation parameters fall inside of those covered by the experiment performed to obtain such correlation; according to Kayser and Shambaugh(1991) the discharge coefficient fitted correlation is expressed as:

$$C_D = 0.120\left(\frac{P_{ups}-P_{dwn}}{P_{crit}-P_{dwn}}\right) + 0.626 \quad \text{----------2.14}$$

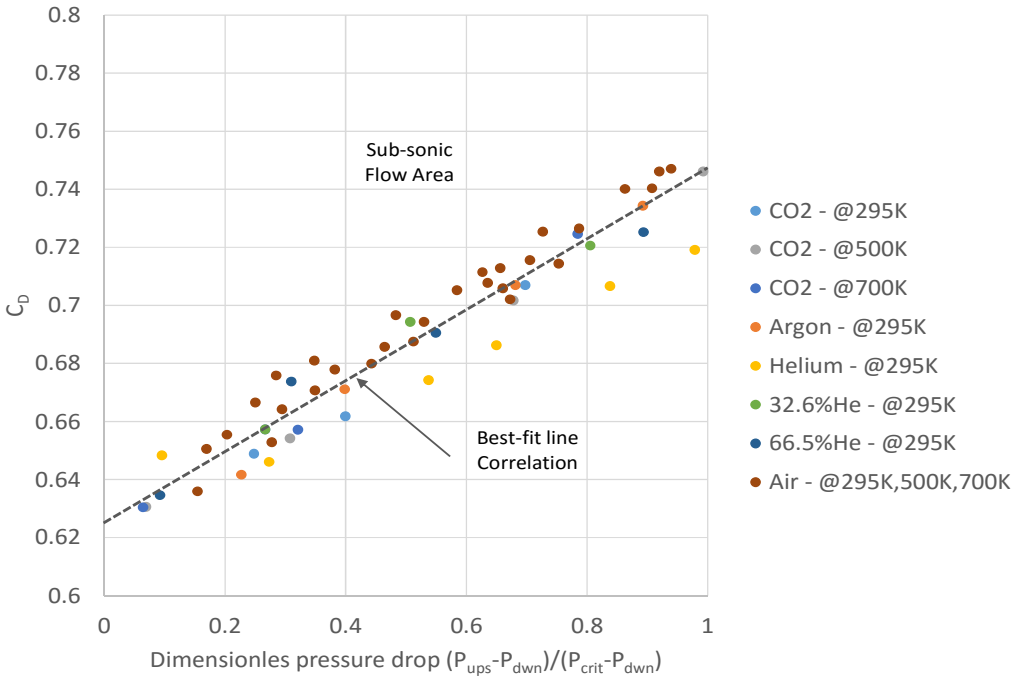

Fig. 2.18 – C_D for multiple sharp-edge orifices with different upstream temperatures and gas compositions at sub-sonic flow conditions. Reprinted with permission from Kayser and Shambaugh, 1991.

- When plotting the discharge coefficient against the throat Reynolds number (fig. 2.19) (Kayser and Shambaugh. 1991) observed that for compressible flow through sharp-edge orifices the discharge coefficient does not show a good correlation with the throat Reynolds number, from the previous results they concluded that while the Reynolds number is usually correlated to the discharge coefficient for incompressible flow, it will not show a correlation to the discharge coefficient for compressible flow when large expansions occur across the sharp-edge orifices.

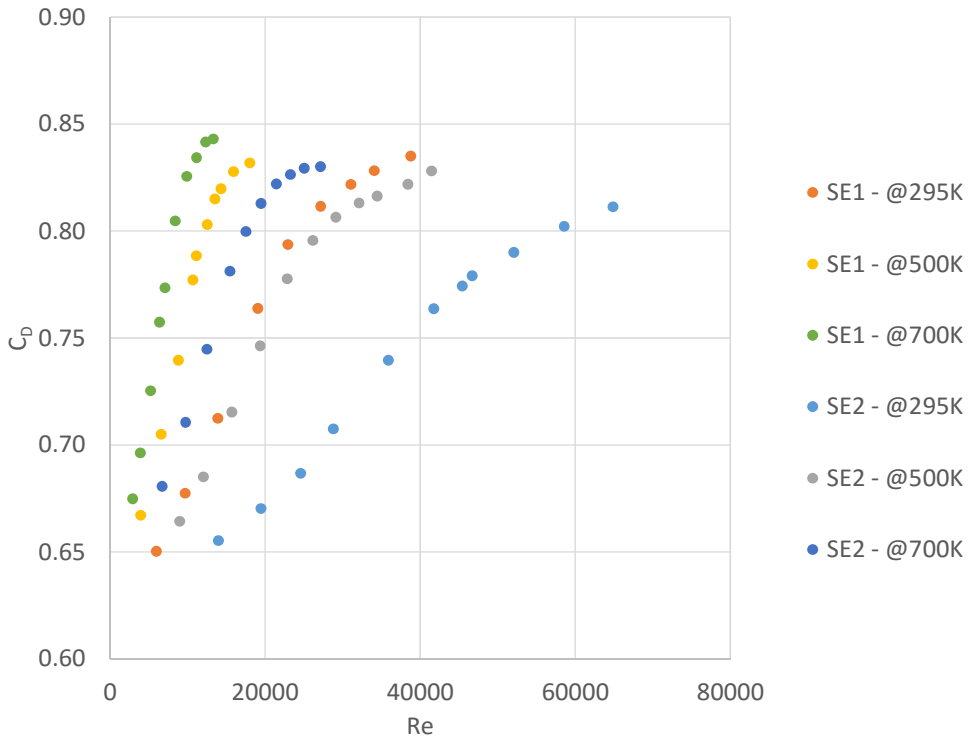

Fig. 2.19 – Reynolds number vs discharge coefficient. Each color represents different orifice diameter at different temperatures. Reprinted with permission from Kayser and Shambaugh, 1991.

Moving to the next orifice geometry of interest for the purposes of the present thesis, the experiments done by (Kayser and Shambaugh. 1991) on straight-bore orifices gave the following results:

- As the length to diameter ratio of the straight-bore orifice is increased, it gradually tends in an unpredictable transition towards a quasi-constant discharge coefficient of ~0.85 at a length to diameter ratio of 1.9, as displayed on Fig. 2.20 where data taken from the experiments performed flowing one gas composition at one temperature through plates with the same bore diameter but increasing length is shown:

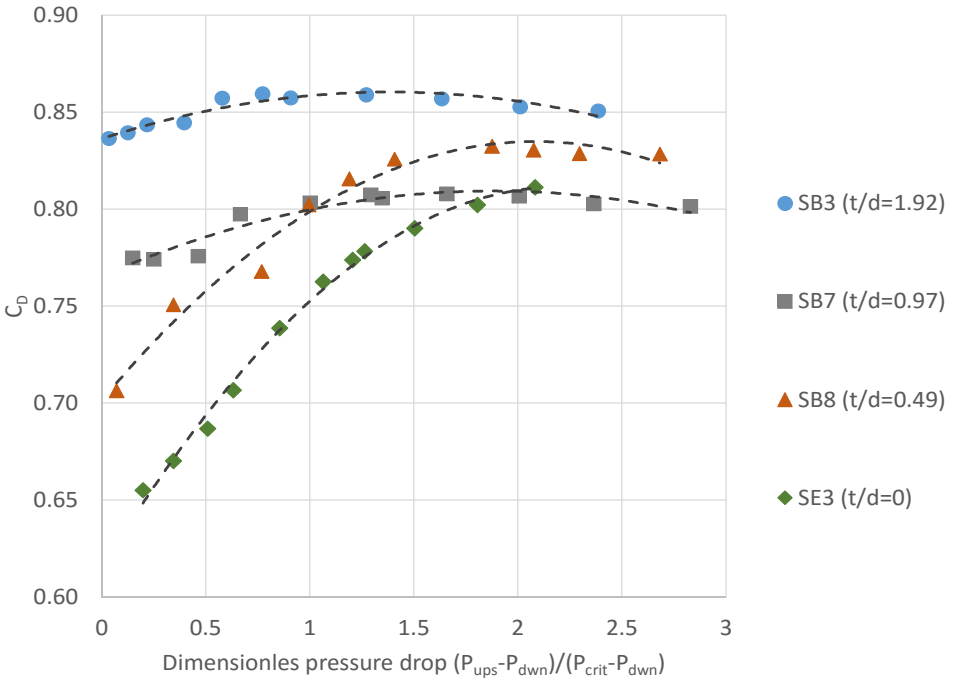

Fig. 2.20 – C_D against the dimensionless pressure drop for straight-bore orifices, complemented by polynomial fits. . Reprinted with permission from Kayser and Shambaugh, 1991.

- From the data obtained performing experiments on 3 plates with different straight-bore diameters and same thickness using multiple gas compositions at different temperatures (Kayser and Shambaugh. 1991) concluded that the C_D profile is basically not affected by temperature changes, the mentioned data is displayed in fig. 2.21 where C_D has been plotted against the pressure differential ratio P_{ups}/P_{dwn}, they concluded from this image that the discharge coefficient basically stays constant for length to diameter ratios above 1.0.

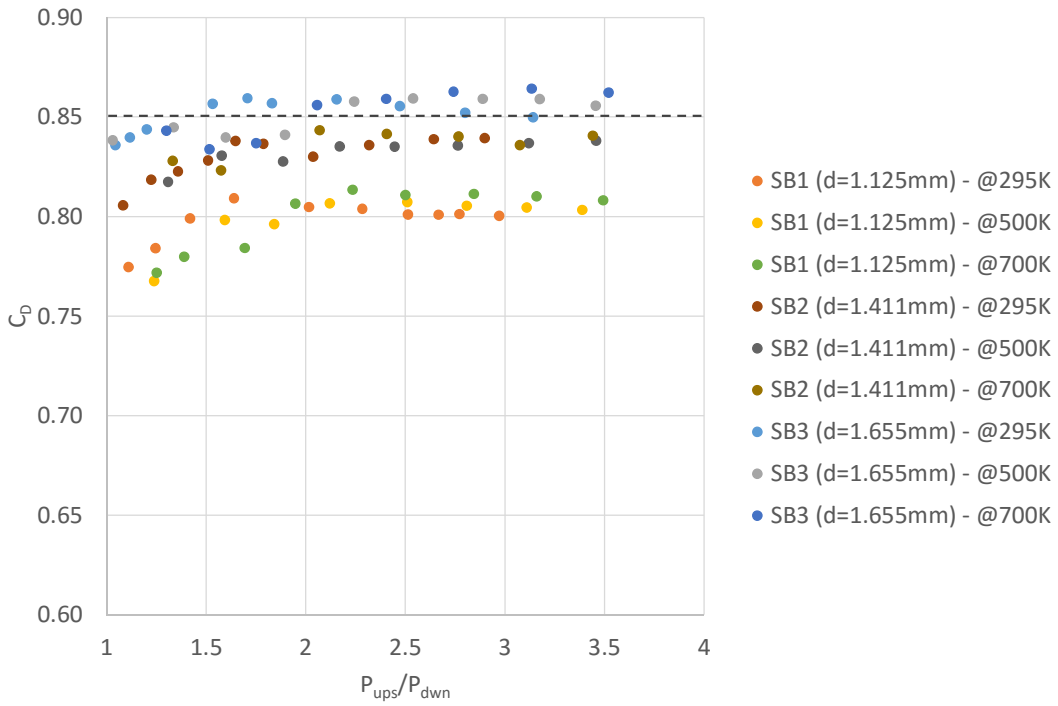

Fig. 2.21 – C_D against the pressure drop ratio Pups/Pdwn, highlighting the flattening of C_D at 0.85. Reprinted with permission from Kayser and Shambaugh, 1991.

- Finally, they also concluded that the relationship between change in gas composition and the discharge coefficient is fairly weak, this conclusion can be observed in fig. 2.22, where data from the experiments performed on a single plate flowing different gas compositions at the same temperature is displayed:

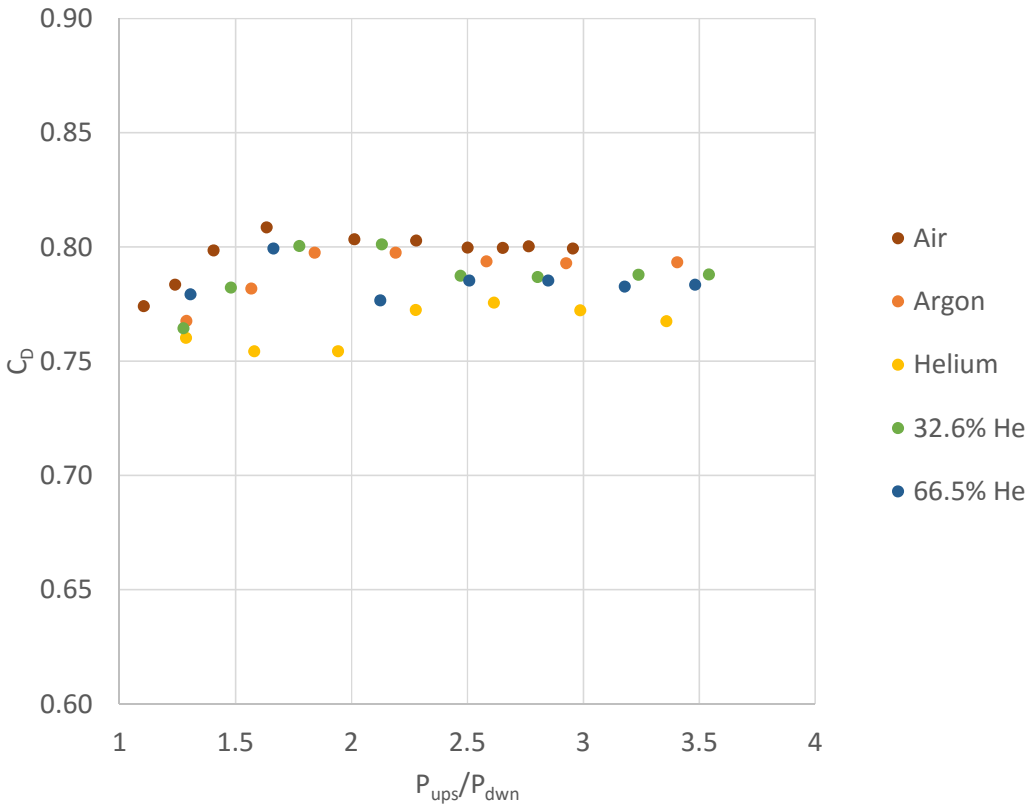

Fig. 2.22 – C_D against the pressure drop ratio Pups/Pdwn. Reprinted with permission from Kayser and Shambaugh, 1991.

The experiment performed by (Kayser and Shambaugh. 1991) gives us a solid base to characterize the discharge coefficient behavior under different geometries and flow conditions; as they state, their results allow to confidently apply the calibration of a small orifice performed with one gas to other gases not mattering variations in temperatures. It is also important to note that for straight-bore orifices, they demonstrated that for the range applicable to gases and temperatures used in their study the discharge coefficient remains almost constant in subsonic and sonic flow when larger length to diameter ratios are designed for the orifices.

2.9 Fluid Gradients Calculation

When analyzing bottom hole pressure data it is very important to be familiar to fluid gradients theory, in order to take advantage of the information that can be obtained from the different fluids present in a well; there exist two different types of gradients, depending on the flowing conditions of the well; when the well is flowing, pressure metering at different depths will result in a flowing gradient. If by the contrary the well is shut in, and enough time has passed allowing for the pressure to stabilize, pressure metering at different depths will result in a static gradient (Onyekonwu. 1997).

For a two point metering survey where only exists one fluid, like in fig. 2.23, to calculate the fluid gradient between the two points metered we use the following expression:

$$Grad = \frac{P_2 - P_1}{TVD_2 - TVD_1} \quad \text{----------2.15}$$

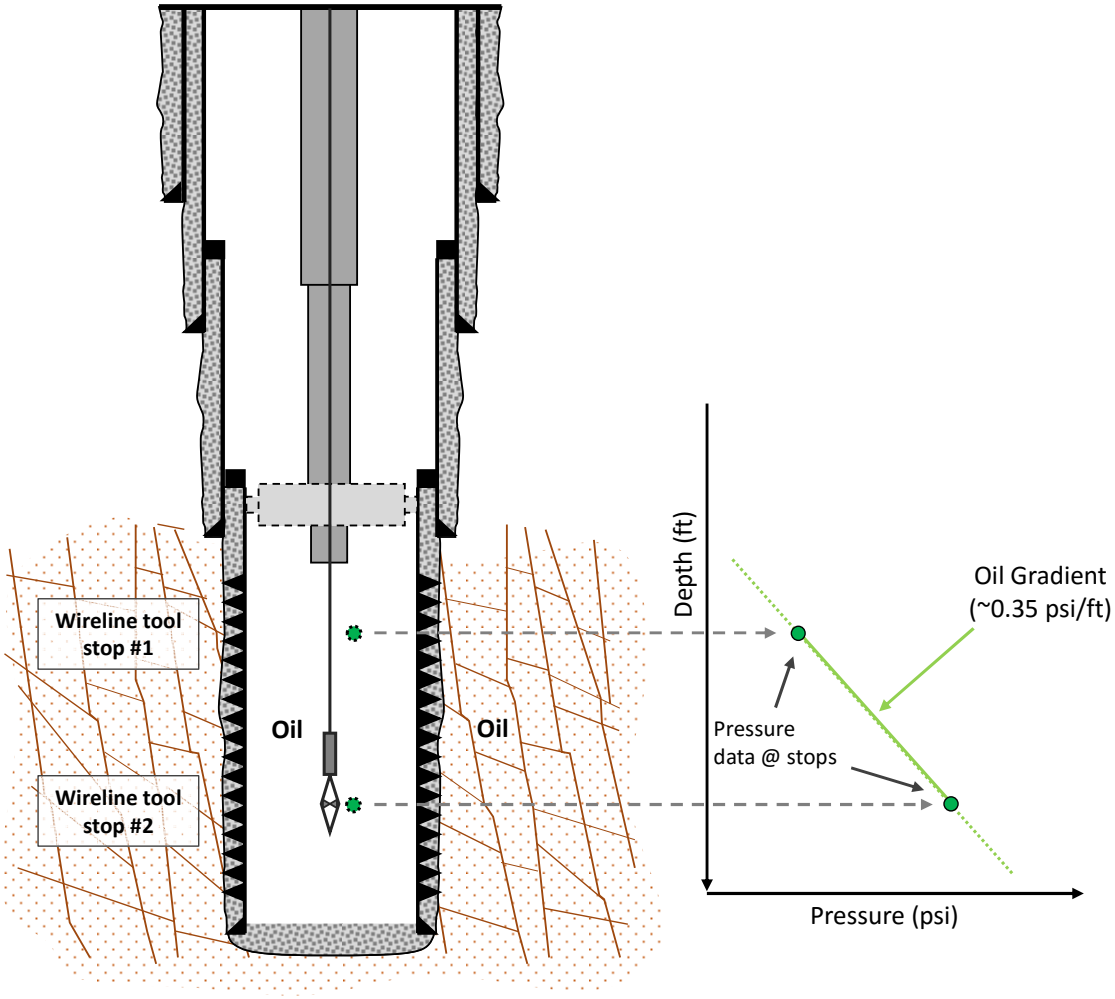

Fig. 2.23 – Diagram of a closed well with a pressure survey at 2 stops.

When we are surveying a well that crosses a fluids contact like the gas oil contact, as stated by (Onyekonwu. 1997), in order to correctly determine the fluid contact position using a

gradient survey at least 2 stops have to be performed in each phase as the gauge travels across the well total depth (fig. 2.24), this will allow for each fluid gradient to be calculated and extrapolated, using a graphical methodology like the one in fig. 2.24 each depth where the gradients extrapolation cross is determined to be the depth of the fluids contacts. If the fluids are well characterized beforehand and their fluid gradients are already known, one pressure point should be enough to use as reference point to estimate the fluids contact depth.

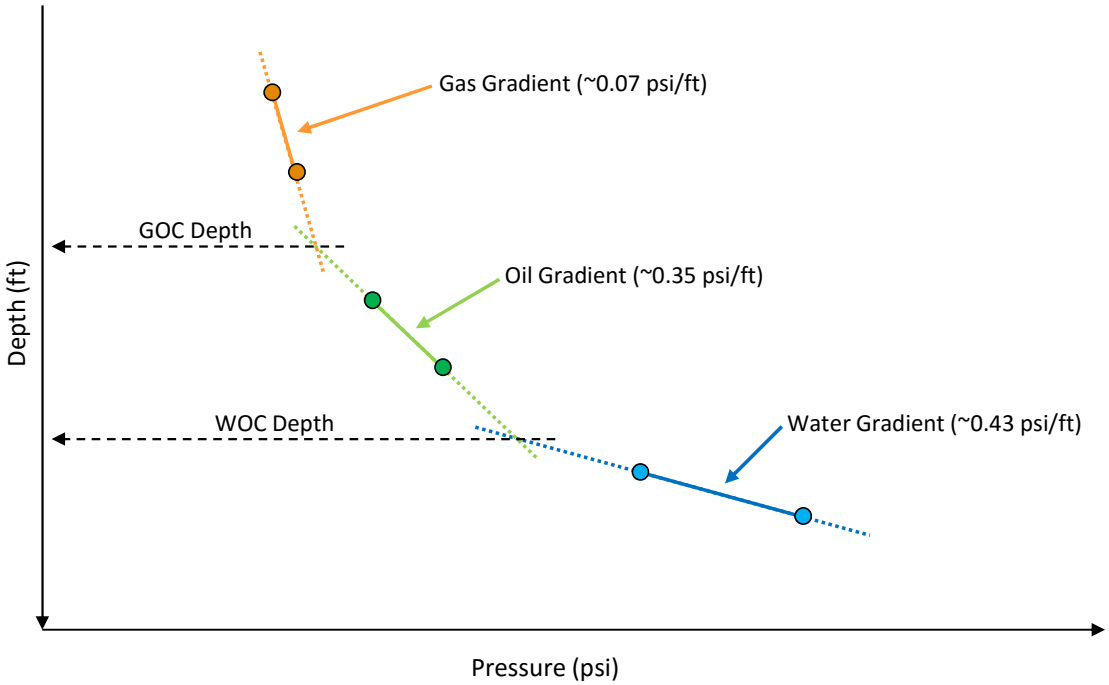

Fig. 2.24 – Gradients and Fluid contacts estimation based on a pressure survey with two stops on each fluid in a gas/oil/water well.

There are some cases when a survey cannot be run all the way to the bottom of a well, if the pressure needs to be obtained at a depth outside of the survey range, it can be extrapolated using a mathematical correlation as long as pressure data is available for another depth inside the same fluid interval and that fluid gradient is also known (Onyekonwu. 1997), if extrapolating bellow the known pressure data acquired depth:

$$P_{@required-depth} = P_{@gauge-depth} + \left(Grad_{fluid} * \Delta z\right) \text{ ----------2.16}$$

If extrapolating above the known pressure data acquired depth:

$$P_{@required-depth} = P_{@gauge-depth} - \left(Grad_{fluid} * \Delta z\right) \text{ ----------2.17}$$

Pressure surveys performed in an open-hole well were direct connection to the reservoir is available are an excellent source of pressure data for reservoir datum pressure monitoring (Onyekonwu. 1997), the usual procedure consist on transporting the pressure measured at the gauge depth inside a well to the reservoir datum depth using the equation 2.16 or 2.17 depending on the relative position of the datum depth to the measured pressure depth. With the previous statements in mind, it becomes relevant that knowing the actual vertical position of the measurements is of primordial importance, since any variation in depth will affect the fluid gradients and directly change the pressure data extrapolated (Onyekonwu. 1997).

3. PROPOSED METHODOLOGY

3.1 Current Background, Limitations, Problem Analysis and General Assumptions

The oil industry has gradually evolved to an integral philosophy that aims not only to find and produce hydrocarbons for a revenue, but to do so in a way that optimizes the resources required to accomplish such goal, while securing the safety of the people developing these projects, and making an effort to minimize the environmental damage, applying multidisciplinary approaches to solve the increasingly complex problems that current hydrocarbon reservoirs imply.

A core pillar of such philosophy is the continuous field monitoring, a very wide term that usually spans, but is not limited to, from the hydrocarbon reservoir to the end of the line of the production transport tubing at the surface that gathers the field production and transports it either outside of the field or to a collecting vessel to be stored and transferred or processed later.

A field monitoring philosophy has multiple advantages, including the reduction of uncertainties and risks that have to be continuously evaluated and included into the equation before any action regarding the operation or development of a field can be taken.

A very specific component of the field monitoring practice is the surveillance of the movement of the gas-oil contact depth inside a producing or monitoring well through time; knowing the position of the gas-oil contact allows the reservoir and production engineers to have a better understanding of the fluid dynamics governing the interaction between the "near well reservoir rock" and the well completion installed; the engineers can apply this knowledge to estimate a well productive life expectancy, to monitor the thinning of the oil rim during the exploitation of the reservoir, or to use the data as a reference point when designing a future well completion in the same production area, among other uses; this knowledge can also help reservoir and simulation engineers to improve the characterization of the reservoir behavior under specific conditions, and design future field development and operating plans to optimize the exploitation of the reservoir.

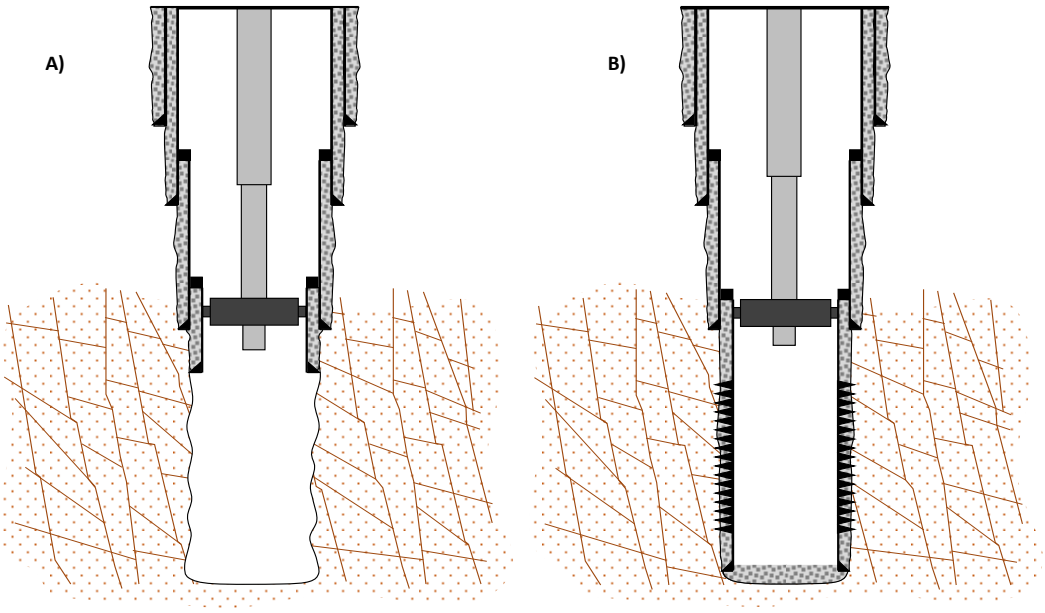

Fig. 3.1 – A) Open-hole completion B) Cemented and perforated completion.

The surveillance methodology selected to monitor the fluid level inside a producing well depends on the type of well completion, some of the most common well completion types that allow a fluids monitoring are depicted in fig. 3.1; Wells in a Naturally Fractured Reservoir that already have developed a gas cap have shown improved performance when completed using an Intelligent well completion design known as "Instrumented deep tubing tail completion" (Ladron De Guevara et al. 2012) as shown in the previous chapter, for wells with this type of well completion, surveillance of the fluid level is generally performed installing permanent pressure sensors outside of the production tubing completion, hence the name instrumented deep tubing tail completion; the data gathered through the permanent sensors can then be used to calculate the position of the fluids contacts inside the well at any given time where data was taken. The IDTTC requires candidate wells to have specific characteristics detailed in the previous chapter, when such wells does not meet the required characteristics other monitoring technologies or methodologies must be implemented. For the case of non-candidate wells for IDTTC implementation because of small hole diameter restrictions (Fig. 2.8), one approach to provide such wells with a fluids monitoring methodology is presented by Lagunas Tapia et al. (2015) explained in detail in the previous chapter, their methodology relies in the manufacturing of small diameter orifices though the tubing tail length to allow a small amount of gas to enter the non-instrumented tubing tail through each orifice in contact to the gas cap, in this way evidence of gas inlet gives an estimate of the gas-oil contact depth.

The main limitation for the methodology presented by (Lagunas Tapia et al. 2015) is the low resolution that their method can achieve without risking to allow too much gas to be produced, this limitation provides an area of opportunity for their approach to the DGOC monitoring requirements on well with small hole diameters to be improved or substituted with one that is more efficient and provides better resolution.

3.2 Proposed Methodology, Details and Considerations

The work presented in this thesis takes as starting point the methodology presented for monitoring fluid contacts in wells with reduced hole diameter and/or economically restricted resources by (Lagunas Tapia et al. 2015) and modifies it to develop a mathematical correlation, making use of pressure data, liquid rates and gas rates data collected primarily inside the production tubing; Generating as a result a simpler and more efficient way of estimating the DGOC, reducing the number of orifices required in the tubing tail to estimate the position of the fluids contact to just one or two, and thus reducing the gas required to enter the tubing tail, but increasing the resolution of the estimate, allowing for a specific depth point inside the well to be calculated for the position of the DGOC.

The proposed methodology will allow for candidate wells to have a fluid contact monitoring system, when otherwise would have to settle for a non-instrumented well completion, where monitoring of the fluids contacts movement could not be achieved.

To achieve the previous objectives, we aim to make use of compressible flow though orifices correlations, but before that, the first step is to clearly detail the configuration of a candidate well, the required data to perform the well DGOC monitoring, and the limitations it exhibits under current, not improved well completion configurations.

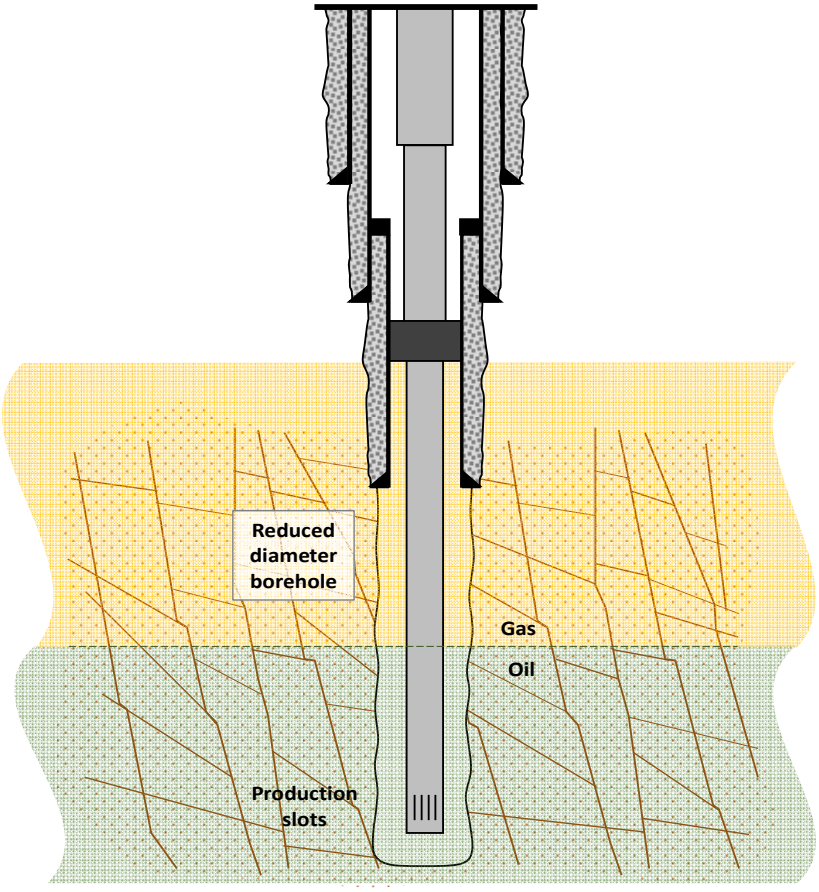

Fig. 3.2 – Reduced diameter borehole producing well with tubing tail completion, isolated from the gas cap.

Well completions like the one displayed in fig. 3.2 generally are implemented in naturally fracture reservoirs with presence of a gas cap, GOC and DGOC monitoring is a relevant activity for reservoir and production engineer working with this type of completions; due to the lack of space, or other restrictive parameters, it is not possible to install permanent pressure and temperature gauges at the exterior of the tubing tail like in the IDTTC (Ladron De Guevara et al. 2012; Tovar Rodriguez et al. 2011); the type of completion displayed in fig. 3.2 does not allow to monitor the position of the fluid contacts since any metering done inside the tubing will only result in parameters related to the liquid phase, which alone do not provide enough information to estimate the position of the fluid contacts, even when the well is shut in, the nature of this completion will result in a liquids level inside the tubing different to the fluids level at the fracture network in reservoir with normal pressure distributions. For the fluids contact position to be defined, the liquids data has to be complemented with pressure data from the gas phase, as explained by (Onyekonwu. 1997) and further developed in the previous chapter. In a well where pressure gauges can be implemented outside the tubing tail covering all fluids of interest (gas/oil/water) the graphic process to calculate the fluids contact follows the next steps:

- Pressure gauges vertical depth position and fluids gradients are known parameters or can be easily obtained.
- A graph displaying pressure versus depth is generated.
- In the generated graph we proceed to plot the pressure measurements obtained by the pressure gauges at their corresponding depths.

- If there exist full certainty of the position of a given or multiple gauges inside a specific fluid, the gradient of such fluid is plotted and extrapolated crossing the measured pressures of those respective gauges. If there exists uncertainty of the fluid around a given gauge, a gradient can be computed between that gauge and the next one in order to identify the fluid, if the gradient does not correspond to neither fluid (in this case usually the gradient calculated value will be lighter than one of the fluids gradient but heavier than the other) this mean that the fluids contact must be residing between those gauges and the next gauge to the opposite direction should be used to calculate the gradient.
- Once the gradients have been extrapolated, the depths where the gradients cross will be the depth where the fluid contacts reside at the time of the pressure measurements. An example of such diagram can be seen in fig. 3.3.

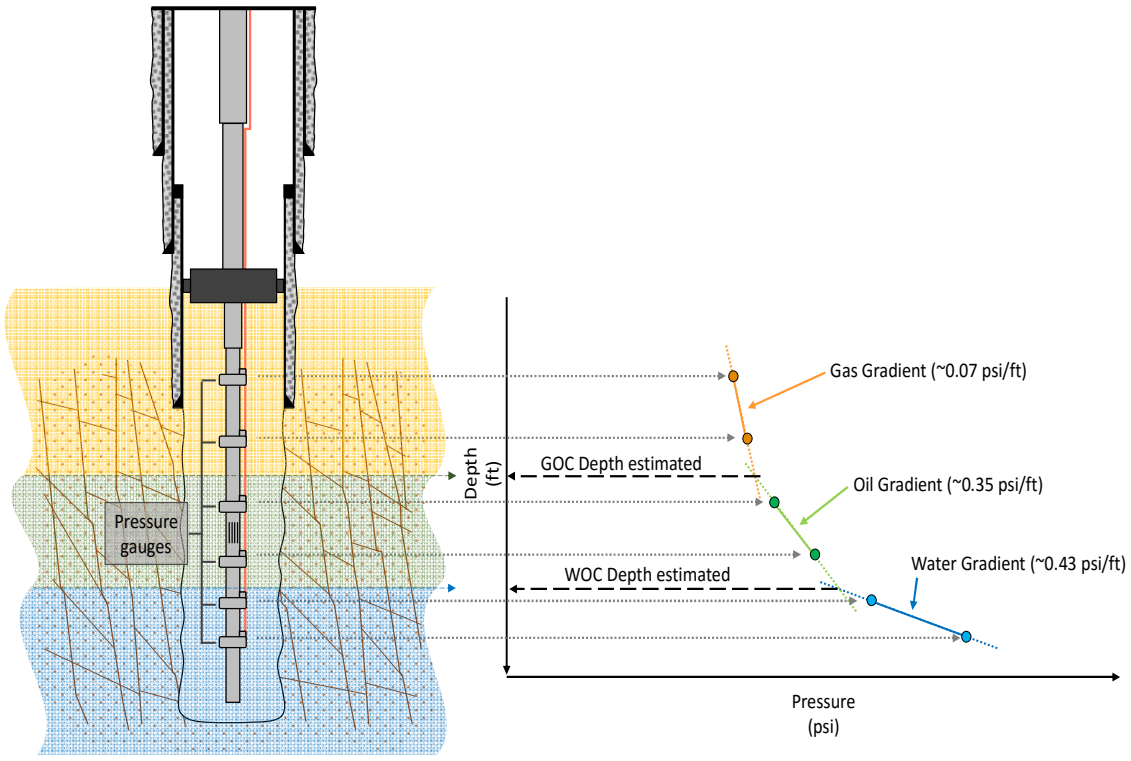

Fig. 3.3 – IDTTC schematics and gradients plot example generated from pressure gauges data.

Such calculation of the fluid contacts position can also be achieved applying eq. 2.16 and 2.17.

3.3 Development of the Theory Background for the Proposed Methodology to Estimate the DGOC Position

Fig. 3.4 displays a reduced diameter borehole producing well with a non-instrumented tubing tail completion, isolated from the gas cap, the minimum required data to calculate the fluids contact position is pressure data at the oil and at the gas taken at the same time,

their respective measurement depths and the fluid gradients; from fig. 3.4 we can see that the pressure measurement at the gas cap is not available:

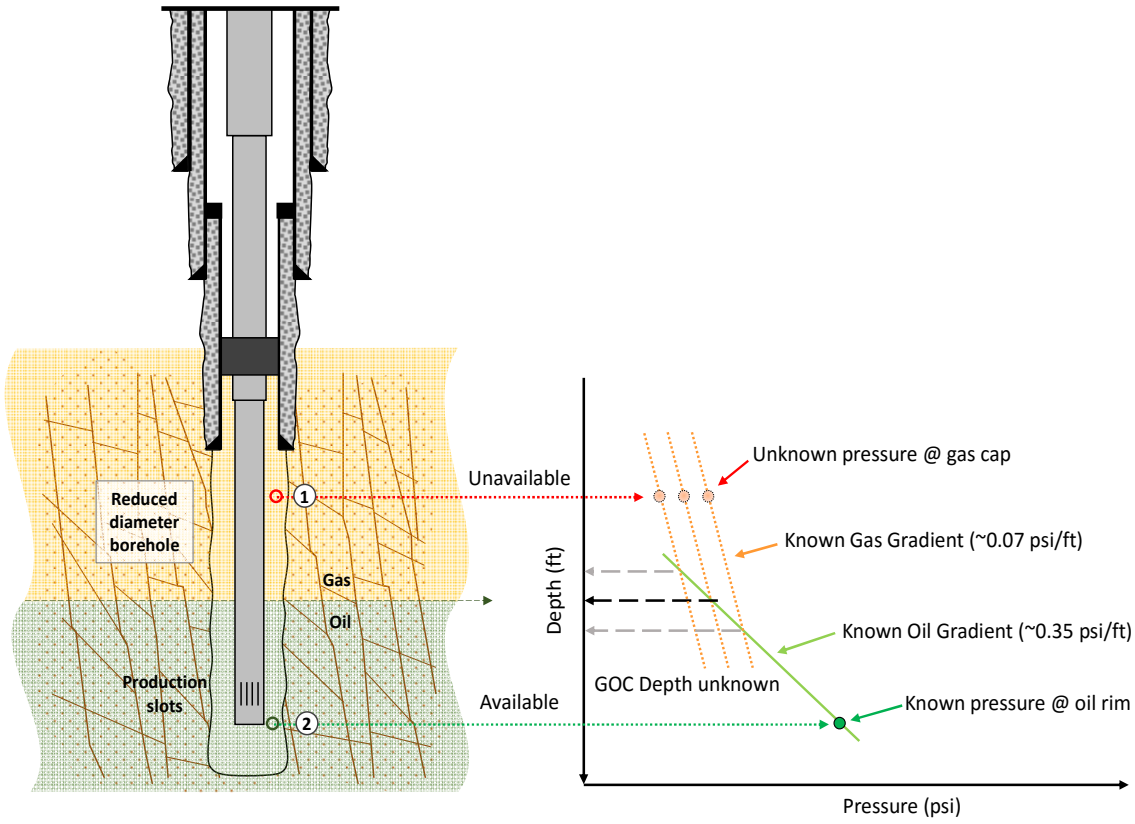

Fig. 3.4 – DTTC schematics an gradient plot displaying uncertainty on the DGOC position.

If all the required data was available, the position of the DGOC could be calculated deriving the position from equations 2.16 and 2.17; since the two equations represent a straight line of their respective fluid gradients, we can make equal both equations at the point where their pressure is the same, this allows us to subsequently Isolate the depth

where the gradients cross and calculate such value; based on the diagram from fig. 3.4 the corresponding DGOC depth derivation is as follows:

Parting from position "1":

$$P_{@DGOC,depth1} = P_1 + \left(Grad_{gas} * (Depth_{@DGOC1} - Depth_1)\right) \quad \text{--- 3.1}$$

Now parting from position "2":

$$P_{@DGOC,depth2} = P_2 - \left(Grad_{oil} * (Depth_2 - Depth_{@DGOC2})\right) \quad \text{--- 3.2}$$

Equaling both equations when the pressure is the same for both gradients:

$$P_{@DGOC,depth1} = P_{@DGOC,depth2} \quad \text{--- 3.3}$$

$$Depth_{@DGOC1} = Depth_{@DGOC2} = Depth_{@DGOC} \quad \text{--- 3.4}$$

$$P_1 + \left(Grad_{gas} * (Depth_{@DGOC} - Depth_1)\right) = P_2 - \left(Grad_{oil} * (Depth_2 - Depth_{@DGOC})\right) \quad \text{--- 3.5}$$

Leaving the Depth of the DGOC at the L.H.S. of the equation:

$$(Grad_{oil} * Depth_2 - Grad_{oil} * Depth_{@DGOC}) + \Big(\big(Grad_{gas} * Depth_{@DGOC} - Grad_{gas} * Depth_1\big)\Big) = P_2 - P_1 \quad \text{3.6}$$

$$Grad_{oil} * Depth_2 - Grad_{oil} * Depth_{@DGOC} + Grad_{gas} * Depth_{@DGOC} - Grad_{gas} * Depth_1 = P_2 - P_1 \quad \text{3.7}$$

$$-Grad_{oil} * Depth_{@DGOC} + Grad_{gas} * Depth_{@DGOC} = P_2 - P_1 + Grad_{gas} * Depth_1 - Grad_{oil} * Depth_2 \quad \text{3.8}$$

$$Depth_{@DGOC} * \big(Grad_{gas} - Grad_{oil}\big) = P_2 - P_1 + Grad_{gas} * Depth_1 - Grad_{oil} * Depth_2 \quad \text{3.9}$$

$$Depth_{@DGOC} = \frac{P_2 - (Grad_{oil} * Depth_2) + \big(Grad_{gas} * Depth_1\big) - P_1}{Grad_{gas} - Grad_{oil}} \quad \text{3.10}$$

The previous equation is the expression that will allow us to calculate the depth of the DGOC, as long as P_1, P_2, $Depth_1$, $Depth_2$, $Grad_{gas}$ and $Grad_{oil}$ are known; in order to be able to use this equation, we have to find a way to obtain the pressure value at the gas cap, for this purpose we propose to manufacture a small orifice in the tubing tail in direct contact to the gas cap, letting a small volume of gas to enter the tubing tail and flow to the surface along the oil production coming from the production slots or the open bottom of the tubing. Such modification is performed in order to allow for a tool installed inside the

production tubing to perform measurements in front of the orifice manufactured and correlate the data gathered to the conditions in the annular space, where the data is required to perform the DGOC calculation. A schematic of such completion is displayed in fig. 3.5:

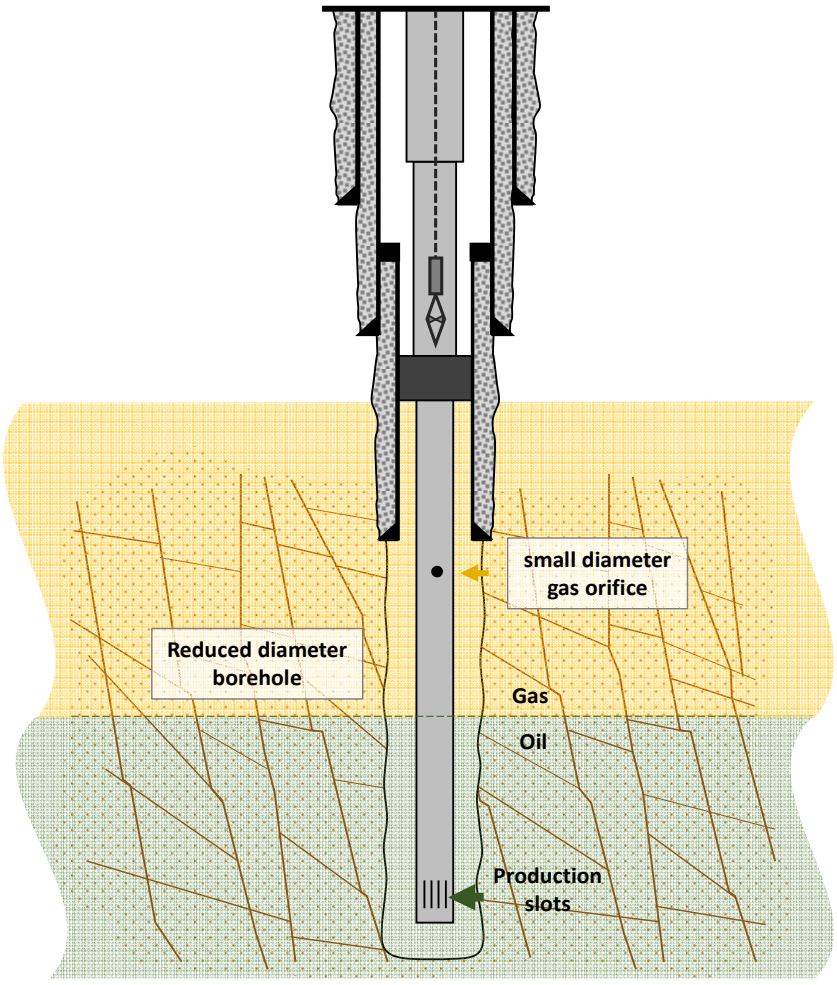

Fig. 3.5 – Schematics of a DTTC with the inclusion of a manufactured small diameter orifice at the gas cap level.

From the literature review we obtain the following general expression for the compressible flow through round orifices (Szilas. 1985a):

$$Q_g = \sqrt{2R}\frac{\pi}{4}d_{ch}^2 P_{ups}\frac{T_{sc}}{p_{sc}}C_D\sqrt{\frac{1}{MT_1}\frac{k}{k-1}\left[\left(\frac{p_{dwn}}{p_{ups}}\right)^{\frac{2}{k}}-\left(\frac{p_{dwn}}{p_{ups}}\right)^{\frac{k+1}{k}}\right]} \text{----------3.11}$$

Using field units, the expression takes the form:

$$Q_g = (3.505)C_D d_{64}^2\frac{P_{ups}}{P_{sc}}\sqrt{\frac{1}{\gamma_g T}}\sqrt{\frac{k}{k-1}\left[\left(\frac{p_{dwn}}{p_{ups}}\right)^{\frac{2}{k}}-\left(\frac{p_{dwn}}{p_{ups}}\right)^{\frac{k+1}{k}}\right]} \text{----------3.12}$$

One important characteristic of this correlation is that the gas rate will be independent from the conditions downstream (on the inside of the production tubing) at sonic flow (Szilas. 1985a; Economides et al. 2012; Kayser and Shambaugh. 1991), is a required condition for the present thesis proposal that the gas must pass through the orifice under subsonic flow conditions for the changes in the measured pressure downstream to be correlated to the pressure upstream the orifice (the annular space between the tubing tail and the open hole wellbore).

To ensure that the flow is subsonic, we can perform a two steps procedure; first we calculate the critical pressure ratio for the gas flowing through the orifice, usually the gas cap gas will be well characterized and properties like the heat capacity ratio are known so

this step should not represent any problem, the critical pressure ratio is obtained from the following equation:

$$\left(\frac{P_{dwn}}{P_{ups}}\right)_c = \left(\frac{2}{k+1}\right)^{\frac{k}{k-1}} \quad \text{----------3.13}$$

Once we have the value for the critical pressure ratio, using the measured pressure downstream inside the production tubing, we calculate the minimum required pressure upstream (critical pressure) for the flow to be sonic:

$$P_{crit} = \frac{P_{dwn}}{\left(\frac{P_{dwn}}{P_{ups}}\right)_c} \quad \text{----------3.14}$$

If the required pressure upstream (critical pressure) for the flow to be sonic given the measured pressure downstream is smaller than the average reservoir static pressure P_{WS} then there exists the possibility that the flow is sonic, and such data should not be used, but in the contrary, if the required pressure upstream (critical pressure) for the flow to be sonic given the measured pressure downstream is bigger than the average reservoir static pressure P_{WS} then it is not possible for the flow to be sonic, that means that the current gas flow through the orifice is happening under subsonic flow, and the methodology given in this thesis is applicable.

Example.- Let's assume that the heat capacity ratio for the gas flowing through the choke has a value of 1.28, a wireline tool measured a data point of 750 psi at the outlet of the orifice inside the tubing tail, and the reservoir has a recent acquired data of P_{ws}=1000 psi, then:

$$\left(\frac{P_{dwn}}{P_{ups}}\right)_c = \left(\frac{2}{k+1}\right)^{\frac{k}{k-1}} = \left(\frac{2}{1.28+1}\right)^{\frac{1.28}{1.28-1}} = 0.549 \text{ ----------} \textit{3.15}$$

Obtaining P_{crit} from the data calculated:

$$P_{crit} = \frac{P_{dwn}}{\left(\frac{P_{dwn}}{P_{ups}}\right)_c} = \frac{750\ psi}{0.549} = 1366.12\ psi \text{ ----------} \textit{3.16}$$

Comparing the minimum required pressure upstream (critical pressure) for the flow to be sonic against the current reservoir static pressure:

$$P_{crit} > P_{ws} \text{ ----------} \textit{3.17}$$

$$1366.12\ psi > 1000\ psi \text{ ----------} \textit{3.18}$$

We can conclude from this that it would be required a pressure greater than that of the reservoir in order for the flow to achieve sonic conditions, those conditions are just not possible, since the pressure at any point referenced to the reservoir datum pressure cannot

be greater that P_{ws} under normal circumstances (being really close to an injector well could in theory void the previous assumption, additional precautions should be taken given such scenario).

Once it has been concluded that the flow is subsonic, we can confidently make use of equation 3.12.

The previous expression has a polynomial form, for this reason it will not be directly solvable for the pressure upstream and an iterative method will prove effective regarding this matter; before trying to solve the polynomial expression we isolate the required known parameters in one side of the equation and leave the pressure terms in the other side of the equation:

$$\frac{Q_g}{(3.505)d_{64}^2\sqrt{\frac{1}{\gamma_g T}}} = C_D \frac{P_{ups}}{P_{sc}} \sqrt{\frac{k}{k-1}\left[\left(\frac{p_{dwn}}{p_{ups}}\right)^{\frac{2}{k}} - \left(\frac{p_{dwn}}{p_{ups}}\right)^{\frac{k+1}{k}}\right]} \quad \text{----------3.19}$$

For practical purposes we will introduce the dimensionless rate term from equation 3.19:

$$Q_{gD} = \frac{Q_g}{(3.505)d_{64}^2\sqrt{\frac{1}{\gamma_g T}}} \quad \text{----------3.20}$$

The R.H.S. of equation 3.19 is dimensionless since the heat capacity ratio, the discharge coefficient and the pressure differential ratio present in that side are dimensionless; this expression gives us the capacity to generate multiple type-curves for a graphic methodology to obtain the DGOC position, which will be developed in the next section. Dissecting equation 3.19 for the required elements to be computed, the list goes as follows:

- Q_g – Known variable, the gas rate flowing through the orifice is measured along the pressure downstream inside the tubing tail at the gas orifice depth.
- d_{64} – Known variable, the diameter of the orifice where the gas is flowing through, expressed in 64ths of an inch (this means that 16/64 of an inch is expressed just as 16)
- γ_g – Known variable, gravity of the gas (relative to air), usually around 0.70~0.65.
- T – Known variable, temperature upstream of the flow, since the system in the reservoir is usually under relative thermal equilibrium, it is acceptable to use the reservoir temperature.
- C_D – The orifice discharge coefficient will depend on the geometry of the orifice, details about the geometries are given in the previous chapter, depending on one or another geometry the discharge coefficient for compressible flow through small orifices will have a constant value or will be represented by a correlation dependent of the pressure differential across the orifice.
- P_{sc} – Known variable, is the pressure magnitude at standard conditions.
- k – Known variable, is the heat capacity ratio of the gas flowing through the choke.

- P_{dwn} – Known variable, the pressure downstream is measured along the gas rate flowing through the orifice inside the tubing tail at the gas orifice depth.
- P_{ups} – Unknown variable, the pressure upstream (at the gas in the annular space of the well completion) is the wanted variable.

We will provide two different equations to obtain the pressure magnitude upstream of the gas flow orifice, the orifices should be small enough that the gas volume flowing through them does not affect negatively the productivity of the well, for this purpose orifice geometries with diameters ranging from 6/64" to 14/64" are recommended; the decision of the orifice diameter size and geometry should be made taking into account the maximum amount of gas volume that can be produced without affecting negatively the productivity of the well, it should also be taken into account the ability and precision of the tools selected to measure pressure and gas rates, if the accuracy and resolution of the tools is not good enough, more gas would be required to enter the well, if the tools excel at accuracy and resolution, less amount of gas is required to enter the well and smaller diameters can be chosen; the following equations are proposed depending on the chosen orifice geometry:

Straight-bore orifice.- When the orifice has a straight-bore geometry, the discharge coefficient C_D for compressible flow through small orifices tends to maintain a constant value of around 0.85 for subsonic and sonic flow in orifices with length-to-diameter ratios of 1.9 or higher (Kayser and Shambaugh. 1991; Szilas. 1985a; Economides et al. 2012),

the following formula will leave open the decision of which value to assign to the discharge coefficient used since some manufacturers tend to provide their own discharge coefficient values; when constant discharge coefficients are to be used, sometimes is useful to calibrate said discharge coefficient prior to its implementation, in order to reduce the risk of accuracy errors:

$$Q_{gD} = C_D \frac{P_{ups}}{P_{sc}} \sqrt{\frac{k}{k-1}\left[\left(\frac{p_{dwn}}{p_{ups}}\right)^{\frac{2}{k}} - \left(\frac{p_{dwn}}{p_{ups}}\right)^{\frac{k+1}{k}}\right]} \quad \text{----------3.21}$$

This expression is the first of two equations presented in this thesis for the calculation of the pressure at the annular space between the tubing tail and the wellbore at the gas level.

Sharp-edge orifice.- When the orifice has a sharp-edge geometry, the discharge coefficient C_D for compressible flow through small round orifices tends to follow a behavior governed by the expression presented in (Kayser and Shambaugh. 1991; Szilas. 1985a; Economides et al. 2012) work which is only dependent of the pressure differential across the orifice, independent of the orifice diameter, flow temperature or gas composition:

$$C_D = 0.120 * (\omega) + 0.626 \quad \text{----------3.22}$$

Where:

$$\omega = \left(\frac{P_{ups}-P_{dwn}}{P_{crit}-P_{dwn}}\right) \text{ ----------3.23}$$

P_{crit} is in function of P_{dwn} and is defined as the minimum pressure required upstream given a specific pressure downstream for the sonic flow through the orifice to manifest; the physical interpretation for the dimensionless pressure drop "ω" is that it defines the flow condition of the gas passing through the orifice, for "ω" values below 1.0 the flow will be subsonic, when "ω" achieves values greater that unity, the flow will be considered sonic. P_{crit} should be calculated for every P_{dwn} in order to be in accordance with the previous statement, and requires the knowledge of the critical pressure ratio of the gas flowing through the orifice, the expression to calculate P_{crit} is:

$$P_{crit} = \frac{P_{dwn}}{\left(\frac{P_{dwn}}{P_{ups}}\right)_c} \text{ ----------3.24}$$

Now replacing the discharge coefficient correlation for compressible flow through small sharp-edge orifices in equation 3.21:

$$Q_{gD} = \left(0.120 * \left(\frac{(P_{ups}-P_{dwn})*\left(\frac{P_{dwn}}{P_{ups}}\right)_c}{P_{dwn}-P_{dwn}*\left(\frac{P_{dwn}}{P_{ups}}\right)_c}\right) + 0.626\right)\frac{P_{ups}}{P_{sc}}\sqrt{\frac{k}{k-1}\left[\left(\frac{p_{dwn}}{p_{ups}}\right)^{\frac{2}{k}} - \left(\frac{p_{dwn}}{p_{ups}}\right)^{\frac{k+1}{k}}\right]} \text{ 3.25}$$

The last expression is the second of two equations presented in this thesis for the calculation of the pressure at the annular space between the tubing tail and the wellbore at the gas level.

Since expressions 3.21 and 3.25 are of the polynomial type, they require an iterative process to be solved and obtain a value for P_{ups}, we recommend either to use a solver software like the ones included in Microsoft excel, or programing one using Matlab or any other programing software suitable.

Now that we have stablished a reliable method to acquire pressure data at the gas zone in the annular space of the well completion through data measured at the same level inside the production tubing, all the variables required in the implementation of equation 3.10 to define the position of the DGOC have been acquired and the calculation can take place, for:

$$P_1 = P_{ups@gas} \ ; \ P_2 = P_{measured@oil}$$

$$Depth_{@DGOC} = \frac{P_2 - (Grad_{oil} * Depth_2) + (Grad_{gas} * Depth_1) - P_1}{Grad_{gas} - Grad_{oil}}$$

The theory explained in this section is the base for the methodologies proposed in this thesis, consisting of a numerical approach to the problem, and a graphical, type-curve approach, the next sections will present a structured approach to each methodology.

Previous arrangements have to be performed before applying any of the methodologies proposed here, the minimum key elements that should be covered prior to calculate the DGOC position in a candidate well for the present methodologies are:

- Design and installation of the well completion finished, including the length of the tubing tail with an open bottom or any other oil flow design like production slots that allow for the pressure at the oil phase in the wellbore to be calculated, and the gas orifice manufactured as part of the tubing or as an attachable component, we have selected an open bottom tubing tail since it allows for the most direct readings of pressure directly to the oil in the wellbore, but other configurations are also applicable as long as the pressure calculations are taken into account.
- The surface equipment and the well configuration must allow for surface-run tools like wireline tools or C.T. tools to be run inside the well in order to take pressure and rate measurements at the gas orifice depth and at the oil phase, if possible at the bottom of the tubing tail.

3.4 Proposed Methodology: A Numerical Approach

If the user has the tools to develop a mathematical tool like a spreadsheet or a program software like a Matlab script, the numerical approach is recommended over the graphical approach since it will give a better accuracy to the estimation of the DGOC position. The numerical approach goes as follows:

1) Data gathering.- first of all pressure and rates data has to be gathered inside the tubing, either by temporary tool or permanent tools, like wireline tools or hanging gauges. Data should be collected under steady-state flow conditions at both the orifice depth and at the oil phase at same flowing conditions, this will ensure that the fluid contacts are stable and their position calculation will be valid.
2) Gas flow validation.- for the methodology to be valid, gas flow through the gas orifice must exists under subsonic flow, if the orifice is currently below the DGOC, or the pressure differential ratio is below the critical pressure ratio, gas flow through the orifice under subsonic flow won't happen. Using equations 3.13 and 3.14 allows us to define such conditions comparing the critical pressure to P_{ws}.

$$\left(\frac{P_{dwn}}{P_{ups}}\right)_c = \left(\frac{2}{k+1}\right)^{\frac{k}{k-1}} \quad \rightarrow \quad P_{crit} = \frac{P_{dwn}}{\left(\frac{P_{dwn}}{P_{ups}}\right)_c} \quad \rightarrow \quad P_{crit} > P_{ws} \quad or \quad P_{crit} < P_{ws}$$

If risk of sonic flow exists, then the next steps are not applicable to the current conditions and this methodology cannot be performed to estimate the DGOC position.

3) Dimensionless gas rate calculation.- If subsonic gas flow through the orifice is confirmed, we proceed to obtain the Dimensionless gas rate using expression 3.20:

$$Q_{gD} = \frac{Q_g}{(3.505)d_{64}^2\sqrt{\frac{1}{\gamma_g T}}}$$

4) Gas upstream pressure calculation.- Once the dimensionless gas rate has been calculated we proceed to select the adequate compressible flow through small diameter orifices polynomial expression and solve for the pressure upstream of the gas orifice "P_{ups}" using iterative methods for solving polynomial equations; the corresponding equations are 3.21 and 3.25:

Straight-bore orifice

$$Q_{gD} = C_D \frac{P_{ups}}{P_{sc}} \sqrt{\frac{k}{k-1}\left[\left(\frac{p_{dwn}}{p_{ups}}\right)^{\frac{2}{k}} - \left(\frac{p_{dwn}}{p_{ups}}\right)^{\frac{k+1}{k}}\right]}$$

Sharp-edge orifice

$$Q_{gD} = \left(0.120 * \left(\frac{(P_{ups}-P_{dwn})*\left(\frac{P_{dwn}}{P_{ups}}\right)_c}{P_{dwn}-P_{dwn}*\left(\frac{P_{dwn}}{P_{ups}}\right)_c}\right) + 0.626\right) \frac{P_{ups}}{P_{sc}} \sqrt{\frac{k}{k-1}\left[\left(\frac{p_{dwn}}{p_{ups}}\right)^{\frac{2}{k}} - \left(\frac{p_{dwn}}{p_{ups}}\right)^{\frac{k+1}{k}}\right]}$$

5) DGOC calculation.- Finally, with the pressure upstream of the gas orifice "P_{ups}" obtained and the data gathered at the oil phase, we proceed to use equation 3.10:

$$P_1 = P_{ups@gas} \ ; \ P_2 = P_{measured@oil}$$

$$Depth_{@DGOC} = \frac{P_2 - (Grad_{oil} * Depth_2) + (Grad_{gas} * Depth_1) - P_1}{Grad_{gas} - Grad_{oil}}$$

Following steps 1 to 5 will allow us to estimate the position of the DGOC under the previously mentioned conditions, if a continuous monitoring was performed where multiple pressure data points and rates were measured over a period of time under steady-state flow, steps 3 to 5 can be programed to be repeated on the whole data set in order to generate a plot of the dynamic gas-oil contact depth position over a period of time like fig. 2.1 and fig. 2.7.

3.5 Proposed Methodology: A Type-curve Approach

If the user doesn't have the tools to develop a mathematical tool like a spreadsheet or a program software like a Matlab script, the graphical approach is recommended over the numerical approach since it does not require the use of iterative methods for the solution of polynomial equations and the required calculations to estimate the DGOC position are easily performed using a regular calculator. The graphical approach goes as follows:

1) Data gathering.- first of all pressure and rates data has to be gathered inside the tubing, either by temporary tool or permanent tools, like wireline tools or hanging gauges. Data should be collected under steady-state flow conditions at both the orifice depth and at the oil phase at same flowing conditions, this will ensure that the fluid contacts are stable and their position calculation will be valid.

2) Gas flow validation.- for the methodology to be valid, gas flow through the gas orifice must exists under subsonic flow, if the orifice is currently below the DGOC, or the pressure differential ratio is below the critical pressure ratio, gas flow through the orifice under subsonic flow won't happen. Using equations 3.13 and 3.14 allows us to define such conditions comparing the critical pressure to P_{ws}.

$$\left(\frac{P_{dwn}}{P_{ups}}\right)_c = \left(\frac{2}{k+1}\right)^{\frac{k}{k-1}} \quad \rightarrow \quad P_{crit} = \frac{P_{dwn}}{\left(\frac{P_{dwn}}{P_{ups}}\right)_c} \quad \rightarrow \quad P_{crit} > P_{ws} \quad or \quad P_{crit} < P_{ws}$$

If risk of sonic flow exists, then the next steps are not applicable to the current conditions and this methodology cannot be performed to estimate the DGOC position.

3) Dimensionless gas rate calculation.- If subsonic gas flow through the orifice is confirmed, we proceed to obtain the Dimensionless gas rate using expression 3.20:

$$Q_{gD} = \frac{Q_g}{(3.505)d_{64}^2\sqrt{\frac{1}{\gamma_g T}}}$$

4) Dimensionless type-curve reading.- Once the dimensionless gas rate has been calculated we proceed to select the adequate type-curve from the curve family presented in the results chapter of this thesis, depending on the geometry of the orifice, pressure downstream of the orifice, heat capacity ratio of the gas and the dimensionless gas rate; the type-curves are generated based on the compressible flow through small

diameter orifices polynomial expressions presented in previous chapters for straight-bore orifices and sharp-edge orifices; examples of such type-curves are given below:

If dimensionless type-curve for straight-bore orifices are selected, a similar plot to the one in fig. 3.6 will be used:

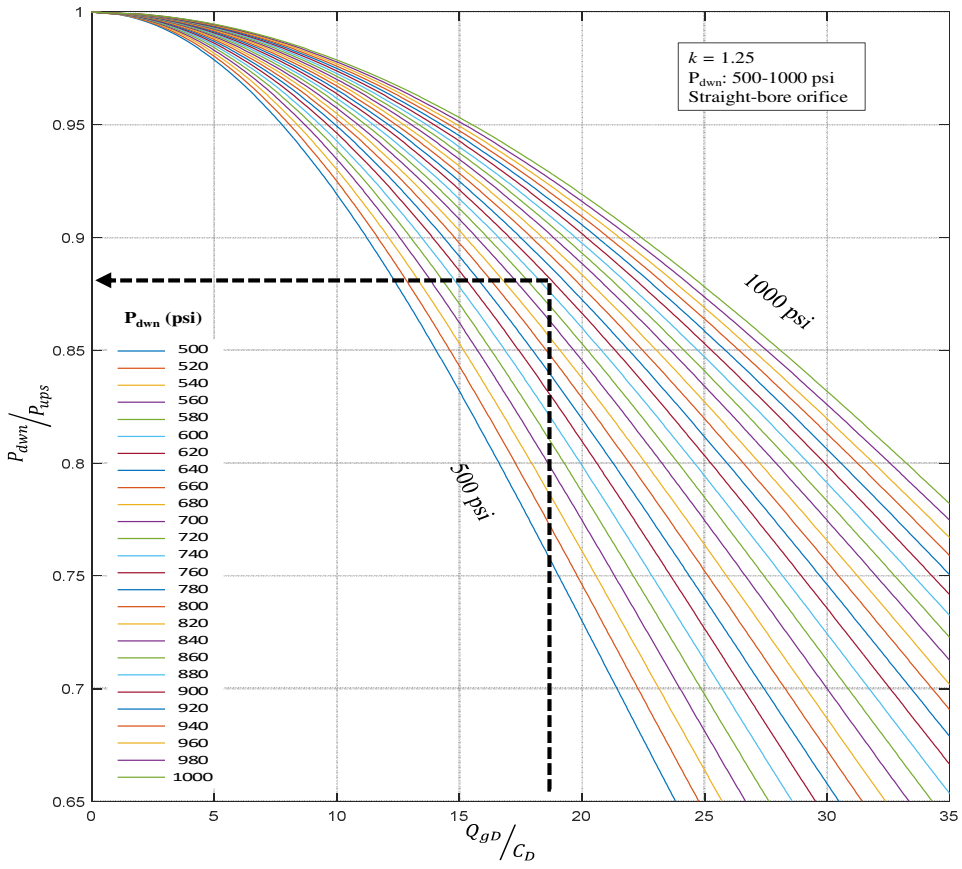

Fig. 3.6 – Dimensionless gas rate vs pressure differential ratio for straight-bore orifices example.

The way to read the dimensionless type-curves presented here for straight-bore orifices consist on entering from the horizontal axis with the previously calculated dimensionless gas rate value divided by the corresponding discharge coefficient (Q_{gD}/C_D), intersect the corresponding isobaric curve that best represents the pressure measured downstream of the gas orifice, and finally read the corresponding value on the vertical axis for the pressure differential ratio (P_{dwn}/P_{ups}).

If dimensionless type-curve for sharp-edge orifices are selected, a similar plot to the one in fig. 3.7 will be used:

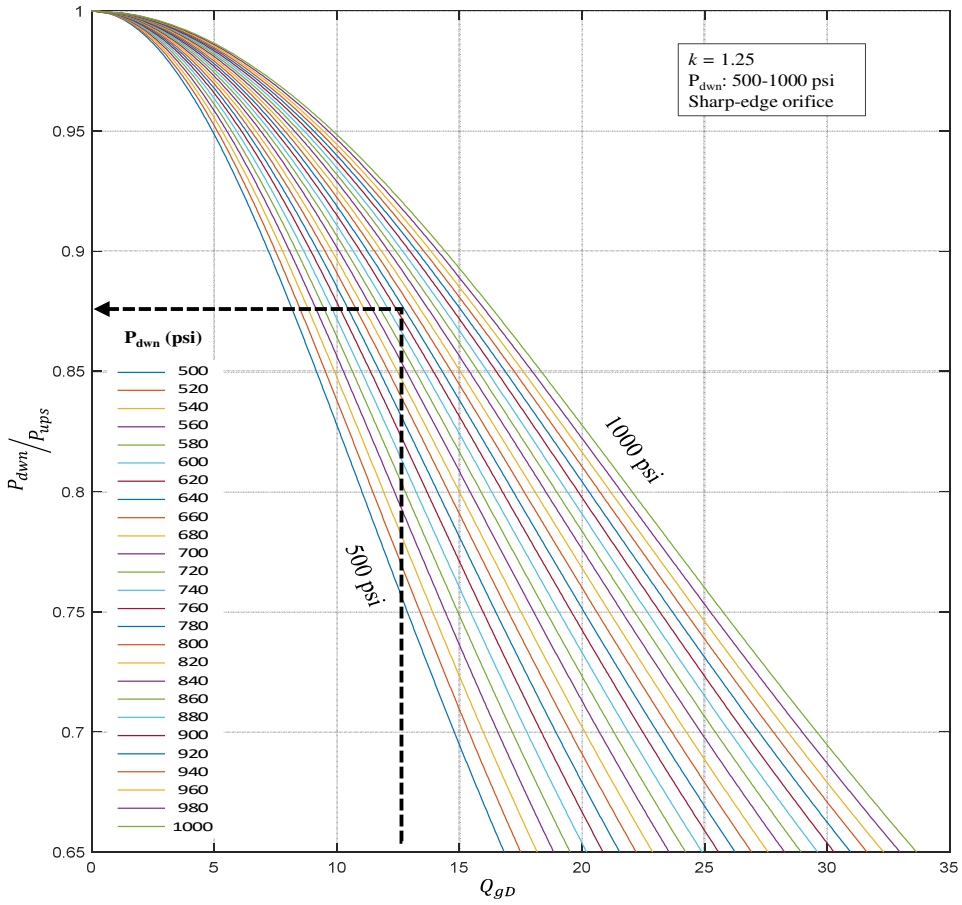

Fig. 3.7 – Dimensionless gas rate vs pressure differential ratio for sharp-edge orifices example.

The way to read the dimensionless type-curves presented here for sharp-edge orifices consist on entering from the horizontal axis with the previously calculated dimensionless gas rate value (Q_{gD}), intersect the corresponding isobaric curve that best represents the pressure measured downstream of the gas orifice, and finally read the corresponding value on the vertical axis for the pressure differential ratio (P_{dwn}/P_{ups}).

5) Gas upstream pressure calculation from type-curve read data.- Once the pressure differential ratio (P_{dwn}/P_{ups}) has been graphically obtained, we calculate the pressure upstream of the gas orifice using the following expression:

$$P_{ups} = \frac{P_{dwn-measured}}{\left(\frac{P_{dwn}}{P_{ups}}\right)_{read\ from\ type-curve}} \text{ ----------3.26}$$

6) DGOC calculation.- Finally, with the pressure upstream of the gas orifice "P_{ups}" obtained and the data gathered at the oil phase, we proceed to use equation 3.10:

$$P_1 = P_{ups@gas}\ ;\ P_2 = P_{measured@oil}$$

$$Depth_{@DGOC} = \frac{P_2 - (Grad_{oil} * Depth_2) + (Grad_{gas} * Depth_1) - P_1}{Grad_{gas} - Grad_{oil}}$$

Following steps 1 to 6 will allow us to estimate the position of the DGOC under the previously mentioned conditions, if a continuous monitoring was performed where multiple pressure data points and rates were measured over a period of time under steady-state flow, steps 3 to 6 can be applied to the whole data set in order to generate a plot of the dynamic gas-oil contact depth position over a period of time, but such procedure will be slow and tedious, it is then recommended to make use of the numerical approach for cases where a large amount of data is going to be processed.

4. RESULTS

4.1 Equations, Methodologies and Type-curves Developed

From the work developed in this thesis, a dimensionless gas rate term is being implemented for gas flow through a small diameter orifice:

$$Q_{gD} = \frac{Q_g}{(3.505)d_{64}^2\sqrt{\frac{1}{\gamma_g T}}} \text{ ---------- } 4.1$$

Taking advantage of the dimensionless gas rate, 2 dimensionless equations have been developed in order to calculate the pressure upstream of a small diameter orifice based on compressible gas flow theory; depending on the geometry of the orifice the final form of the expressions mentioned are:

For orifices with straight-bore geometries:

$$Q_{gD} = \frac{Q_g}{(3.505)d_{64}^2\sqrt{\frac{1}{\gamma_g T}}} = C_D \frac{P_{ups}}{P_{sc}} \sqrt{\frac{k}{k-1}\left[\left(\frac{p_{dwn}}{p_{ups}}\right)^{\frac{2}{k}} - \left(\frac{p_{dwn}}{p_{ups}}\right)^{\frac{k+1}{k}}\right]} \text{ ---------- } 4.2$$

For orifices with sharp-edge geometries:

$$Q_{gD} = \left(0.120 * \left(\frac{(P_{ups} - P_{dwn}) * \left(\frac{P_{dwn}}{P_{ups}}\right)_c}{P_{dwn} - P_{dwn} * \left(\frac{P_{dwn}}{P_{ups}}\right)_c} \right) + 0.626 \right) \frac{P_{ups}}{P_{sc}} \sqrt{\frac{k}{k-1}\left[\left(\frac{p_{dwn}}{p_{ups}}\right)^{\frac{2}{k}} - \left(\frac{p_{dwn}}{p_{ups}}\right)^{\frac{k+1}{k}}\right]} \quad \textit{4.3}$$

The upstream pressure data calculated using any of the previous two equations can be used to estimate the position of fluid contacts inside a well at the moment of the measurement of well parameters; parting from the aforementioned equations 2 main methodologies to estimate the DGOC for wells in naturally fractured reservoirs have been developed; the numerical methodology main points are:

1) Data gathering.
2) Gas flow validation.
3) Dimensionless gas rate calculation.
4) Gas upstream pressure calculation though mathematical correlations.
5) DGOC calculation.

The type-curve methodology main points are:

1) Data gathering.
2) Gas flow validation.
3) Dimensionless gas rate calculation.
4) Dimensionless type-curve reading.
5) Gas upstream pressure calculation from type-curve read data.

6) DGOC calculation.

The details for each of the steps are explained in their corresponding proposed methodology sub-sections.

For the type-curve methodology a series of dimensionless curve families have been constructed, aiming to cover a wide range of conditions, if the reader requires type-curves for conditions outside of those presented here, they can always be built using any computer programing software and equations 3.21 and 3.25; the curve families are grouped according to orifice geometry and heat capacity ratio, figures 4.1 to 4.12 conform the straight-bore orifice geometry dimensionless curves family, figures 4.13 to 4.24 conform the sharp-edge orifice geometry dimensionless curves family:

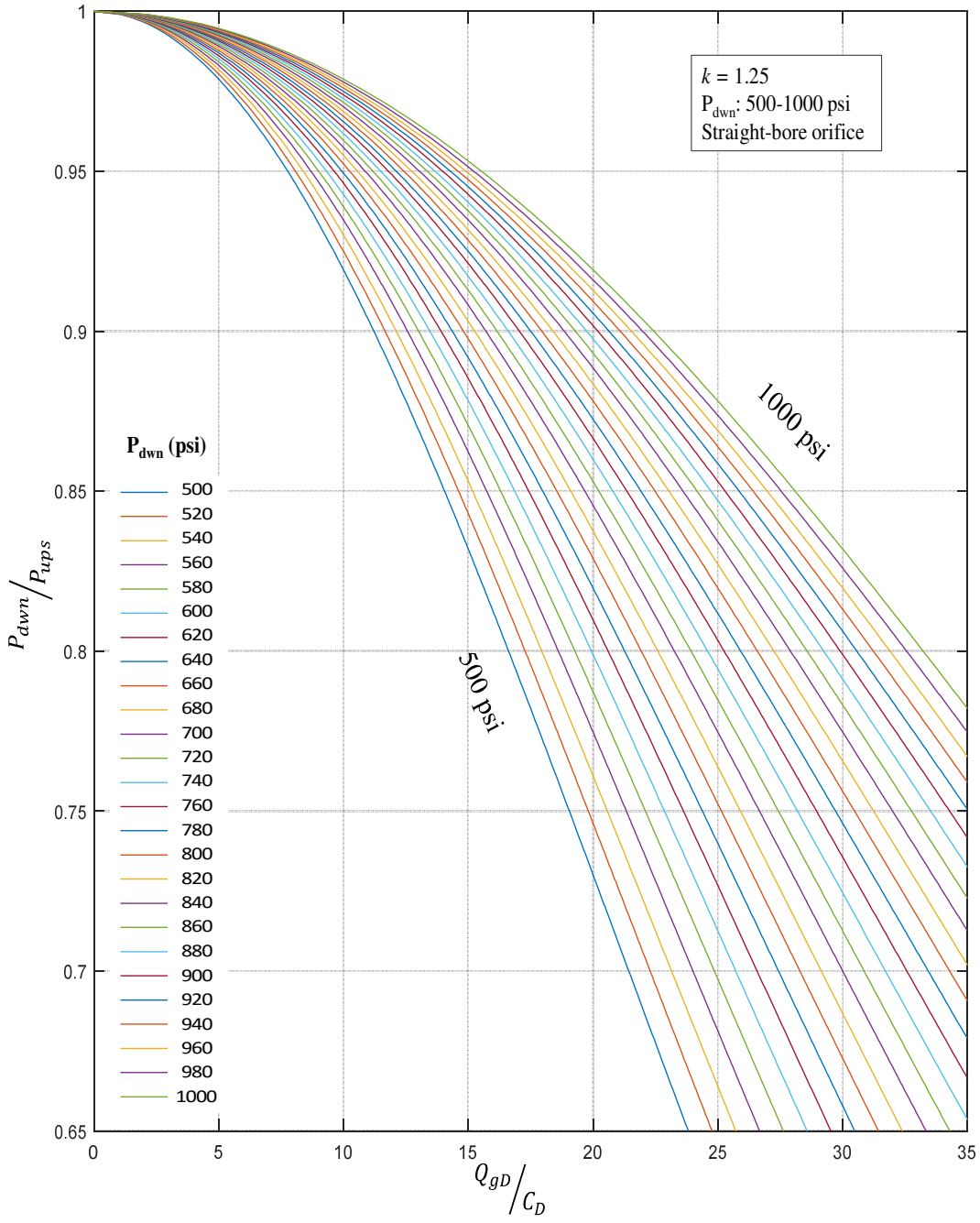

Fig. 4.1 – Dimensionless gas rate vs pressure differential ratio. k = 1.25, P_{dwn}: 500-1000 psi, straight-bore orifice.

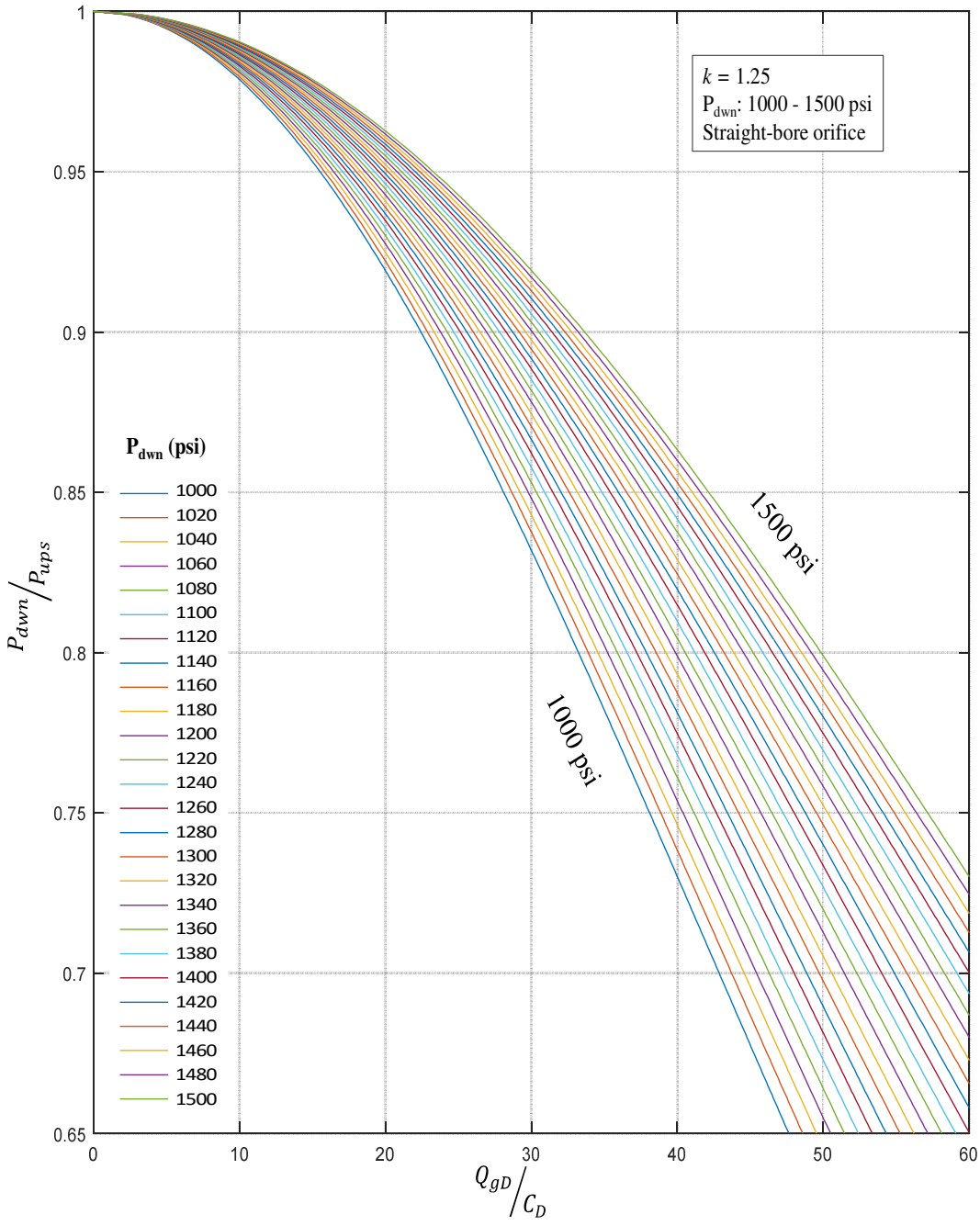

Fig. 4.2 – Dimensionless gas rate vs pressure differential ratio. k = 1.25, P_{dwn}: 1000-1500 psi, straight-bore orifice.

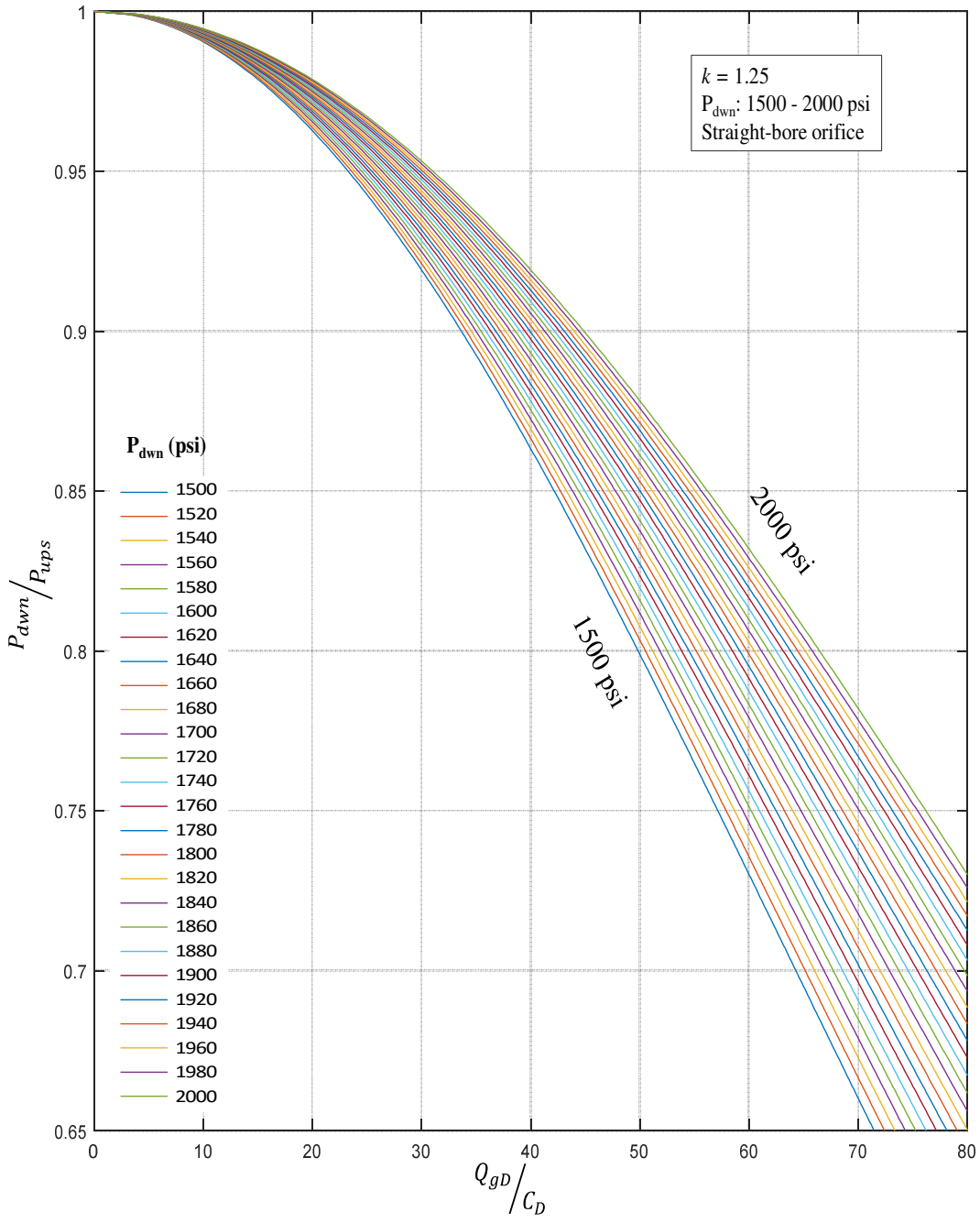

Fig. 4.3 – Dimensionless gas rate vs pressure differential ratio. k = 1.25, P_{dwn}: 1500-2000 psi, straight-bore orifice.

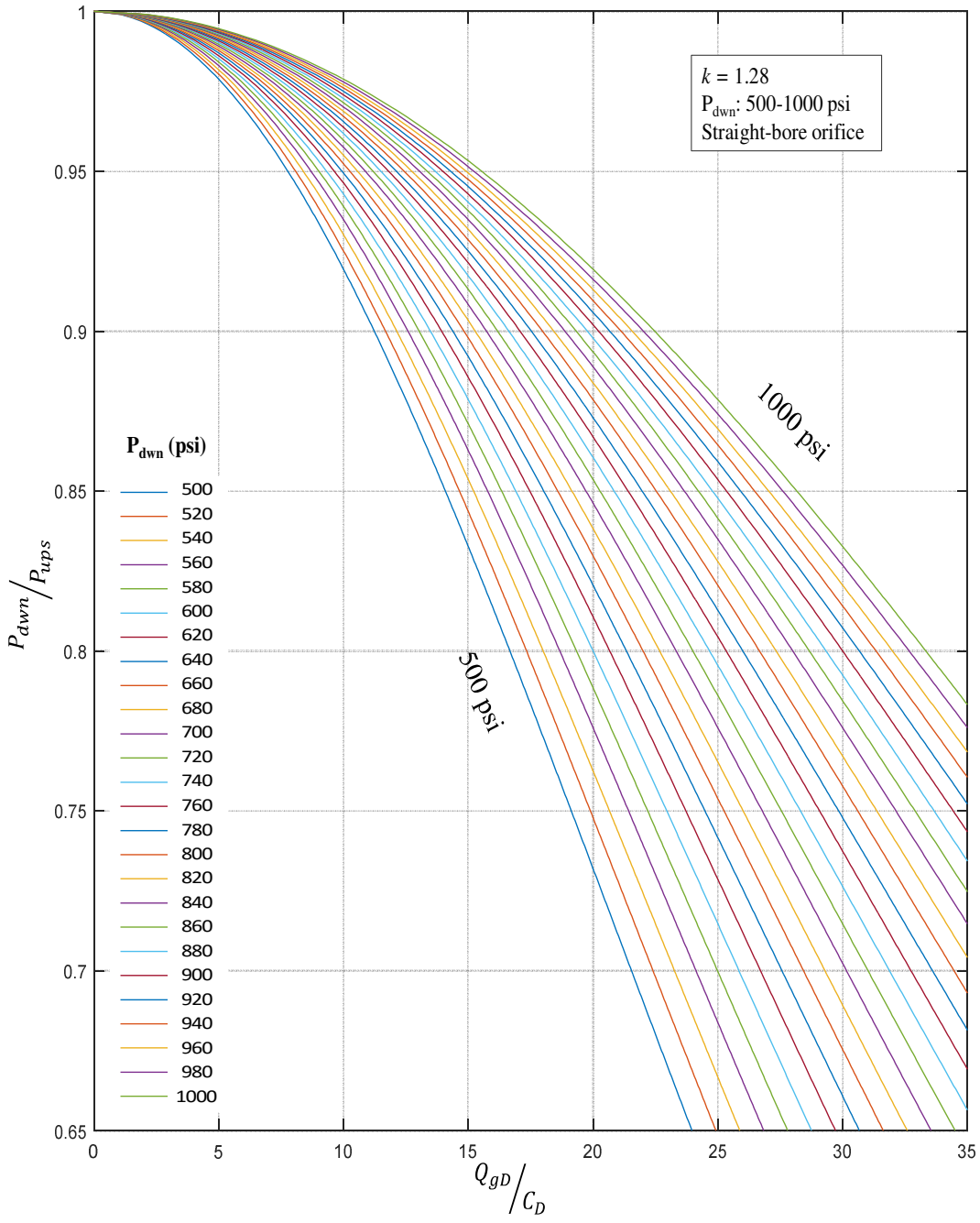

Fig. 4.4 – Dimensionless gas rate vs pressure differential ratio. k = 1.28, P_{dwn}: 500-1000 psi, straight-bore orifice.

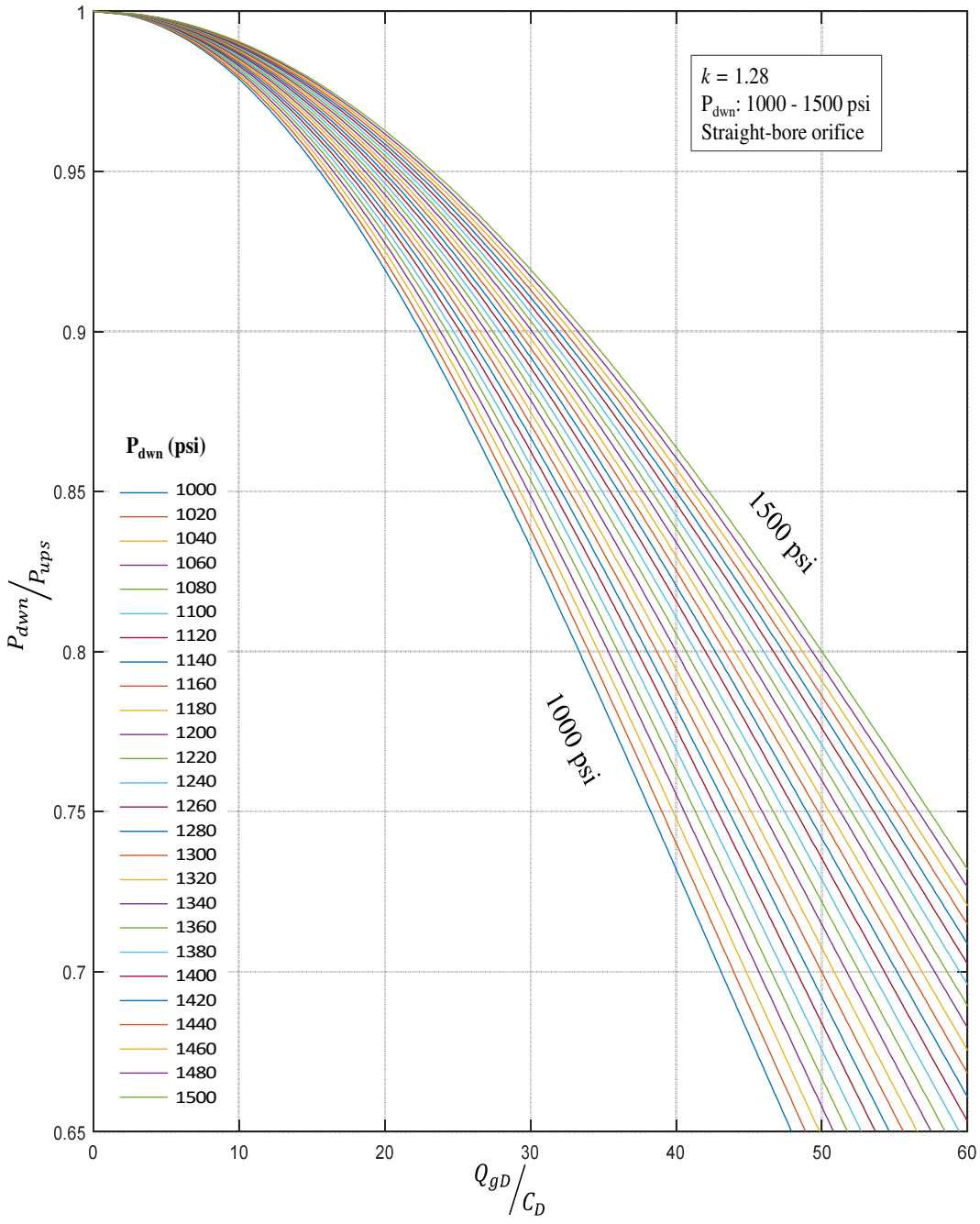

Fig. 4.5 – Dimensionless gas rate vs pressure differential ratio. k = 1.28, P_{dwn}: 1000-1500 psi, straight-bore orifice.

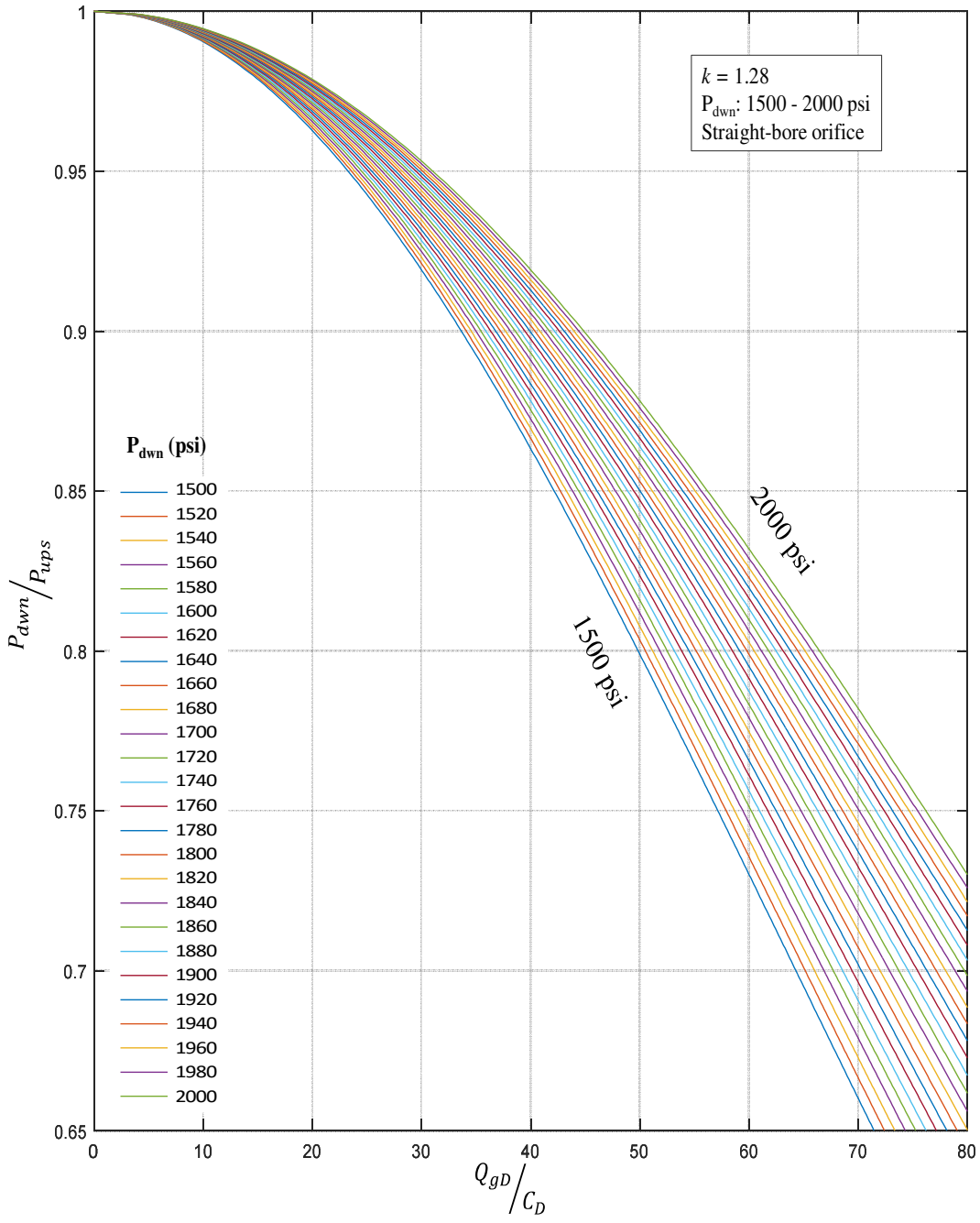

Fig. 4.6 – Dimensionless gas rate vs pressure differential ratio. k = 1.28, P_{dwn}: 1500-2000 psi, straight-bore orifice.

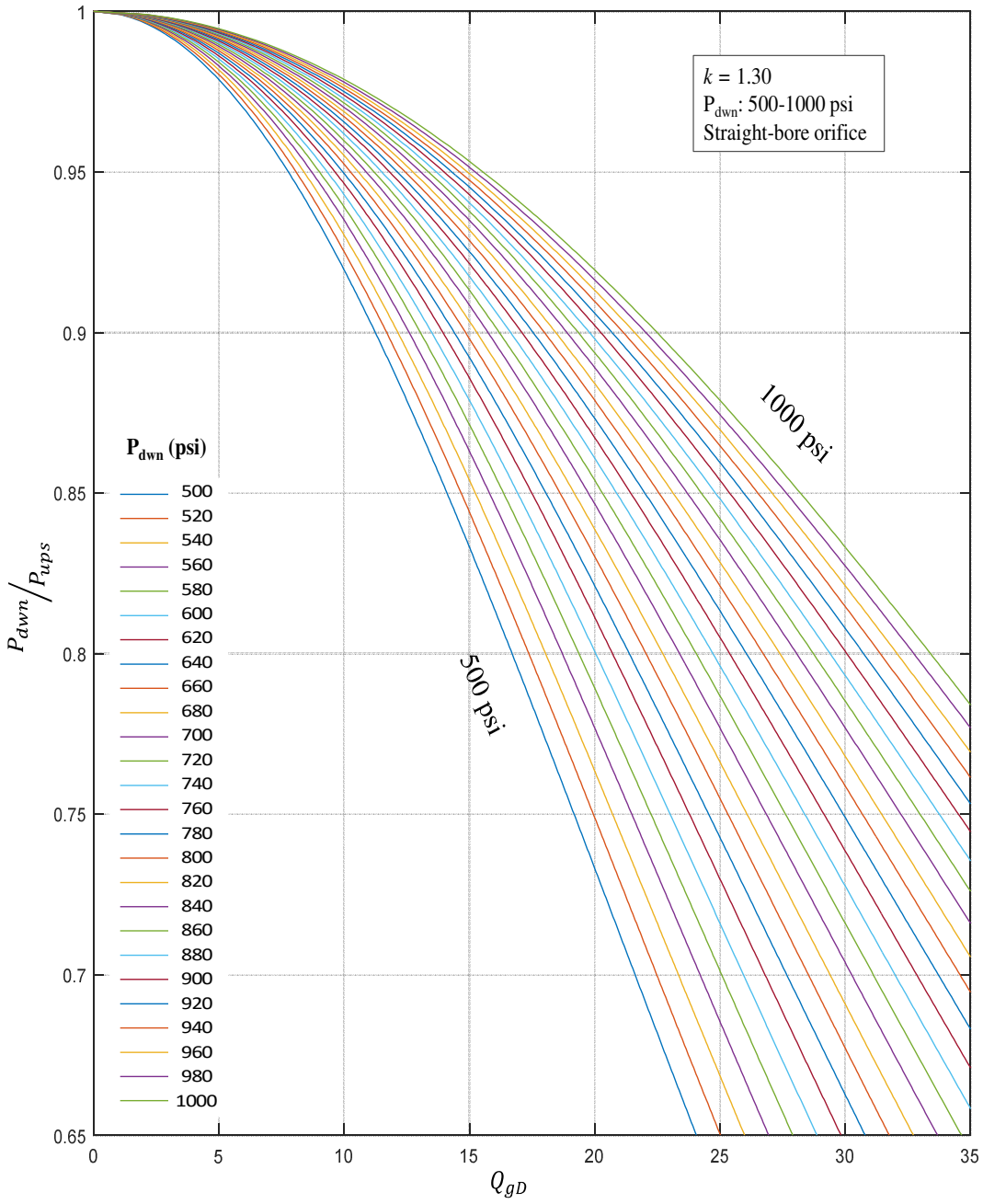

Fig. 4.7 – Dimensionless gas rate vs pressure differential ratio. k = 1.30, P_{dwn}: 500-1000 psi, straight-bore orifice.

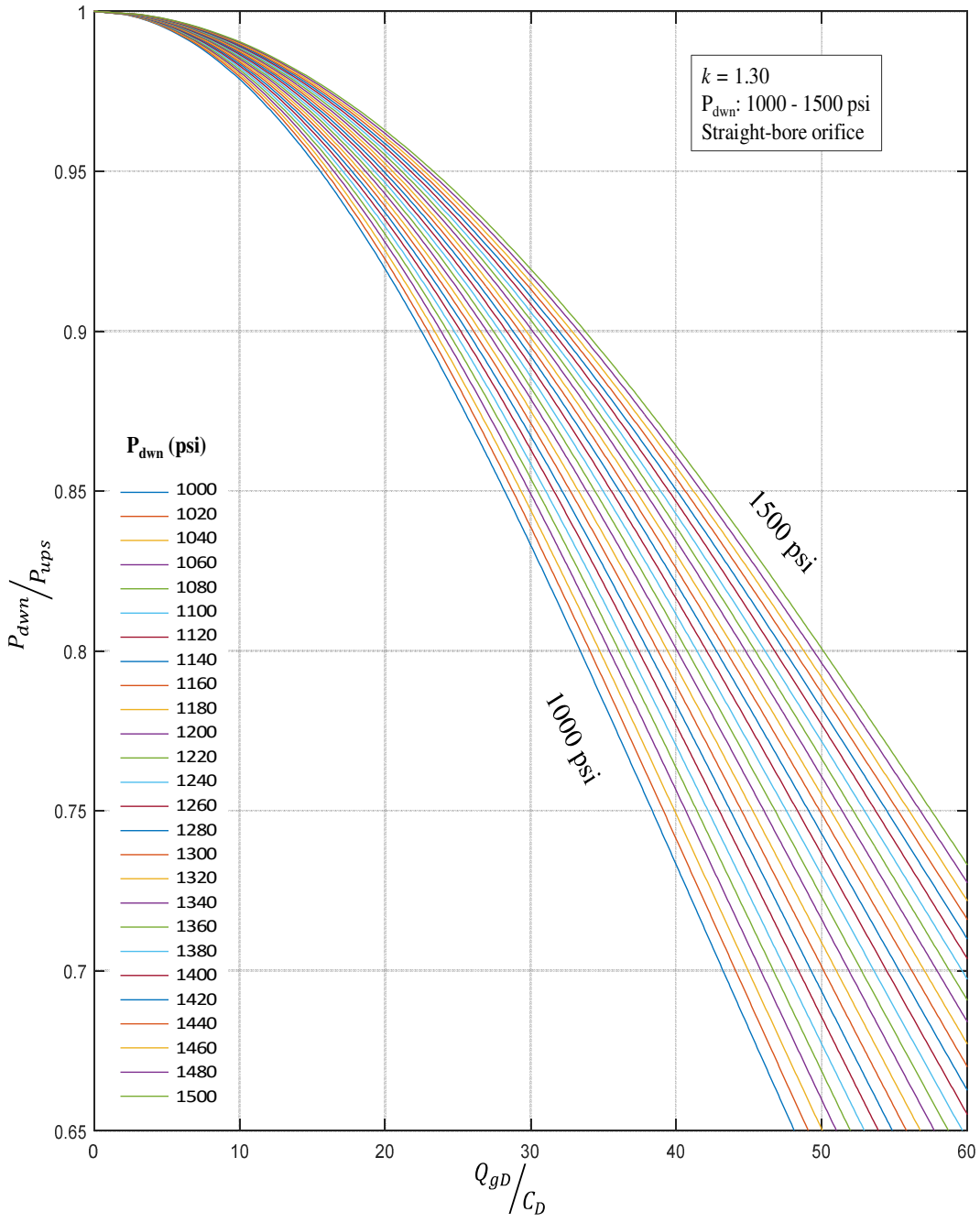

Fig. 4.8 – Dimensionless gas rate vs pressure differential ratio. k = 1.30, P_{dwn}: 1000-1500 psi, straight-bore orifice.

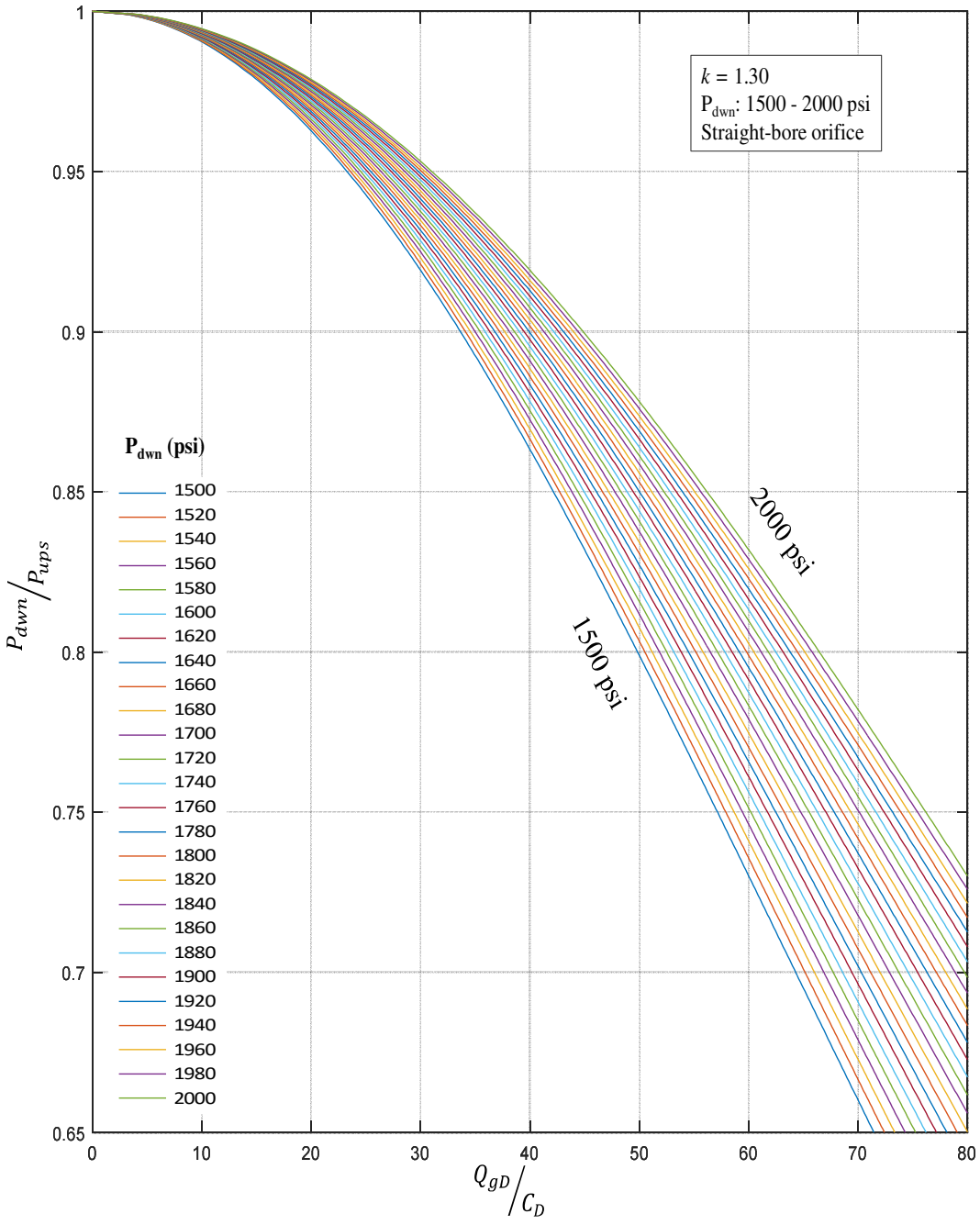

Fig. 4.9 – Dimensionless gas rate vs pressure differential ratio. k = 1.30, P_{dwn}: 1500-2000 psi, straight-bore orifice.

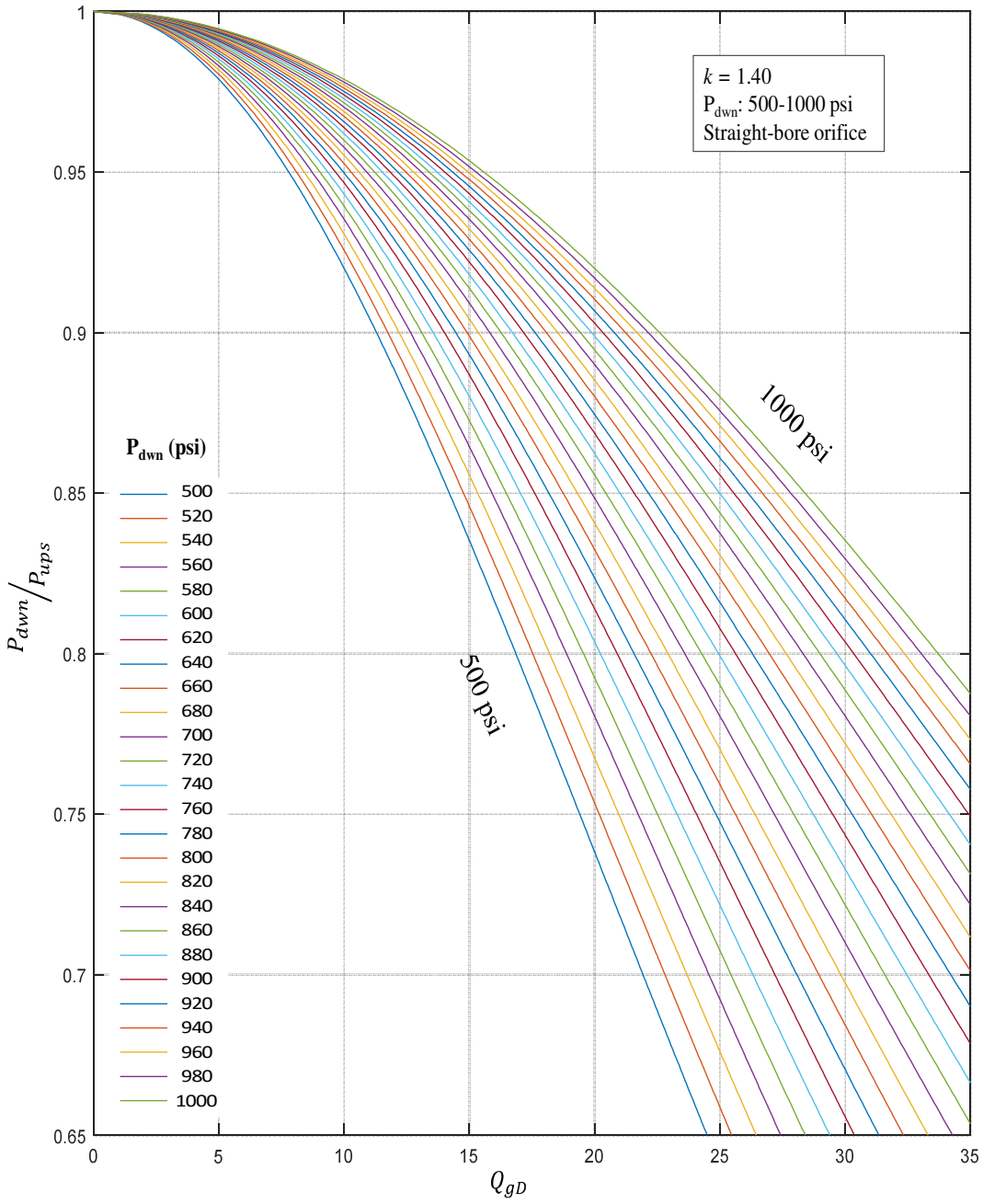

Fig. 4.10 – Dimensionless gas rate vs pressure differential ratio. k = 1.40, P_{dwn}: 500-1000 psi, straight-bore orifice.

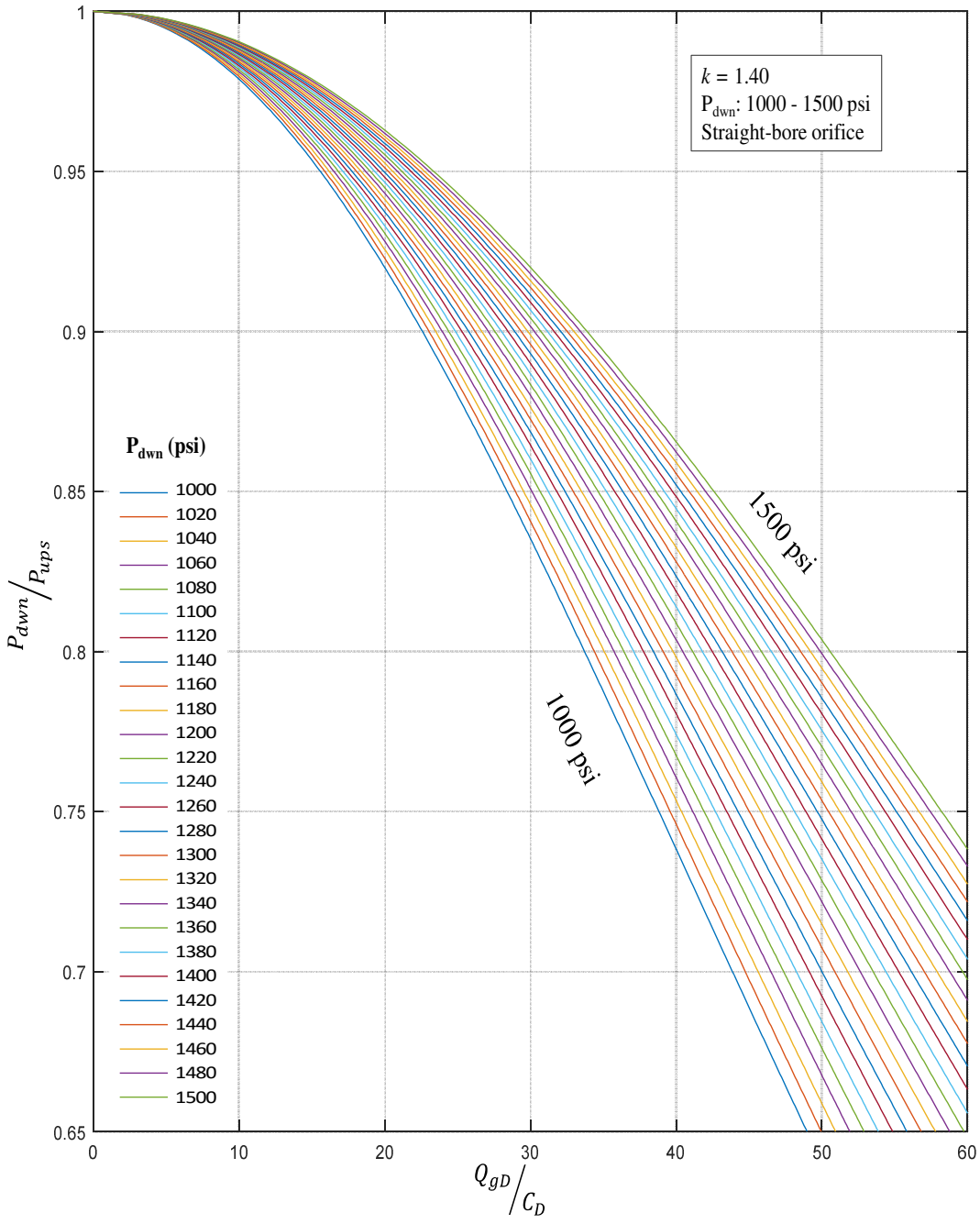

Fig. 4.11 – Dimensionless gas rate vs pressure differential ratio. k = 1.40, P_{dwn}: 1000-1500 psi, straight-bore orifice.

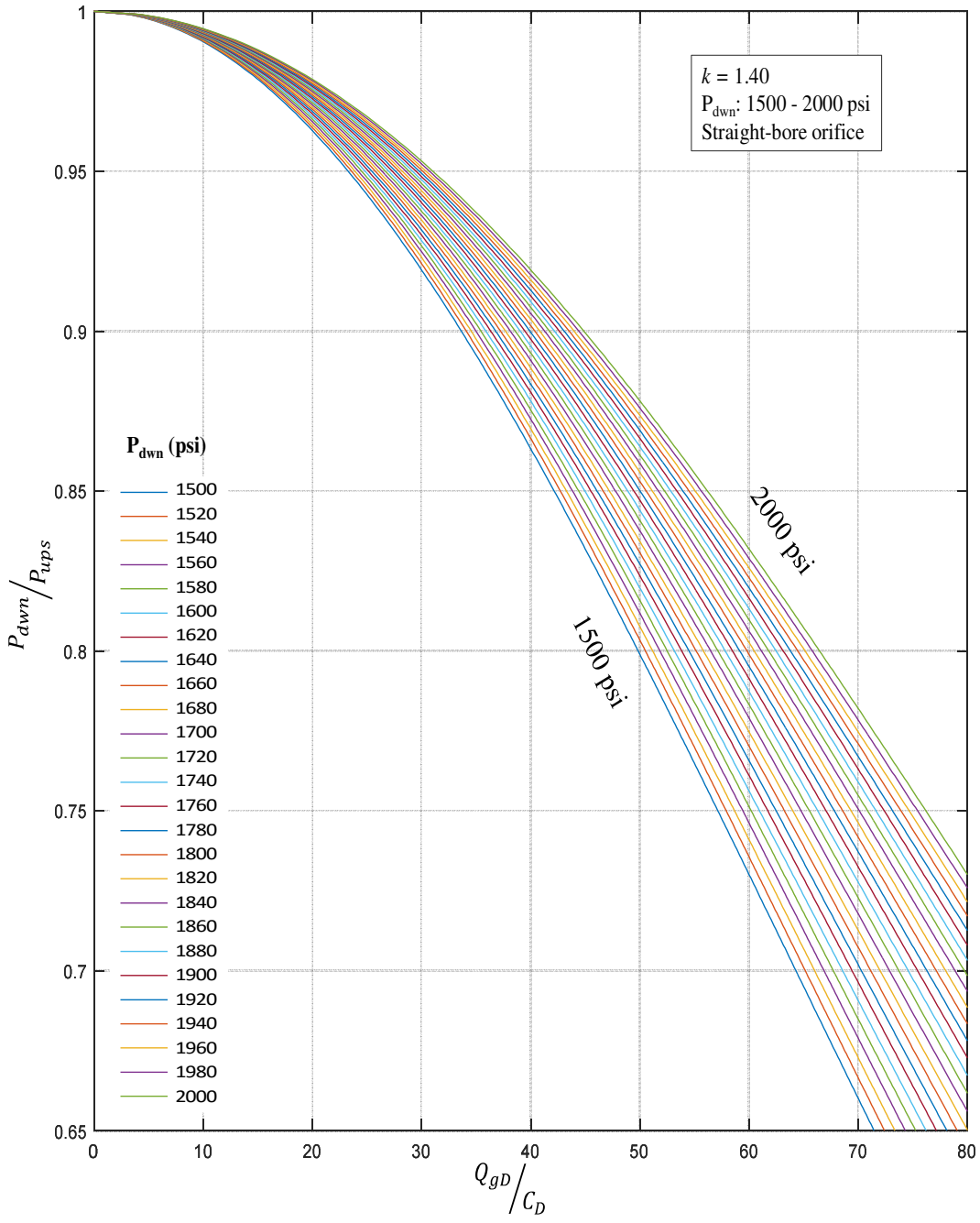

Fig. 4.12 – Dimensionless gas rate vs pressure differential ratio. k = 1.40, P_{dwn}: 1500-2000 psi, straight-bore orifice.

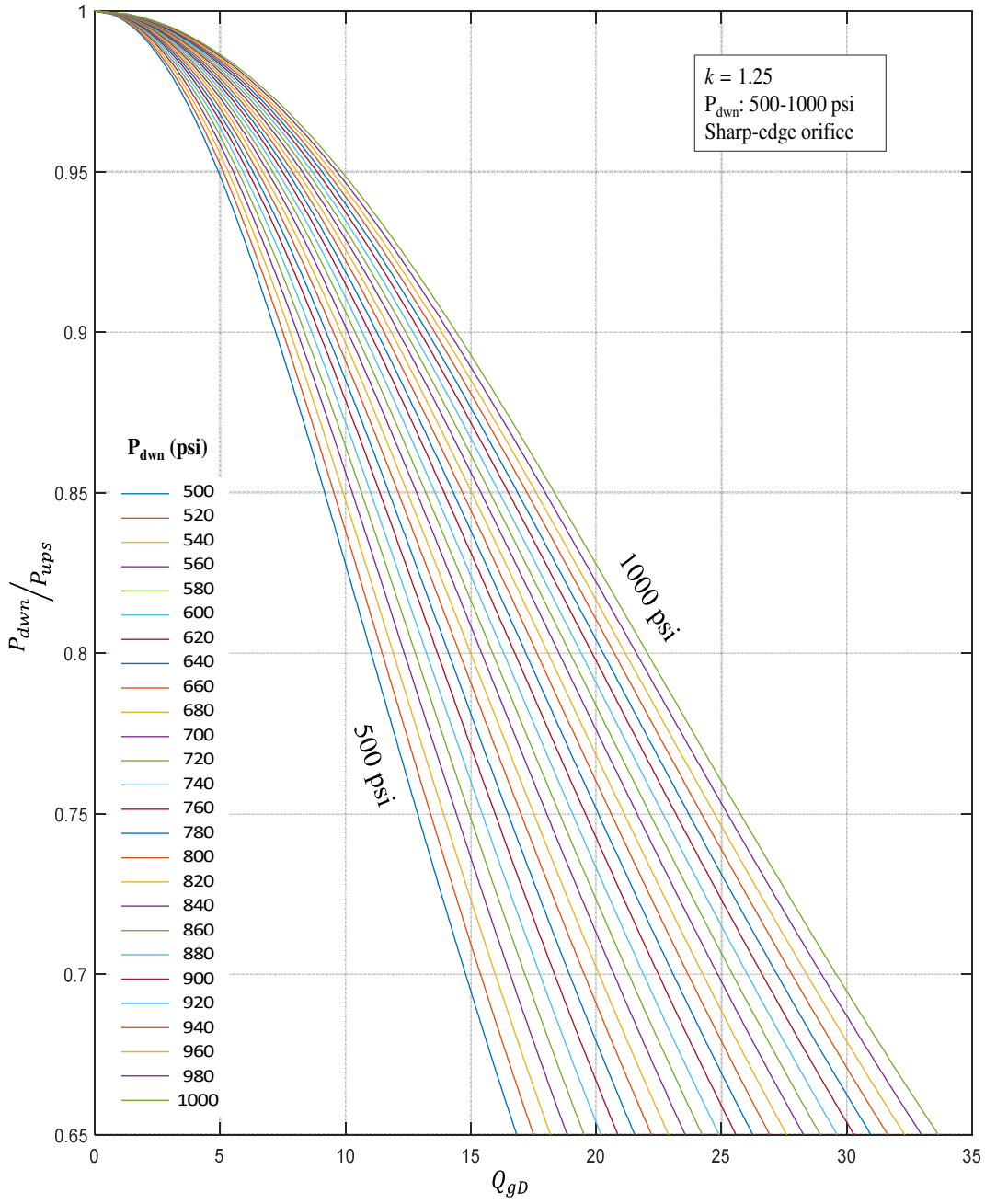

Fig. 4.13 – Dimensionless gas rate vs pressure differential ratio. k = 1.25, P_{dwn}: 500-1000 psi, sharp-edge orifice.

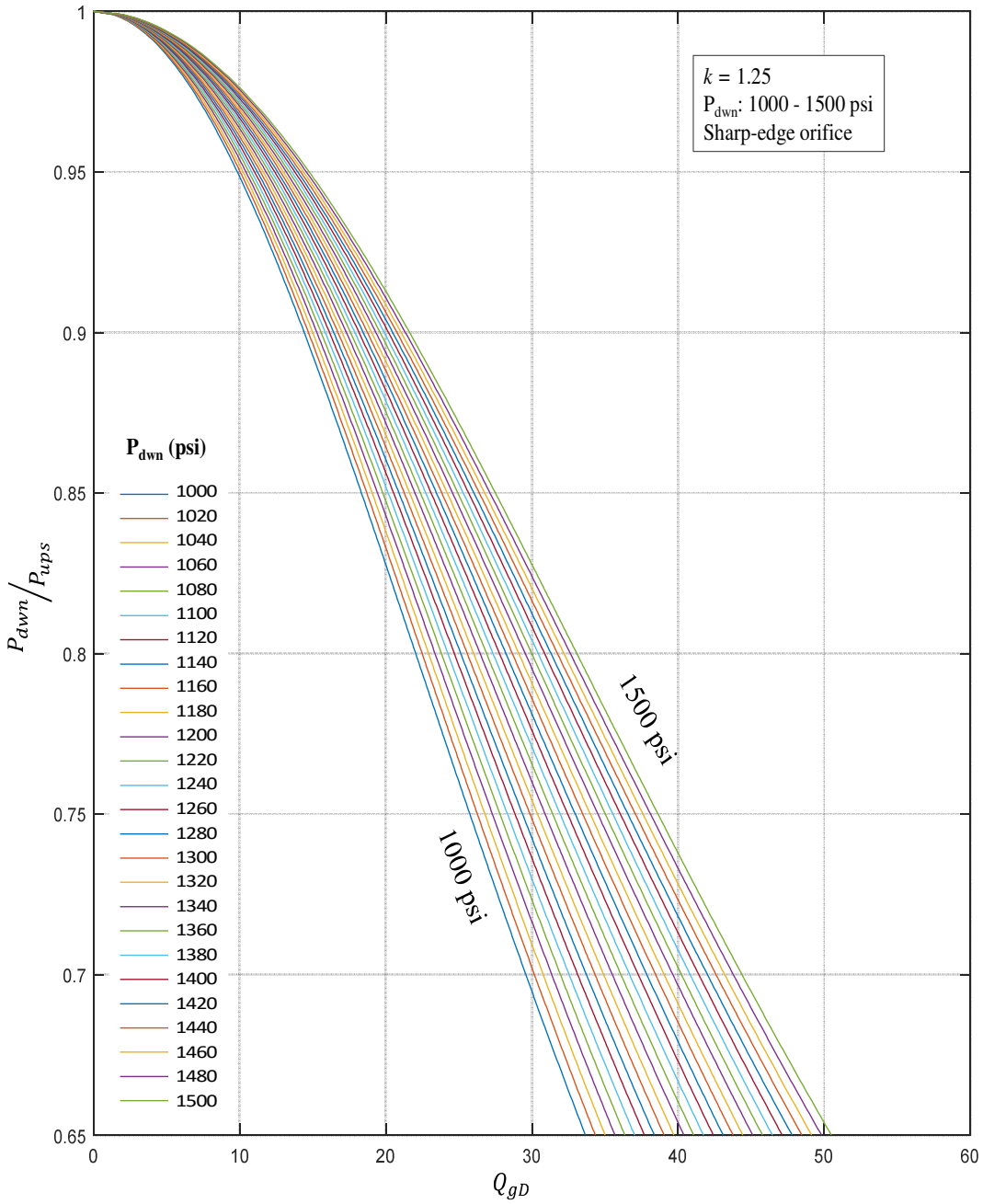

Fig. 4.14 – Dimensionless gas rate vs pressure differential ratio. k = 1.25, P_{dwn}: 1000-1500 psi, sharp-edge orifice.

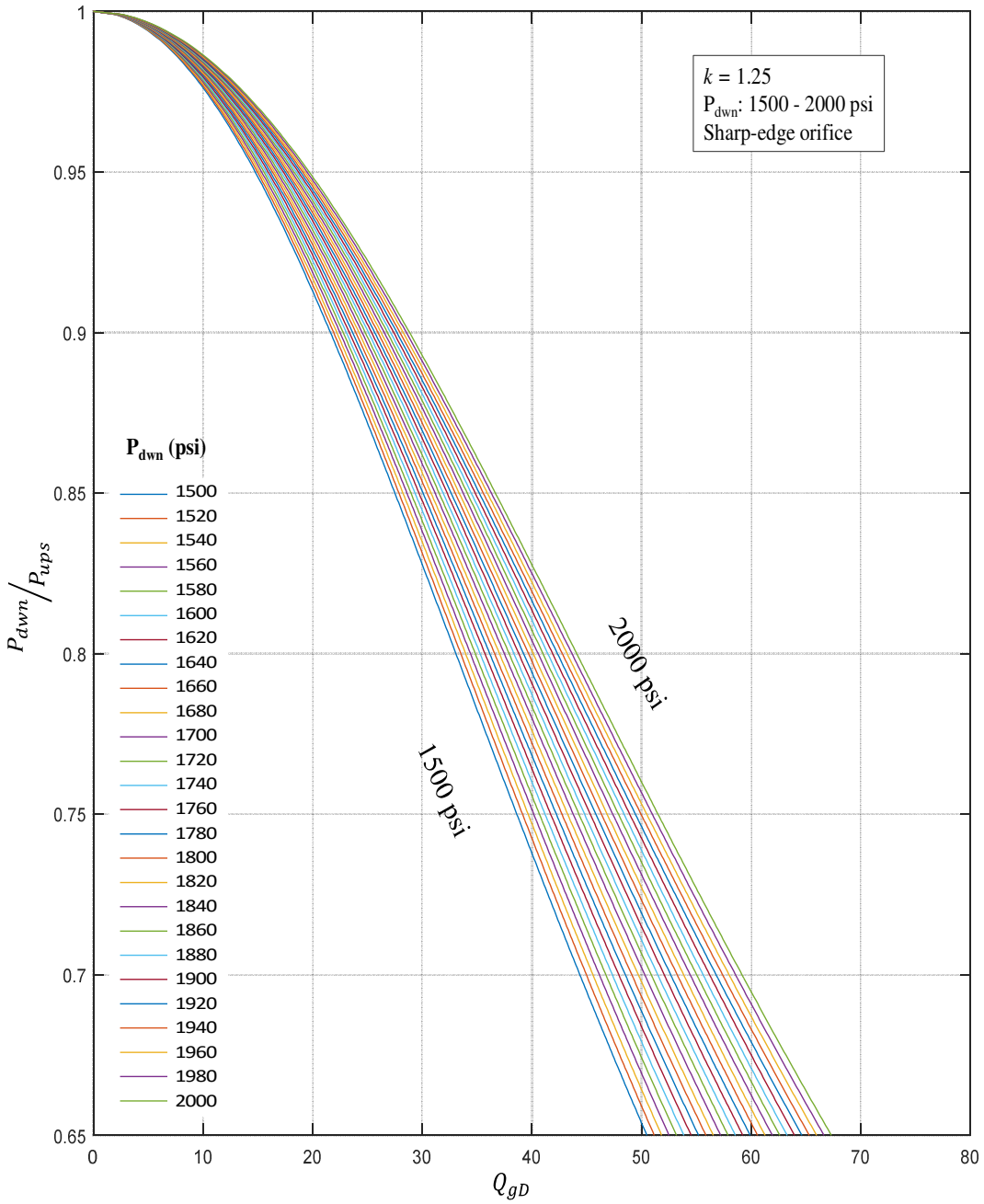

Fig. 4.15 – Dimensionless gas rate vs pressure differential ratio. k = 1.25, P_{dwn}: 1500-2000 psi, sharp-edge orifice.

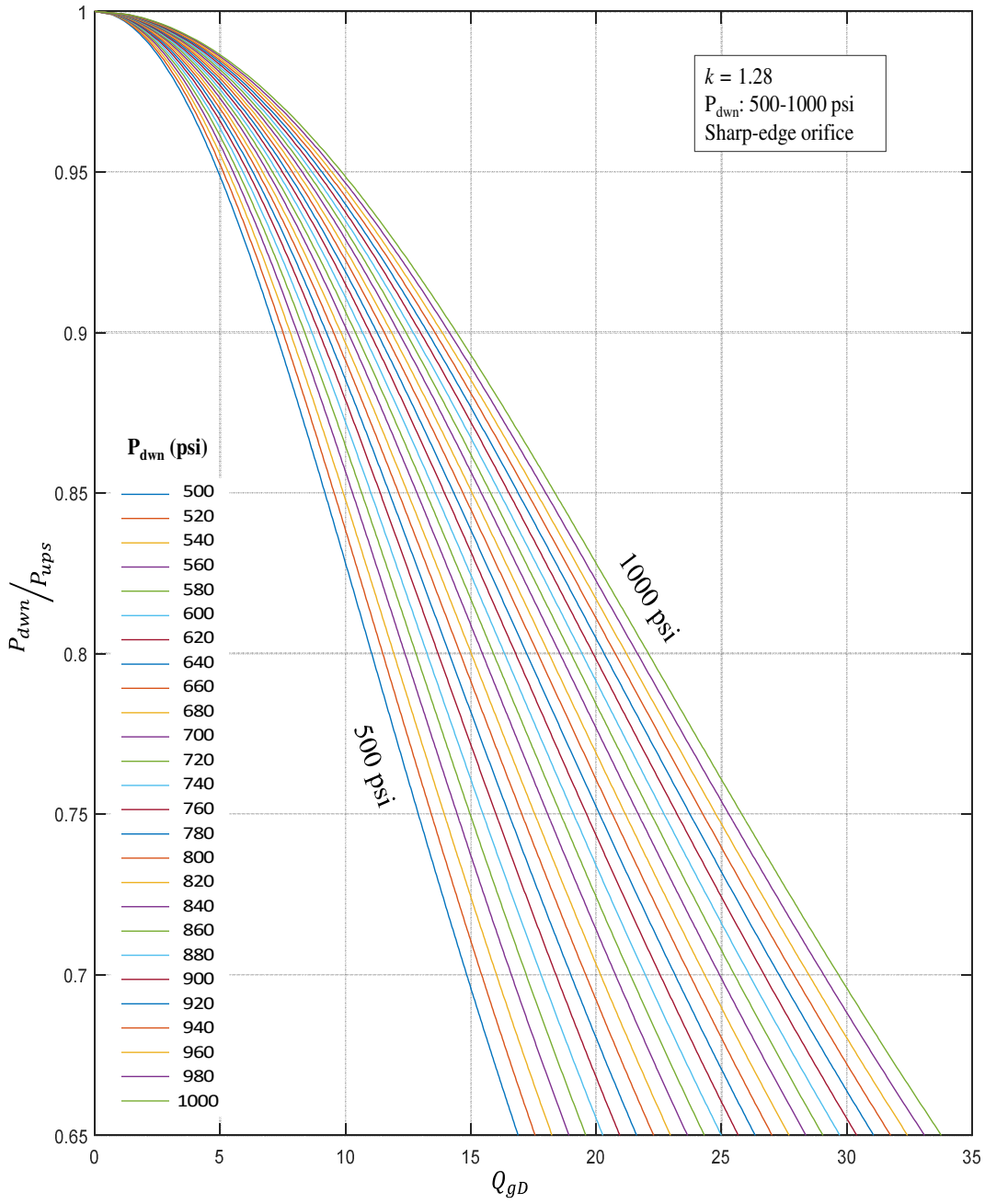

Fig. 4.16 – Dimensionless gas rate vs pressure differential ratio. k = 1.28, P_{dwn}: 500-1000 psi, sharp-edge orifice.

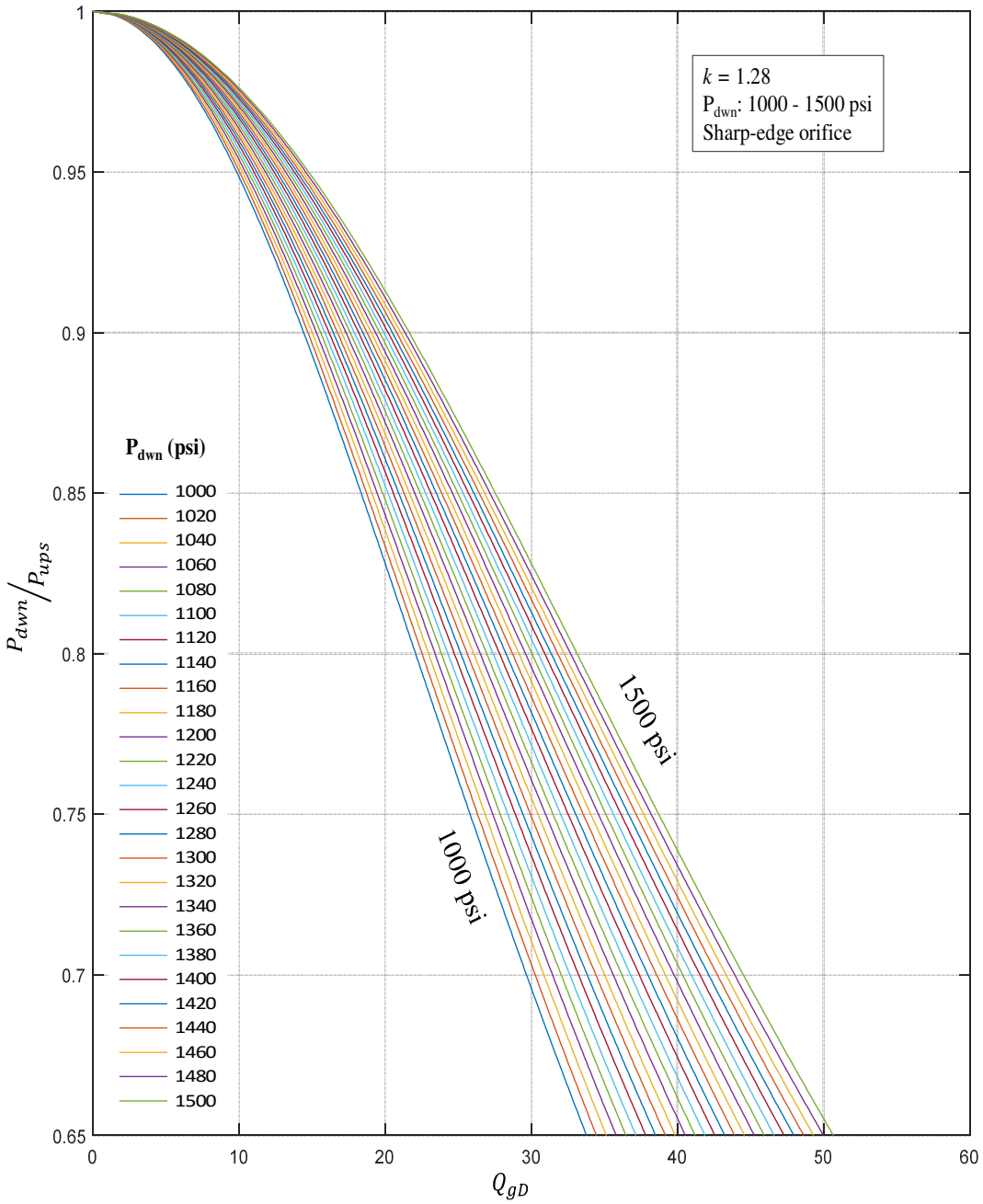

Fig. 4.17 – Dimensionless gas rate vs pressure differential ratio. k = 1.28, P_{dwn}: 1000-1500 psi, sharp-edge orifice.

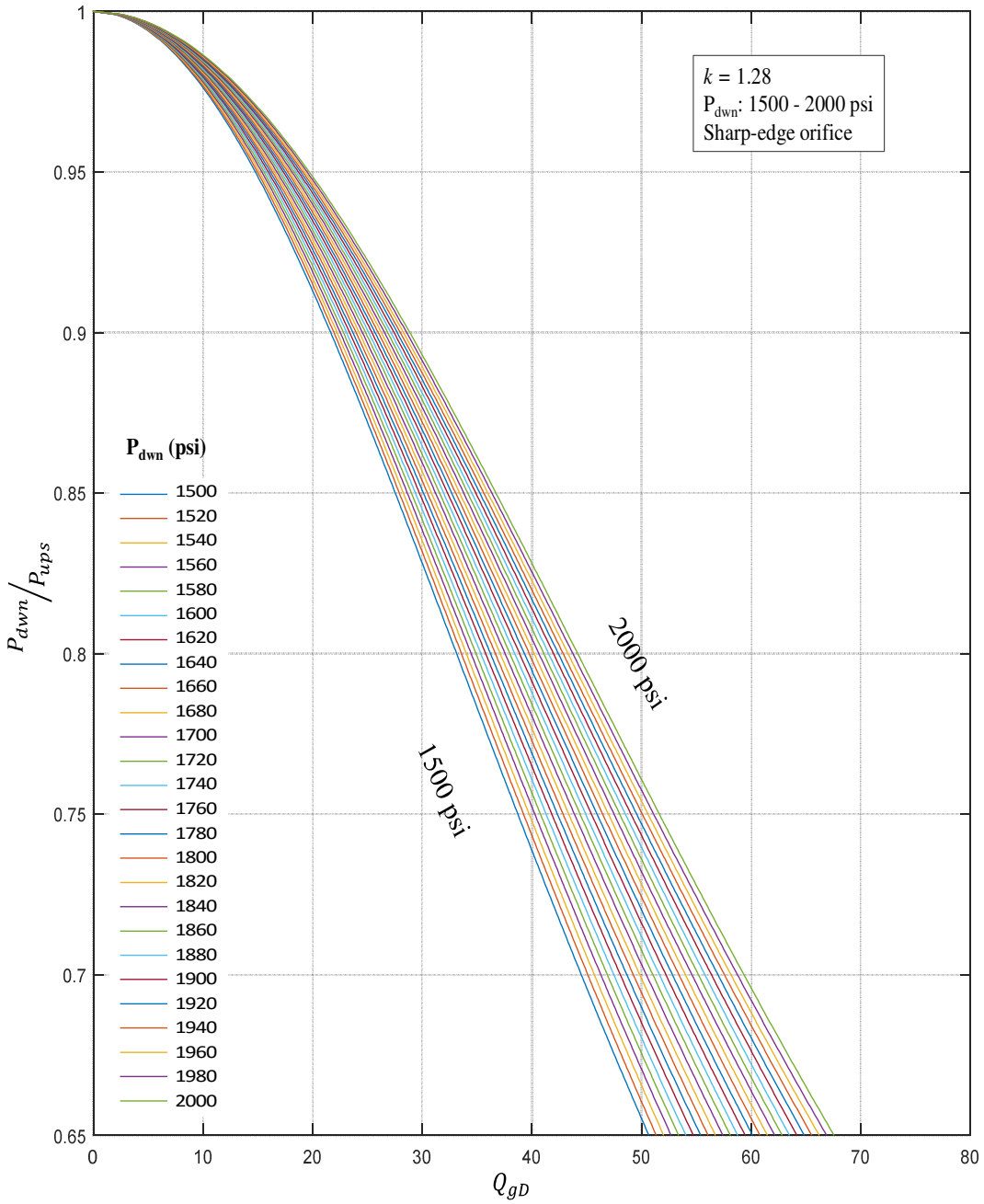

Fig. 4.18 – Dimensionless gas rate vs pressure differential ratio. k = 1.28, P_{dwn}: 1500-2000 psi, sharp-edge orifice.

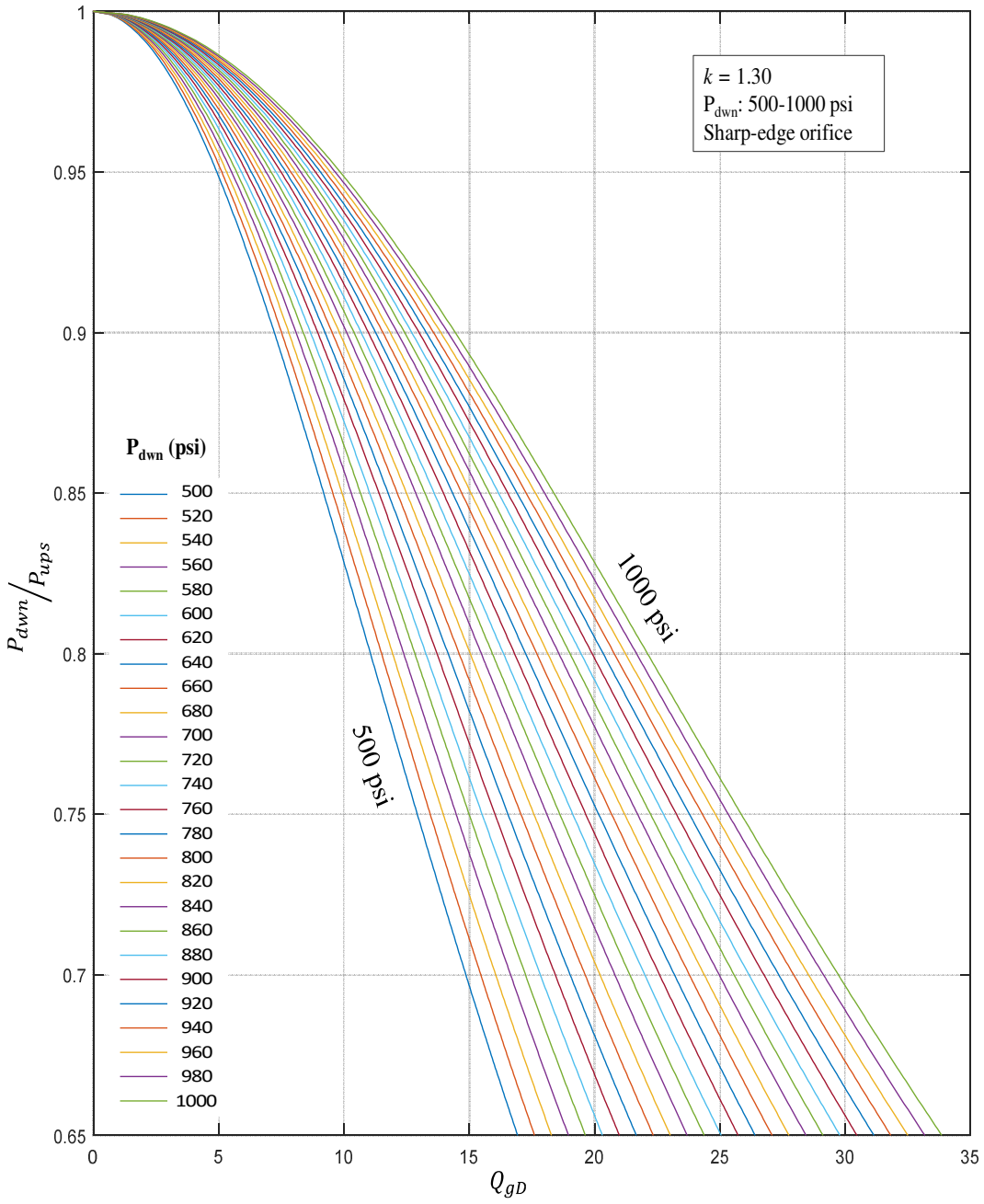

Fig. 4.19 – Dimensionless gas rate vs pressure differential ratio. k = 1.30, P_{dwn}: 500-1000 psi, sharp-edge orifice.

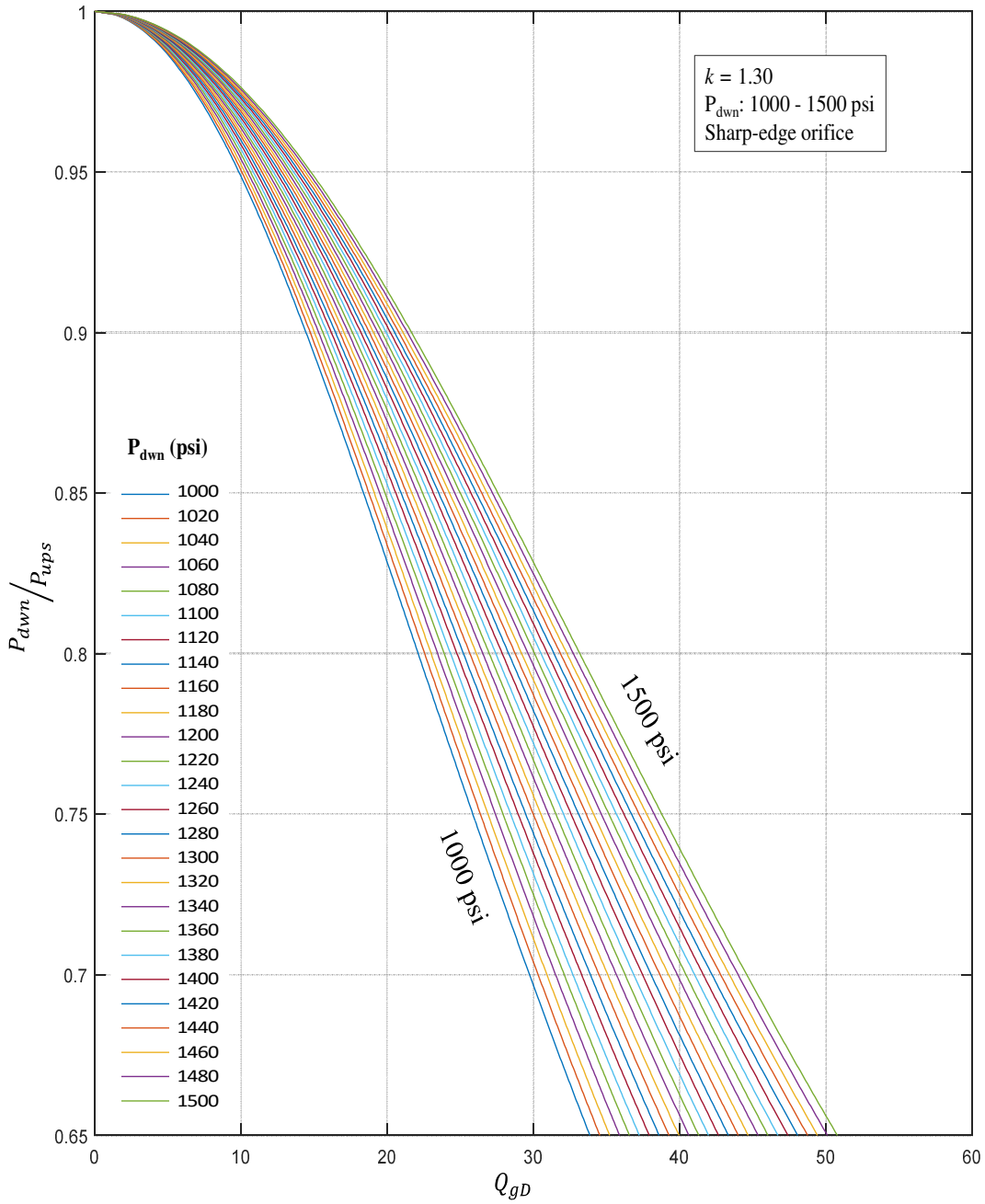

Fig. 4.20 – Dimensionless gas rate vs pressure differential ratio. k = 1.30, P_{dwn}: 1000-1500 psi, sharp-edge orifice.

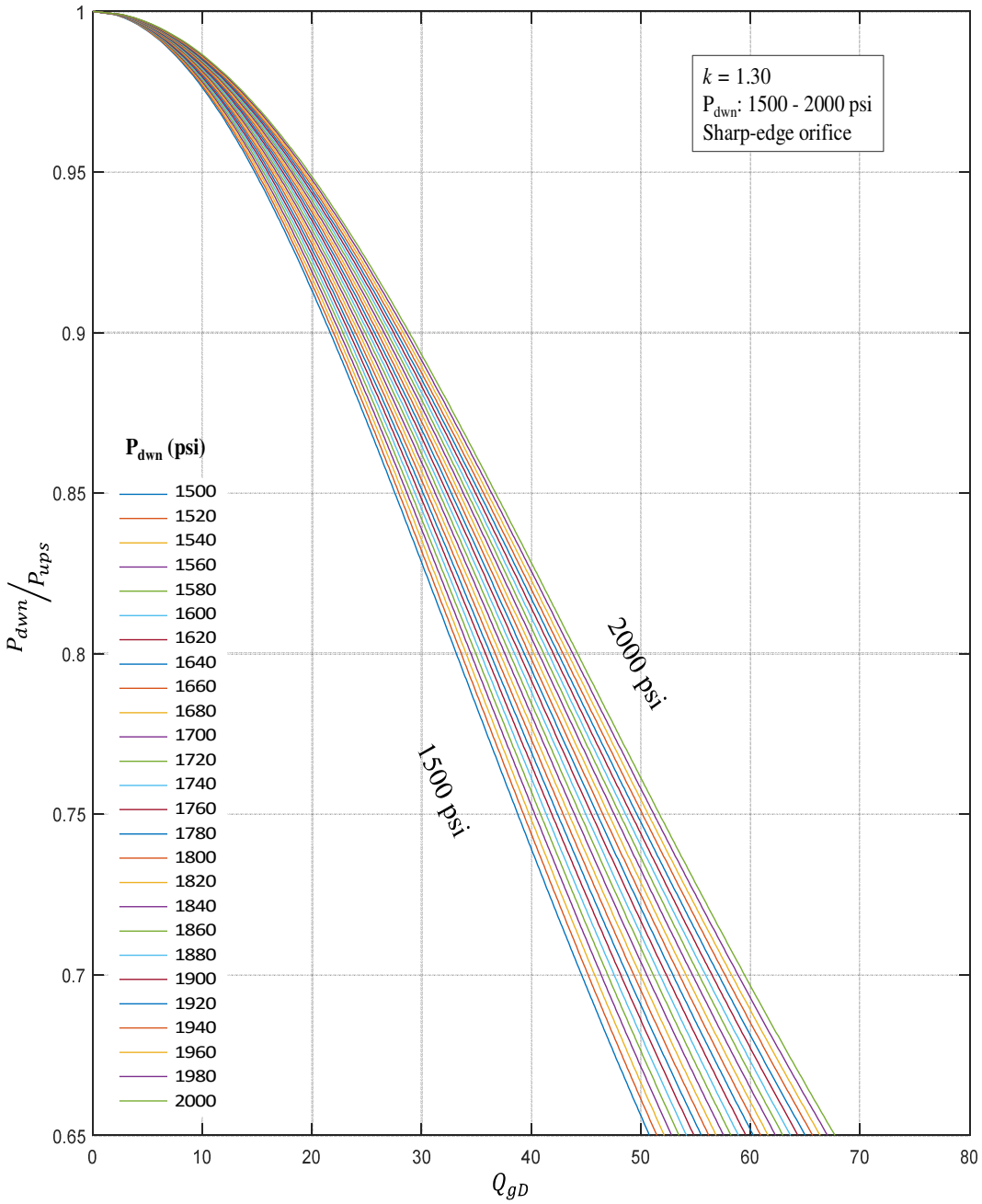

Fig. 4.21 – Dimensionless gas rate vs pressure differential ratio. k = 1.30, P_{dwn}: 1500-2000 psi, sharp-edge orifice.

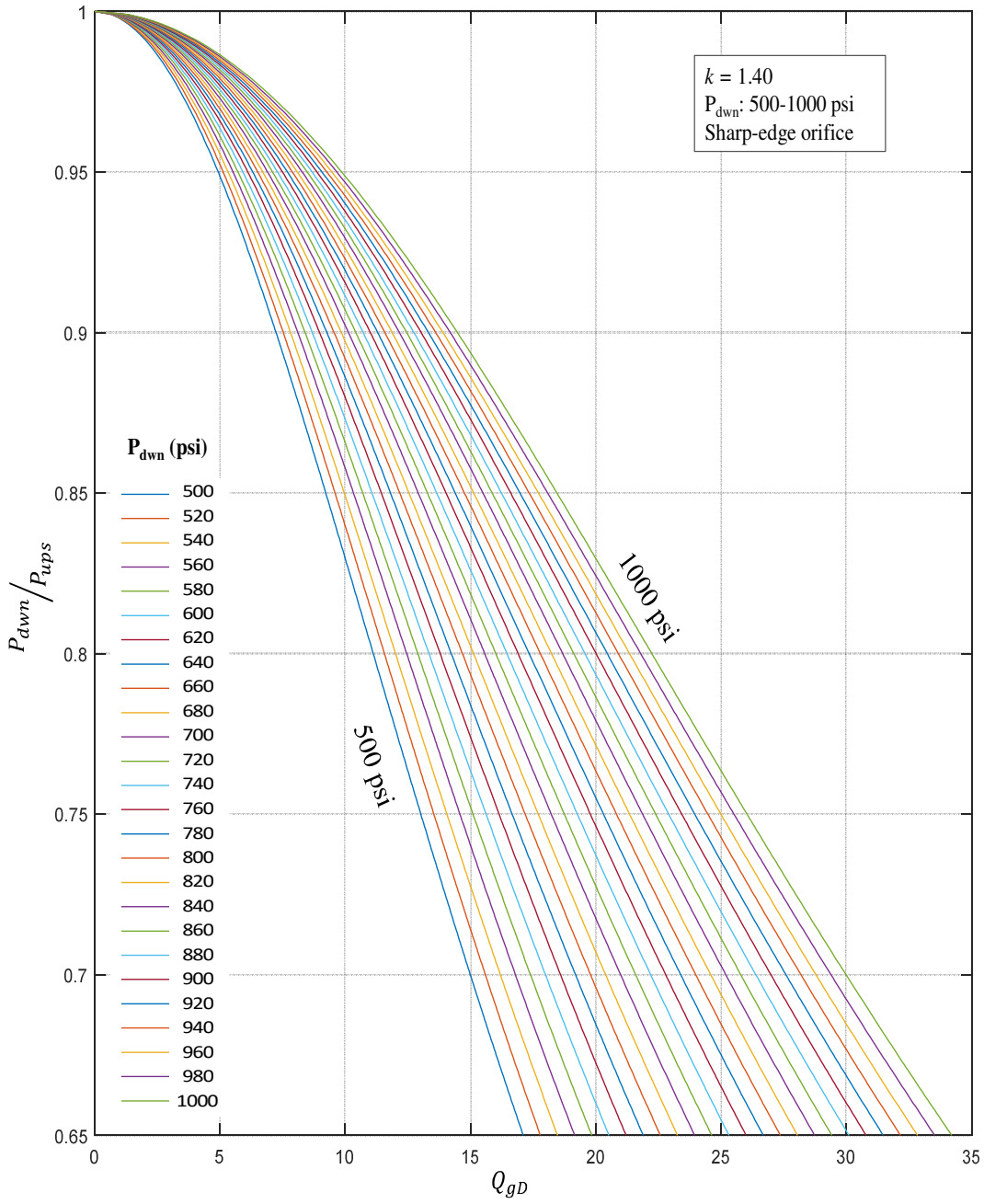

Fig. 4.22 – Dimensionless gas rate vs pressure differential ratio. k = 1.40, P_{dwn}: 500-1000 psi, sharp-edge orifice.

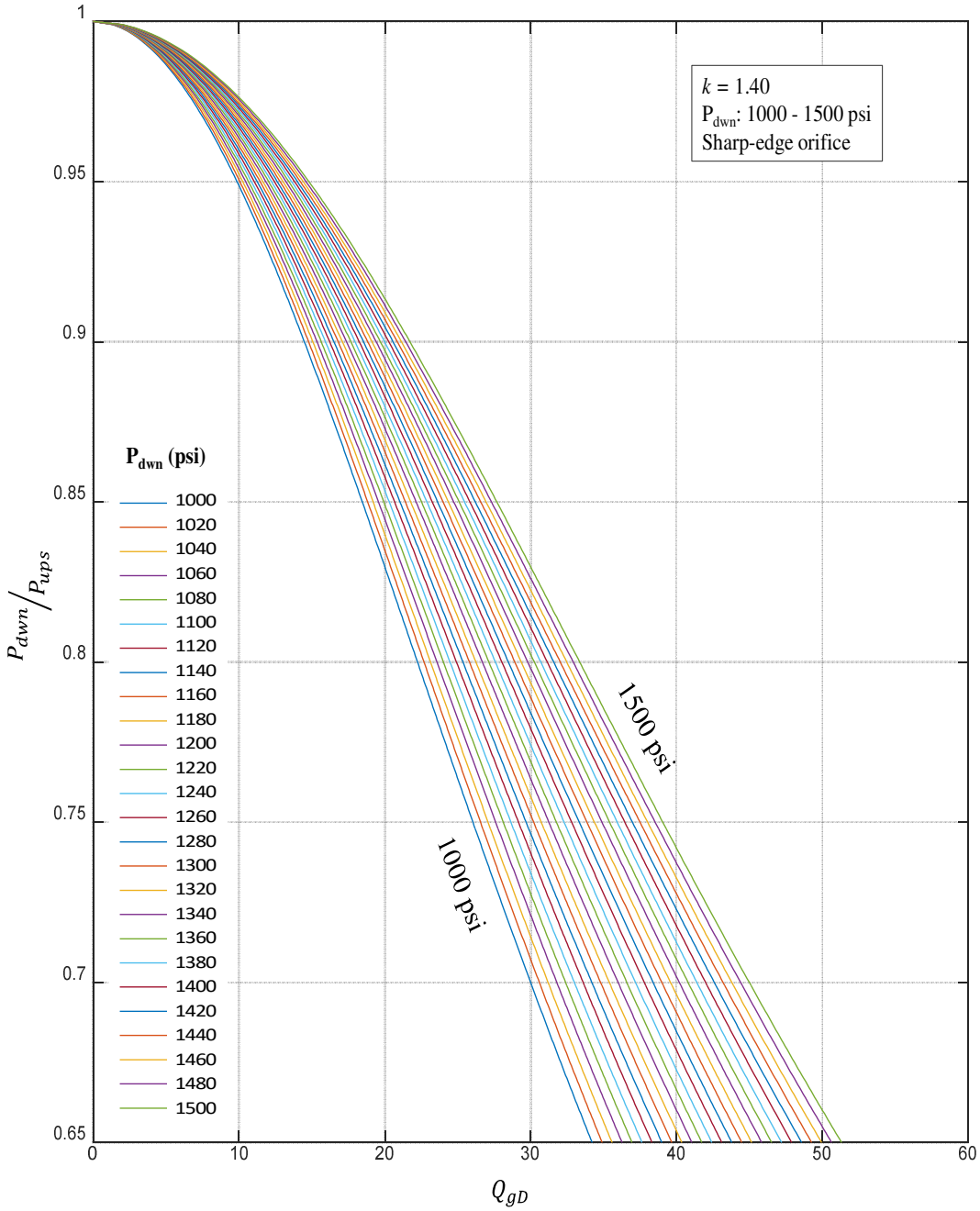

Fig. 4.23 – Dimensionless gas rate vs pressure differential ratio. k = 1.40, P_{dwn}: 1000-1500 psi, sharp-edge orifice.

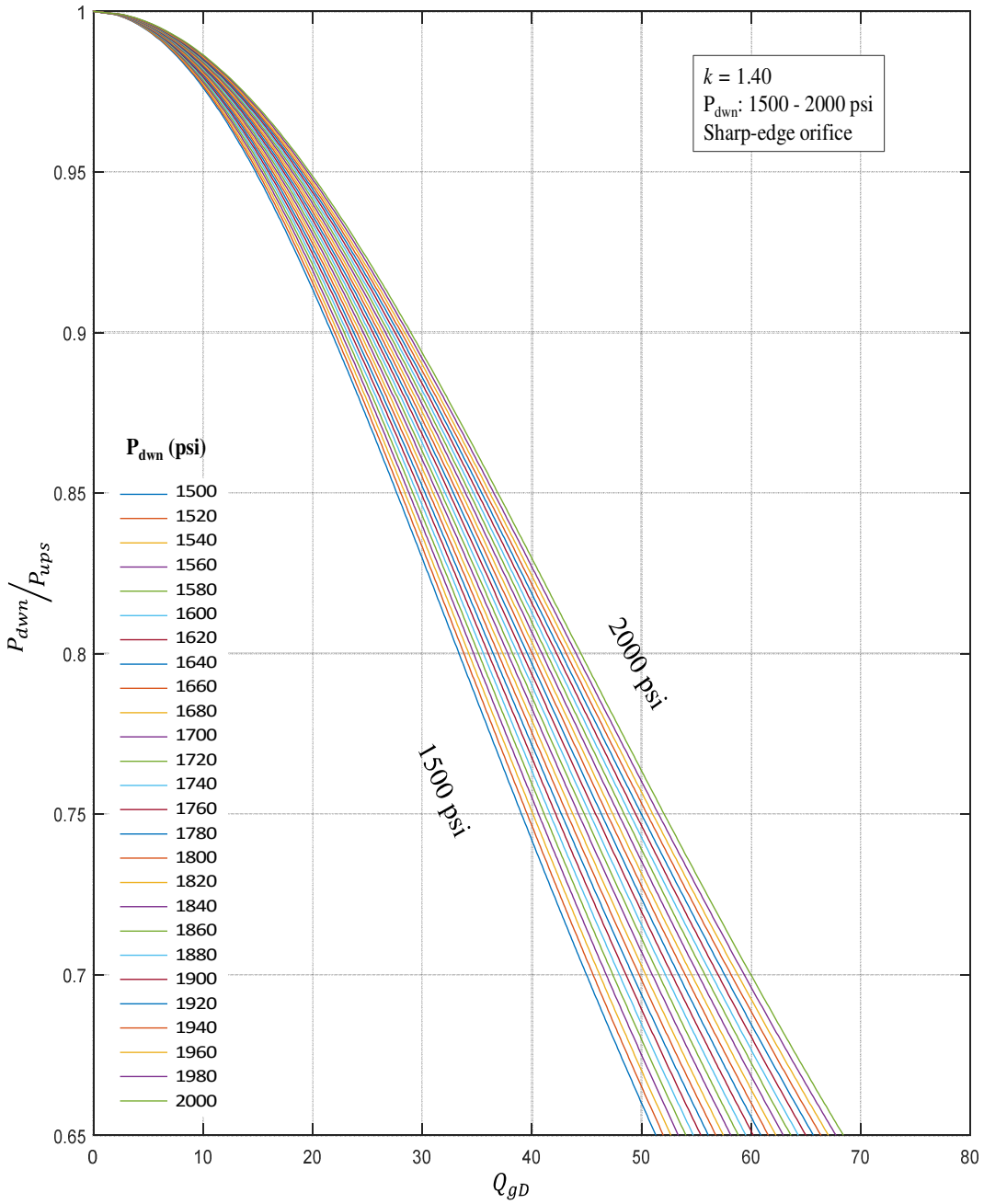

Fig. 4.24 – Dimensionless gas rate vs pressure differential ratio. k = 1.40, P_{dwn}: 1500-2000 psi, sharp-edge orifice.

4.2 Methodology Implementation Example

A hypothetical scenario has been developed in order to exemplify the application of the proposed methodologies; for a well in a naturally fractured reservoir with a deep tubing tail completion hosting a small diameter orifice with a sharp-edge geometry connecting the gas cap with the interior of the tubing tail; the schematics and details are shown in fig. 4.25:

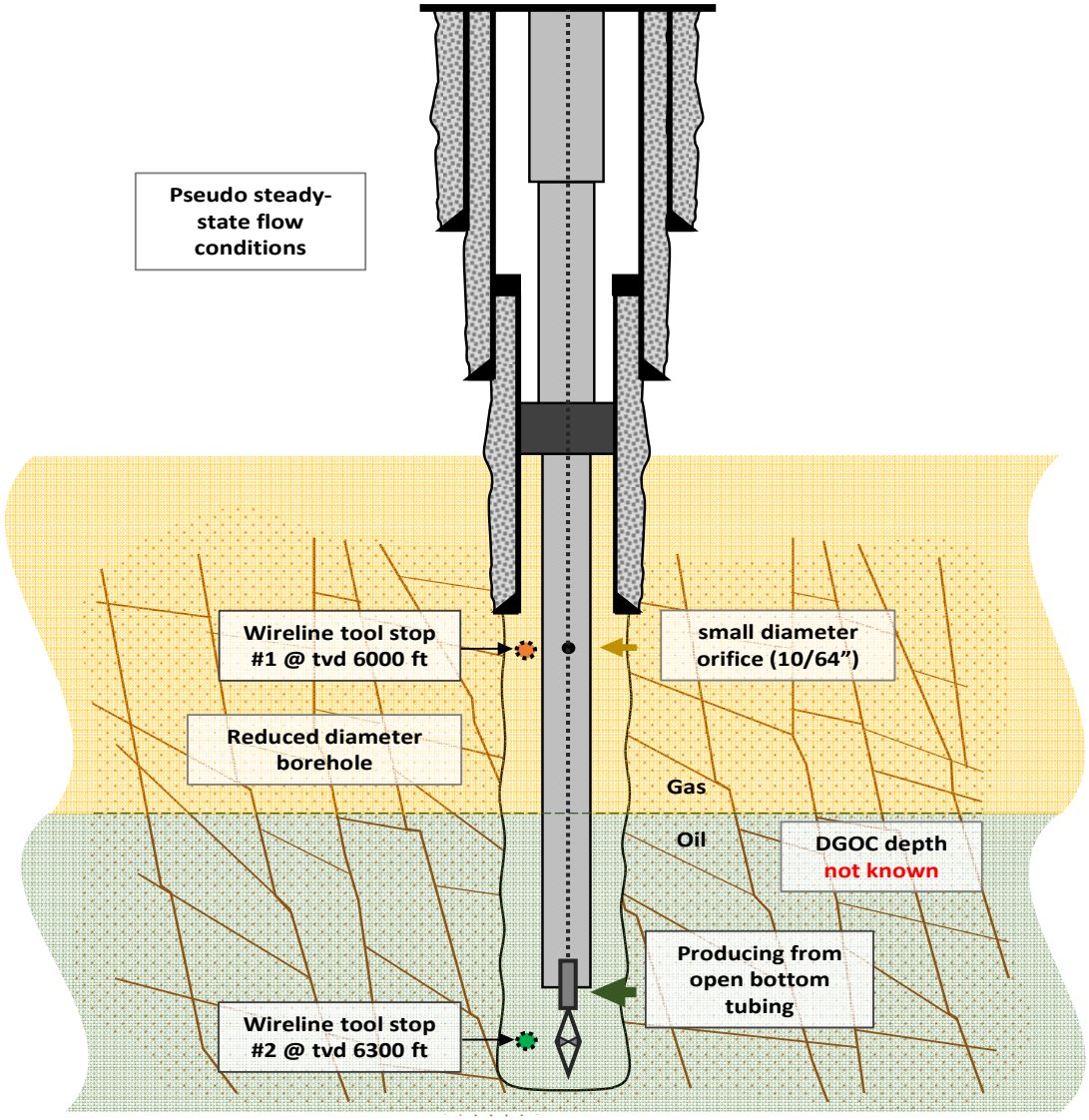

Fig. 4.25 – Example well data and schematics.

Table 4.1 presents the results of a 2 stops survey performed to the well under pseudo steady-state flow:

	Stop #1	Stop #2
TVD (ft)	6000	6300
Pressure (psi)	779.00	882.90
Qg (MSCF/d)	170.1	----

Table 4.1 – Example well data and schematics.

The last reservoir static pressure datum, transported to the depth of the gas orifice, was measured two weeks prior, resulting in a value of P_{ws}= 876.4 psi, temperature at orifice depth is $T = 599.42\ ^{o}R$, the heat capacity ratio for the gas flowing through the choke is $k = 1.28$, the gravity of the gas (to air) is $\gamma_g = 0.69$, the gradient of the oil in the reservoir is $Grad_{oil} = 0.3468\ psi/ft$, and the gradient of the gas in the reservoir is $Grad_{gas} = 0.03858\ psi/ft$, you are required to estimate the position of the dynamic gas-oil contact under current flow conditions.

Solution A. - Following the steps in the numerical methodology:

1) First step has already been finished, consisting in gathering the required data.
2) We have to establish sub-sonic flow conditions, for the fluid properties given, we make use of the corresponding equations:

$$\left(\frac{P_{dwn}}{P_{ups}}\right)_c = \left(\frac{2}{k+1}\right)^{\frac{k}{k-1}} = \left(\frac{2}{1.28+1}\right)^{\frac{1.28}{1.28-1}} = 0.549 \quad \text{----------} \quad 4.4$$

Obtaining P_{crit} from the data calculated:

$$P_{crit} = \frac{P_{dwn}}{\left(\frac{P_{dwn}}{P_{ups}}\right)_c} = \frac{779\ psi}{0.549} = 1418.94\ psi \quad \text{---------- 4.5}$$

Comparing the minimum required pressure upstream (critical pressure) for the flow to be sonic against the current reservoir static pressure:

$$P_{crit} > P_{ws}$$

$$1418.94\ psi > 876.4\ psi$$

We can conclude from this that it would be required a pressure greater than that of the reservoir in order for the flow to achieve sonic conditions, this means that the gas is flowing through the orifice at sub-sonic velocity and we can proceed to the next steps.

3) Now we calculate the dimensionless gas rate:

$$Q_{gD} = \frac{Q_g}{(3.505)d_{64}^2\sqrt{\frac{1}{\gamma_g T}}} = \frac{170.1\ (MSCF/d)}{(3.505)(10)^2\sqrt{\frac{1}{(0.69)*(599.42(\ ^oR\ ))}}} = 9.877 \quad \text{---------- 4.6}$$

4) We can now make use of the dimensionless gas rate calculated and the polynomial expression proposed for sharp-edge orifices to obtain the upstream gas pressure "P_{ups}" using iterative methods for solving polynomial equations:

Sharp-edge orifice proposed expression:

$$Q_{gD} = \left(0.120 * \left(\frac{(P_{ups} - P_{dwn}) * \left(\frac{P_{dwn}}{P_{ups}}\right)_c}{P_{dwn} - P_{dwn} * \left(\frac{P_{dwn}}{P_{ups}}\right)_c} \right) + 0.626 \right) \frac{P_{ups}}{P_{sc}} \sqrt{\frac{k}{k-1}\left[\left(\frac{p_{dwn}}{p_{ups}}\right)^{\frac{2}{k}} - \left(\frac{p_{dwn}}{p_{ups}}\right)^{\frac{k+1}{k}} \right]} \quad 4.7$$

$$Q_{gD} = \left(0.120 * \left(\frac{\left(\boldsymbol{P_{ups}} - 779\ (psi)\right) * 0.549}{779\ (psi) - 779\ (psi) * 0.549} \right) + 0.626 \right) * \frac{\boldsymbol{P_{ups}}}{14.7(psi)} *$$

$$\sqrt{\frac{1.28}{1.28-1}\left[\left(\frac{779\ (psi)}{\boldsymbol{p_{ups}}}\right)^{\frac{2}{1.28}} - \left(\frac{779\ (psi)}{\boldsymbol{p_{ups}}}\right)^{\frac{1.28+1}{1.28}} \right]} \text{ ---------- } 4.8$$

An iterative method for solving polynomial equations using a programming software returned a P_{ups} of:

$$P_{ups} = 846.91\ psi \text{ ---------- } 4.9$$

5) Finally, with the pressure upstream of the gas orifice "P_{ups}" obtained and the data gathered at the second survey stop in the oil phase , we proceed to calculate the DGOC depth:

$P_1 = P_{ups}$; $P_2 = P_{@stop\#2}$

$$Depth_{@DGOC} = \frac{P_2 - (Grad_{oil} * Depth_2) + (Grad_{gas} * Depth_1) - P_1}{Grad_{gas} - Grad_{oil}} \quad \text{----------4.10}$$

$$Depth_{@DGOC} = \frac{882.90\ (psi) - (0.3468(psi/ft) * 6300(ft)) + (0.03858(psi/ft) * 6000(ft)) - 846.91\ (psi)}{0.03858(psi/ft) - 0.3468(psi/ft)} \quad \text{----------4.11}$$

$$Depth_{DGOC@tvd} = 6220.78\ ft \quad \text{----------4.12}$$

The dynamic gas-oil contact for the current well conditions will be located at 6620.78 ft., since the producing section of the tubing tail is located at 6300 ft., there are still around ~80 ft. between the DGOC and the producing section of the tubing tail.

Solution B. - Following the steps in the type-curve methodology:

We can use the information obtained up to step 3 from the numerical methodology to check the solution applying the type-curve methodology.

4) We use fig. 4.26 containing the curves family for a sharp-edge orifice with a heat capacity ratio for the gas flowing through it equal to $k = 1.28$, and a curve close to $P_{dwn} = 779\ psi$; using the calculated dimensionless gas rate $Q_{gD} = 9.877$:

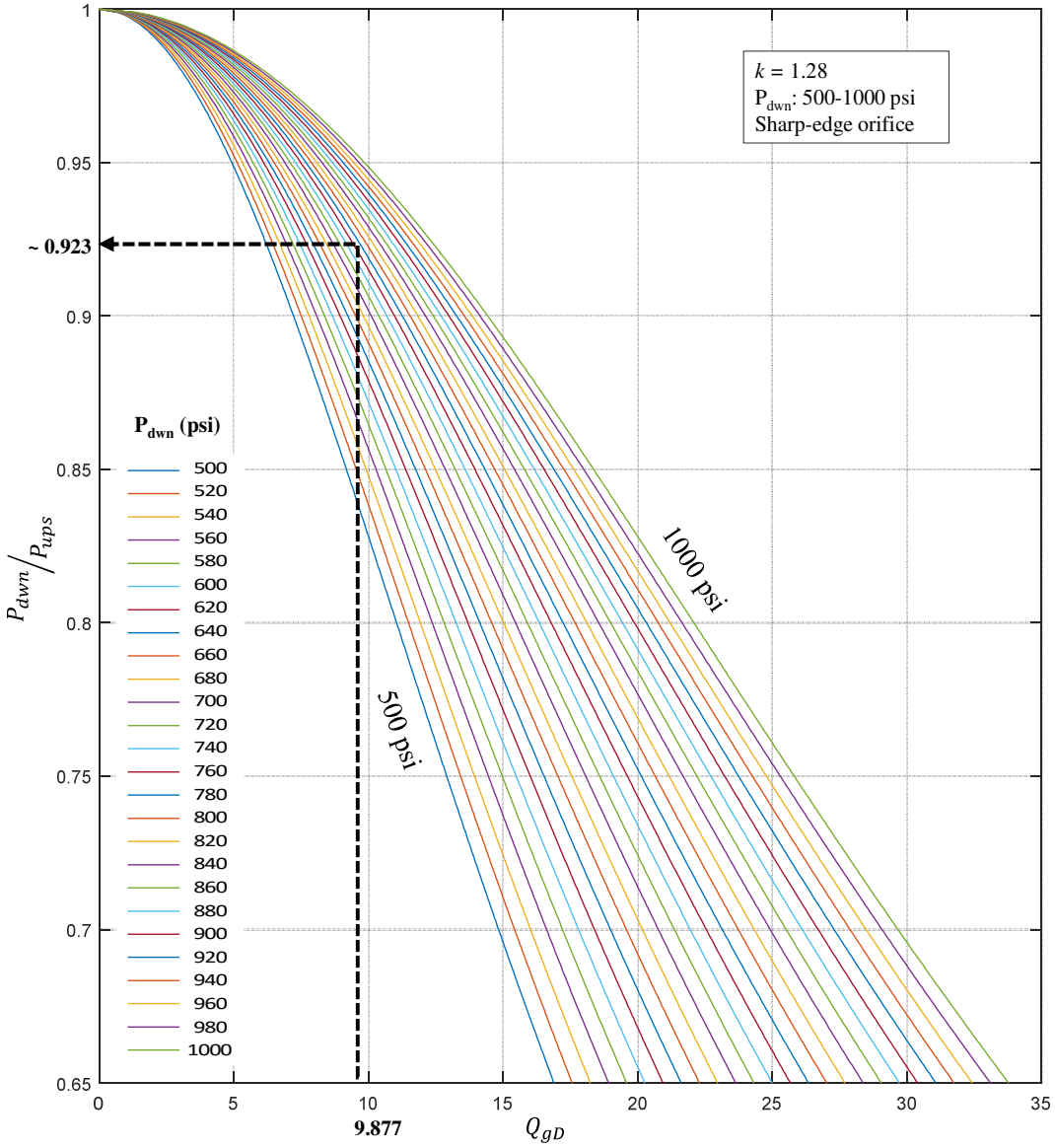

Fig. 4.26 – Dimensionless gas rate vs pressure differential ratio plot selected to solve the example using the type-curve methodology.

Reading the curves family in fig. 4.26 for a dimensionless gas rate of 9.877 will result in a pressure differential ratio of:

$$\frac{p_{dwn}}{p_{ups}} = 0.923 \quad \text{----------4.13}$$

5) Once the pressure differential ratio (P_{dwn}/P_{ups}) has been graphically obtained, we calculate the pressure upstream of the gas orifice using the following expression:

$$P_{ups} = \frac{P_{dwn-measured}}{\left(\frac{P_{dwn}}{P_{ups}}\right)_{read\ from\ type-curve}} \quad \text{----------4.14}$$

$$P_{ups} = \frac{779\ (psi)}{0.923} = 843.98\ psi \quad \text{----------4.15}$$

6) Finally, with the pressure upstream of the gas orifice "P_{ups}" obtained and the data gathered at the second survey stop in the oil phase , we proceed to calculate the DGOC depth:

$$P_1 = P_{ups}\ ;\ P_2 = P_{@stop\#2} \quad \text{----------4.16}$$

$$Depth_{@DGOC} = \frac{P_2 - (Grad_{oil} * Depth_2) + (Grad_{gas} * Depth_1) - P_1}{Grad_{gas} - Grad_{oil}} \quad \text{----------4.17}$$

$$Depth_{@DGOC} =$$

$$\frac{882.90\ (psi) - (0.3468(psi/ft) * 6300(ft)) + (0.03858(psi/ft) * 6000(ft)) - 843.98\ (psi)}{0.03858(psi/ft) - 0.3468(psi/ft)} \quad \text{----------4.18}$$

$$Depth_{DGOC@tvd} = 6211.28\ ft \quad \text{----------} \quad 4.19$$

The dynamic gas-oil contact for the current well conditions will be located at 6611.28 ft., this value is ~9 ft. apart from the results applying the numerical methodology (6620.78 ft.), we consider this to be acceptable due to the errors inherent to reading and estimating values from a plot.

5. SUMMARY AND CONCLUSIONS

5.1 Summary and Conclusions

In the present thesis work two alternate methodologies to the ones existing in available literature to estimate the DGOC in NFR wells with small diameter boreholes have been developed, along with such methodologies comes a series of dimensionless curves to facilitate the computation of the DGOC for cases where software to solve polynomial equations is not easily available. Examples for the implementation of the methodologies to calculate the DGOC have been provided as a support.

In order to being able to use the methodologies presented here, a modification has to be implemented in the deep tubing tail completion design, such modification consists in manufacturing a small diameter orifice at the wall of the tubing tail, directly communicating the interior of the tubing tail with the gas cap, allowing for a small, controlled volume of gas to flow inside the production tubing.

The orifice manufactured at the wall of the tubing tail should be small enough that the gas volume flowing through it does not affect negatively the productivity of the well, for this purpose orifice geometries with diameters ranging from 6/64” to 14/64” are recommended; the decision of the orifice diameter size and geometry should be made taking into account the maximum amount of gas volume that can be produced without

affecting negatively the productivity of the well (max GLR), it should also be taken into account the ability and precision of the tools selected to measure pressure and gas rates, if the accuracy and resolution of the tools is not good enough, more gas would be required to enter the well, if the tools excel at accuracy and resolution, less amount of gas is required to enter the well and smaller diameters can be chosen.

The resulting position of the DGOC using the methodologies proposed should be taken under the assumption that they are the result of measurements taken under semi-steady state conditions, and although this conditions are stable, the multiphase flow given inside the production tubing will have a dynamic impact upon the data measurements performed making it prone to deviation errors, for this reason it is advisable to add as a safety measure a dynamic range interval to the position calculated.

For the methodologies to be valid, the gas passing across the small diameter orifice manufactured at the tubing tail lateral wall must be doing so under sub-sonic flow conditions, when sonic flow conditions govern the flow behavior across the orifice the changes in pressure measured inside the tubing tail at the outlet of the orifice wont modify the pressure upstream and thus can't be related to the conditions on the inlet side of the orifice.

Additional requirements that a deep tubing tail completion has to meet in order to be a candidate for the methodologies presented here have been established regarding well

completion design, data metering tool characteristics and technical specifications and reservoir conditions, recommendations for use and implementation have also been detailed.

The precision of the calculations presented here depend greatly in the quality and design of the small diameter orifice geometry, for this reason extra care should be taken at the time of manufacture.

The actual vertical position of the measurements and key elements of the well completion like the vertical position of the gas inlet orifice and the oil production slots or the tubing open-bottom are of primordial importance, since any variation in depth will affect the fluid gradients used in the calculations and directly change the pressure data extrapolated for the determination of the DGOC position at the time of the measurements.

Well flowing conditions should remain unchanged while performing the corresponding measurements at the gas inlet orifice and at the liquid phase since any change in the flowing conditions will modify the position of the DGOC and the measurements at different depths won't be relatable.

Pressure and rates measurements should be performed under steady-state flow, if such condition can't be achieved the position of the DGOC will be erratic and the measurements performed will be useless.

Sharp-edge orifice geometries are recommended since they provide more advantages than the straight-bore geometry, it also gives a great correlation for the discharge coefficient under sub-sonic flow, independent from the gas composition, temperature or orifice diameter, it only depends on the pressure differential across the orifice; the problem with the sharp-edge orifice relies in the reduced volume of gas flowing through it compared under the same conditions to the straight-bore orifice, if our pressure metering tool does not handle well small volume rates it may be better to choose a straight-bore orifice geometry and sacrifice some estimation accuracy in favor of better data metering reliability.

We recommend the use of the numerical methodology for scenarios where the vertical space available between the orifice and the assume interval where the DGOC is reduced since the gradient and compressible flow equations presented here are quite sensible to changes, because of this, the use of the type-curve methodology could add a slight shift in the calculated position of the DGOC, in wells with enough vertical space this issue does not represent a great problem since a resolution tolerance of +-10 ft. can be acceptable, but in cases where the vertical space is reduced, the shift imposed by a bad type-curve reading could place the DGOC even below the whole well completion.

An additional benefit of the modification proposed to the deep tubing tail completion is that because of the direct connection to the gas cap that the gas inlet orifice provides, when the well is closed, the fluid levels inside the tubing and at the wellbore will balance given

enough time, if such connection is not present, like in well completions isolated from the gas cap, the fluid level inside the tubing will be different to that of the wellbore and the reservoir; this provides the opportunity to also make measurements of the static GOC when the well is shut in using the theory provided in this thesis for gradient calculation and fluid contacts estimation.

If a continuous monitoring was performed where multiple pressure data points and rates were measured over a period of time under steady-state flow, the numerical methodology can be programed using software to be repeated on the whole data set in order to generate a plot of the dynamic gas-oil contact depth position over a period of time.

The fact that the fluid levels inside the tubing and at the wellbore will balance has to be taken into account when opening the well, gas-lift assisted wells rely on the assumption that the fluid levels inside the well will be in concordance with the design of the gas-lift valves, for the well cases presented here an initial induction to start the well using gas injection though a C.T. to raise the level of the fluids inside the tubing to the level of the gas-lift valve and jumpstart the flow inside the well is advisable.

In this thesis we have proposed two methodologies based on a selected set of orifice geometries and compressible flow through small diameter orifices expressions, but it has been easily concluded from available literature that a universal equation does not exist for flow rates estimation across orifices that fits accurately all types of chokes and fluids

passing through them (Bahadori. 2012a; Nøkleberg and Søntvedt. 1995), there exist many models to estimate choke flow behavior, depending on the fluid properties, sonic or subsonic flow and choke configuration, one model or another will be better suited to our specific scenario, and new studies are performed every day with the objective to improve current correlations. Furthermore the same case applies when trying to characterize the discharge coefficient for a specific orifice with a given geometry, for this reason we recommend that if the users require to implement a different set of equations to characterize the behavior of their flow and their orifice geometry, the results obtained in this thesis can still be applied with the condition that steps 3 and 4 of the numerical and type-curve methodologies (steps in charge of correlating the measured data inside of the production tubing to the gas cap) have to be adapted to the user's correlations for compressible flow through orifices and discharge coefficient in the same way it was presented here and generate the corresponding dimensionless curves, this way the pressure at the gas in the user's wellbore can be obtained and the position of the DGOC can be calculated following the steps proposed in the previous methodologies.

5.2 Recommendations for Future Research

Future work on the subject presented on this thesis could involve the results of laboratory tests using a vertical flow system with nested tubing or the results of field implementation, additional compressible flow through orifice equations and discharge coefficient characterization equations could be also studied, different orifice geometries can also be

included as a part of a future work in order to define which is better suited for the purposes of the methodologies presented here; if possible, an experiment with the implementation of both the gas inlet orifice design and external permanent pressure gauges would prove very useful allowing to calibrate and corroborate the estimations of the DGOC done with the proposed methodology with those estimation made parting from the pressure gauges data.

REFERENCES

AlSharif, T., AlMalki, B., Bawazir, M. et al. 2013. Inflow Profiling in Challenging Complex Deep Gas Environment. doi: 10.2118/164467-MS.

Ashford, F.E. and Pierce, P.E. 1975. Determining Multiphase Pressure Drops and Flow Capacities in Down-Hole Safety Valves. doi: 10.2118/5161-PA.

Bahadori, A. 2012b. Estimation Of Flow Coefficient For Subsonic Natural Gas Flow Through Orifice-Type Chokes Using A Simple Method. Journal of Natural Gas Science and Engineering 9: 39-44. Doi: Http://Dx.Doi.Org/10.1016/J.Jngse.2012.05.005.

Bahadori, A. 2012a. A Simple Predictive Tool to Estimate Flow Coefficient for Subsonic Natural Gas Flow Through Nozzle-Type Chokes. Journal of Natural Gas Science and Engineering 7: 1-6. Doi: Http://Dx.Doi.Org/10.1016/J.Jngse.2012.03.002.

Binder, R.C. 1958. Advanced Fluid Mechanics: Prentice-Hall.

Economides, M.J., Hill, A.D., Ehlig-Economides, C. et al. 2012. Petroleum Production Systems, 2nd edition: Pearson Education.

Edwards, J.E., Brown, G.A., Vincent, M. et al. 2011. Reservoir Surveillance - Fluid Contact Monitoring in Fractured Carbonate TA-GOGD Project. doi: 10.2118/145554-MS.

Emanuel, G. 1986. Gasdynamics: Theory and Applications: American Inst. of Aeronautics and Astronautics. New York. ISBN 10: 0930403126.

Emerson Process Management Technologies 2015. Valve Sizing Calculations. In Emerson Process Management Regulator Technologies Natural Gas Application Guide, ed. Emerson Process Management Technologies, Inc., Chap. 605-625. Singapore: Tien Wah Press.

Fling, W.A., Jr. 1988. The API/GPA Orifice-Plate Data Base. Journal of Petroleum Technology 40 (07): 920-922. doi: 10.2118/15393-PA.

Fortunati, F. 1972. Two-Phase Flow through Wellhead Chokes. Society of Petroleum Engineers European Spring Meeting, Amsterdam, Netherlands. doi: 10.2118/3742-MS.

Gould, T.L. 1974. Discussion of An Evaluation of Critical Multiphase Flow Performance Through Wellhead Chokes. Journal of Petroleum Technology 26 (8): 849-850. doi: 10.2118/4541-PA.

Grace, A. and Frawley, P. 2011. Experimental Parametric Equation for the Prediction of Valve Coefficient (Cv) for Choke Valve Trims. International Journal of Pressure Vessels and Piping 88 (2–3): 109-118. doi: http://dx.doi.org/10.1016/j.ijpvp.2010.11.002.

Guo, L., Yan, Y.Y. and Maltson, J.D. 2011. Numerical Study on Discharge Coefficients of a Jet in Crossflow. Computers & Fluids 49 (1): 323-332.
doi: http://dx.doi.org/10.1016/j.compfluid.2011.06.022.

Hüning, M. 2010. Comparison of Discharge Coefficient Measurements and Correlations for Orifices With Cross-Flow and Rotation. Journal of Turbomachinery 132 (3): 031017-01,031017-10.

Kayser, J.C. and Shambaugh, R.L. 1991. Discharge Coefficients for Compressible Flow Through Small-Diameter Orifices and Convergent Nozzles. Chemical Engineering Science 46 (7): 1697-1711. doi: http://dx.doi.org/10.1016/0009-2509(91)87017-7.

Ladron De Guevara, E., Gonzalez-Vasquez, M. and Posadas-Mondragon, R. 2012. Instrumented Deep Tubing Tail Completion: A Good Practice For Monitoring Cantarell Reservoir's Behavior. Society of Petroleum Engineers Latin America and Caribbean Petroleum Engineering Conference, Mexico City, Mexico. doi: 10.2118/153468-MS.

Lagunas-Tapia, R., Sanchez Loera, P., Flores Lima, O. et al. 2015. Development of a Sensorless Well Completion Focused in Monitoring the Dynamic Gas Oil Contact on Akal Field, Mexico. Ingeniería Petrolera 55 (9): 547-557.

Liu, H., Meng, Y., Tang, J. et al. 2007. Research on Multi-stage Choking & Killing System of Oil and Gas Wells. Natural Gas Industry 27 (8): 63.

Majid, F., Jidon, J. and Asadollah, K. 2014-2015. Gas Flow Through Vertical Pipe and Perforated Vertical Pipe. Int. J. ChemTech Res 7 (6): 2589-2595.

McLemore, A., Tyner, J., Yoder, D. et al. 2013. Discharge Coefficients for Orifices Cut into Round Pipes. Journal of Irrigation and Drainage Engineering 139 (11): 947-954. doi: 10.1061/(ASCE)IR.1943-4774.0000641.

Morris, S.D. 1996. Choke Pressure in Pipeline Restrictions. Journal of Hazardous Materials 50 (1): 65-69. doi: http://dx.doi.org/10.1016/0304-3894(96)01786-4.

Nejatian, I., Kanani, M., Arabloo, M. et al. 2014. Prediction of Natural Gas Flow Through Chokes Using Support Vector Machine Algorithm. Journal of Natural Gas Science and Engineering 18: 155-163. doi: http://dx.doi.org/10.1016/j.jngse.2014.02.008.

Nnadi, M., Osho, R., Chima, E. et al. 2015. Fluid Contact Movement Monitoring in Gas Reservoirs Using Pressure Transient Data: Galaxy North Field Example. Society of Petroleum Engineers Nigeria Annual International Conference and Exhibition, Lagos, Nigeria. doi: 10.2118/178398-MS.

Nøkleberg, L. and Søntvedt, T. 1998. Erosion of Oil and Gas Industry Choke Valves Using Computational Fluid Dynamics and Experiment. International Journal of Heat and Fluid Flow 19 (6): 636-643.

Nøkleberg, L. and Søntvedt, T. 1995. Erosion in Choke Valves—Oil and Gas Industry applications. Wear 186: 401-412.

Onyekonwu, M.O. 1997. General Principles of Bottom-Hole Pressure Tests. Petroleum Engineering Department: University of Port Harcourt, Nigeria.

Posadas-Mondragon, R. 2006. 3D Homogeneous Reservoir Simulator, Fortran. PEMEX Software Report.

Ramondenc, P., Franco Delgado, E., Molero, N. et al. 2016. Reviving Oil Production in a Mature Offshore Field Through a Downhole Coiled Tubing Completion. SPE/ICoTA Coiled Tubing and Well Intervention Conference and Exhibition, Houston, Texas, USA. doi: 10.2118/179063-MS.

Schneider, B.D., Hogan,G.P.,,II and Holt, W.N., J. 1996. Using Pulsed Neutron Decay-Spectrum Data and Multi-inflatable Packer Plugdown Assemblies Improve Oil Production Rates in a Mature CO2 Flood. Permian Basin Oil and Gas Recovery Conference, Midland, Texas, USA. doi: 10.2118/35165-MS.

Schuller, R.B., Munaweera, S.J., Selmer-Olsen, S. et al. 2006. Critical and Sub-critical Oil/Gas/Water Mass Flow Rate Experiments and Predictions for Chokes. SPE Production & Operations 21 (03): 372-380. doi: 10.2118/88813-PA.

Szilas, A.P. 1985a. Production and Transport of Oil and Gas: Flow Mechanics and Production. Part A: Elsevier. New York, N.Y.

Szilas, A.P. 1985b. Production and Transport of Oil and Gas: Flow Mechanics and Production. Part B: Elsevier. New York, N.Y.

Tovar Rodriguez, T., Lozada Aguilar, M.A., Torres, M. et al. 2011. Ending Pipe Extension, An Option to Extend the Life of the Well at Low Cost. The Mexican Petroleum Congress, Puebla, Mexico.